Explanatory notes to the thematic geoscientific maps of Ethiopia at a scale of 1 : 50,000

Map sheet 0638-A2 Leku

Tomáš Hroch and Leta Megerssa (eds.)

with co-authors
David Buriánek, Kryštof Verner, Karel Martínek, Mihret Yakob,
Jana Janderková, Jiří Šíma, Eva Kryštofová, Yechale Ali, Ezra Tadesse,
Ferdawok Legesse, Genet Assefa, Jan Valenta, Zoltán Pécskay,
Petra Hejtmánková and Zuzana Krejčí

Czech Geological Survey
Geological Survey of Ethiopia
2018

Reviewed by Daniel Nývlt (Masaryk University, Brno, Czech Republic),
Ameha Atnafu Muluneh (Addis Ababa University, Ethiopia)

© Tomáš Hroch, Leta Megerssa, David Buriánek, Kryštof Verner,
Karel Martínek, Mihret Yakob, Jana Janderková, Jiří Šíma, Eva Kryštofová,
Yechale Ali, Ezra Tadesse, Ferdawok Legesse, Genet Assefa, Jan Valenta,
Zoltán Pécskay, Petra Hejtmánková and Zuzana Krejčí

ISBN 978-80-7075-947-9

ACKNOWLEDGEMENT

Field work, compilation of the map and explanatory notes were done by a combined team of geologists from the Czech Geological Survey, the Geological Survey of Ethiopia and AQUATEST Ltd. within the framework of the Czech Official Development Assistance Program supported by the Czech Government through the Czech Development Agency. The SNNP Region President's Office and SNNP Region Mines and Energy Agency are thanked for their cooperative engagement. Our research benefited from the support and facilitation by the management of the Geological Survey of Ethiopia, particularly Mr. Masresha G/Selassie (Director General), Mr. Hundie Melka (Deputy Director), Mrs. Genet Asefa (acting head of the Geo-Hazards Investigation Directorate) and Mrs. Almaz Mengiste (Secretary of Geo-hazards Investigation Directorate). The team is also very grateful to Mr. Mulugeta Simegn, Mr. Mekonen Hailu, Mr. Mulisa Legese and Mr. Getachew Tegene, the drivers from the Geological Survey of Ethiopia. We would like to acknowledge the support of the local people who assisted the team during the field work.

Thorough reviews by Mr. Daniel Nývlt and Mr. Ameha Atnafu Muluneh improved greatly this explanatory notes and are gratefully acknowledged. We would also like to thank our colleague and Vladimír Žáček for helpful discussion.

Hroch T., Megerssa L., Buriánek D., Verner K., Martínek K., Yakob M., Janderková J., Šíma J., Kryštofová E., Ali Y., Tadesse E., Legesse F., Assefa G., Valenta J., Pécskay Z., Hejtmánková P., Krejčí Z. (2018): Explanatory notes to the thematic geoscientific maps of Ethiopia at a scale of 1 : 50,000, Map sheet 0638-A2 Leku. 123 pages, 2 annexes, 4 maps. Czech Geological Survey, Prague; AQUATEST Ltd., Prague; Geological Survey of Ethiopia, Addis Ababa.Addis Ababa

LIST OF ABBREVIATIONS

apfu:	Atoms per formula units
CES:	Code of Ethiopian Standard
CGS:	Czech Geological Survey
CZDA:	Czech Development Agency
DEM:	Digital Elevation Model
EARS:	East African Rift System
EMA:	Ethiopian Mapping Agency
FAO:	Food Aid Organization
FDRE:	Federal Democratic Republic of Ethiopia
GPS:	Global Positioning System
GSE:	Geological Survey of Ethiopia
IUSS:	International Union of Soil Sciences
JICA:	Japan International Cooperation Agency
Ma:	Million years
MER:	Main Ethiopian Rift
MoWIE:	Ministry of Water Resources, Irrigation and Energy
MoWR:	Ministry of Water Resources
NMA:	National Meteorological Agency of Ethiopia
RSG:	Reference Soil Group
RVLB:	Rift Valley Lakes Basin
SNNP Region:	South Nations, Nationalities and People Region of FDRE
TDS:	Total Dissolved Solid
UNDP:	United Nations Development Program
WFB:	World Food Program
WRB:	world Reference Base (for Soil Resources)
WWDSE:	Water Works Design and Supervision Enterprise

CONTENT

SUMMARY **7**
SUMMARY IN AMHARIC **8**

1) INTRODUCTION **12**
1.1 Background 12
1.2 Objectives 13
1.3 Location and accessibility 14
1.4 Methods 14
1.5 Previous studies 19

2) ENVIRONMENTAL SETTING OF THE STUDY AREA **21**
2.1 Topography and Morphology 21
2.2 Hydrometeorological characteristics 22
2.3 Land use and Land cover 23
2.4 Prominent natural features 24

3) REGIONAL GEOLOGICAL SETTING **25**

4) REMOTE SENSING ANALYSIS **28**
4.1 Data and methods 28
4.2 Morphotectonic analysis 30

5) GEOLOGY OF THE LEKU MAP SHEET **32**
5.1 Lithology and Petrology 32
5.2 Geochemistry 37
5.3 K-Ar dating 37
5.4 Structural and tectonic patterns 39

6) SOIL ENVIRONMENT **42**
6.1 Methods and samples 42
6.2 Reference Soil Groups in the study area 43
6.3 Opportunities for and threats to the soils in the studied area 56

7) HYDROGEOLOGY **61**
7.1 Hydrometeorology and hydrology 61
7.2 Hydrogeological surveys 67
7.3 Hydrogeological Classification/Characterization 70
7.4 Elements of Hydrogeological System of the Area Surveyed (Aquifers) 71
7.5 Hydrogeological Conceptual Model 74
7.6 Hydrogeochemistry 75
7.7 Water resources 82

8) ENGINEERING GEOLOGY 85
8.1 Engineering geological characterization of the Leku area 85
8.2 Engineering geological classification 85
8.2.1 Genetic classification of soils in the area 86
8.2.2 Engineering geological rock mass classification 87

9) GEOLOGICAL HAZARDS 90
9.1 Endogenous hazards 92
9.2 Exogenous hazards 93

10) LOCAL PREVENTION AND MITIGATION MEASURES OF GEOLOGICAL HAZARDS 98
10.1 Manageable geomorphic hazards 98
10.2 Preventive and mitigation measures for rehabilitation of natural environment 101
10.3 Suggested hazard monitoring and emergency response systems 102

REFERENCES 103

ANNEXES 113
Annex 1. Geochemical data and subsequent analytical methods 113
Annex 2. Soil Texture and Chemical data 116
Annex 3. Hydrogeological data 117

LIST OF FIGURES

Fig. 1-1. Political subdivision of the studied map sheet... 14
Fig. 1-2. Map of documentation points (location of analyzed samples). 17
Fig. 2-1. Morphology of the Leku area 21
Fig. 3-1. Digital elevation model showing the East African Rift in Ethiopia and location of the studied area. Black rectangle is frame of the 1 : 250 000 scale map Dila, red rectangle for the map 1 : 50 000 Leku. 25
Fig. 4-1. Landsat image of the Leku map sheet. False colour image with the bands 432 displayed as RGB composite (up) is showing vegetation in red colours. Results of the principal component analysis (PCA) displayed as RGB composite of PCA1, PCA3 and PCA2 (down). Vegetation was obscured (black). Different colours represent different lithologies. For discussion see text. 29
Fig. 4-2. Morphotectonic analysis of the Leku map sheet. Morphotectonic linear indicators are displayed on the color digital elevation model (ASTER DEM) combined with a shaded relief map. 31
Fig. 5-1. Contact between greyish-yellow to reddish strongly weathered ignimbrite of the Nazret Formation and Yubo basalt flow cropping out in a quarry SW of the Yirga Alem town (DE201). 34
Fig. 5-2. Yubo basalt with plagioclase and olivine phenocrysts, amygdale filled with calcite is present in the central part of thin section , an outcrop on an escarpment located SE of Derara town (DE013B), XPL. 34
Fig. 5-3. Classification diagrams for Ca–Fe–Mg pyroxenes (a) and feldspars (b) from the Yubo basalt (DE201, DE013B), the Hantate welded ignimbrite (DE026), the Hawasa ignimbrite(s) (DE001) and rhyolite (DE036). 34
Fig. 5-4. Outcrops of Hantate welded ignimbrite are distributed along an escarpment situated SE of Derara town (DE014). 35
Fig. 5-5. Crystal fragments and fiamme in a fine-grained eutaxitic groundmass (Hantate welded ignimbrite, DE026), PPL. 35
Fig. 5-6. Non-welded Hawasa ignimbrite from a quarry situated WNW of the Leku town (DE024). 35
Fig. 5-7. Crystal fragments and fiamme in a fine-grained welded groundmass (slightly welded Hawasa ignimbrite), PPL. 35
Fig. 5-8. Ash fall deposits with a layer of well-sorted pumice lapilli from the outcrop located N of the Moto village (DE189). 36
Fig. 5-9. Accretionary lapilli in ash fall deposits (an outcrop situated N of the Moto village, DE189) PPL. 36
Fig. 5-10. Quarry situated in the southern part of the Boricha Dome (DE036). 36
Fig. 5-11. Alkali feldspar phenocrysts in rhyolite from the Boricha Dome (DE035), XPL... 36
Fig. 5-12. Chemical composition of volcanic rocks: (a) Total alkalis ($Na_2O + K_2O$) vs. SiO_2 (TAS; LeBas et al., 1986); the filled contours in the background portray the frequency of other volcanic rocks in the southern MER (MacDonald and Gibson 1969; Brown and Carmichaeln 1969, 1971; Di Paola 1971, 1972; Bloomer et al. 1989; Hart et al. 1989; Asfaw et al. 1991; Zanettin et al. 1991; WoldeGabriel et al. 1991, 2005; Wolde and Widenfalk 1994; Stewart and Rogers 1996; Ayalew et al. 1999, 2002, 2006; George

and Rogers 1999; Trua et al. 1999; Yemane et al. 1999; Katoh et al. 2000; Rogers et al. 2000; Furman et al. 2004; Haileab et al. 2004; Rooney 2010; Shinjo et al. 2011; Rooney et al. 2012; Wolela 2014; Rapprich et al. 2016); (b) Nb/Y vs. Ti/Zr discrimination diagram (Pearce 1996); (c) chondrite-normalised REE (rare earth element) patterns (values for normalization are based on Boynton 1984), (d) Primitive mantle-normalised multi-element variation diagrams (values for normalization are based on McDonough and Sun (1995). 38
Fig. 5-13. Structural scheme of the Leku map sheet showing regional fault pattern and bedding in volcano-sedimentary rocks (Dino Formation). 40
Fig. 5-14. Orientation diagrams of brittle structures in the Dino Formation (red – rhyolite ignimbrites; black – pyroclastic fall deposits). (a) – normal faults and fault zones with steeply plunging slickensides; (b) – extensional joints and (c) – rose diagram showing trends in extensional joints in all units. Equal projection to the lower hemisphere. 41
Fig. 5-15. Bedding in unwelded pyroclastic fall deposits and minor ash-flows affected by NNE-SSE trending normal fault (west of Chirecha village) 41
Fig. 5-16. Moderately dipping flow-foliation in rhyolite (Boricha Rhyolite Dome; DE035). 41
Fig. 5-17. Orientation diagram of the primary structures in volcano-sedimentary sequences of the Dino Formation: (a) – Bedding planes in rhyolite ignimbrite, and (b) – Bedding planes in welded pyroclastic fall deposits. Equal projection to the lower hemisphere. 41
Fig. 6-1. Chromic Luvisol. 42
Fig. 6-2. Rill erosion on a dirt road in Skeletic Luvisols. 43
Fig. 6-3. Dystric Nitisols (JJ046 left and JJ047 right) 46
Fig. 6-4. Pellic Vertisols. 48
Fig. 6-5. Surface drainage of Vertisols. 50
Fig. 6-6. Vitric Andosol (Thaptomollic) (left) and Mollic Andosol (Thaptovitric) from tuff (right) 52
Fig. 6-7. Chromic Cambisol from tuff deposited on top of a buried soil (left) and Eutric Cambisol from ignimbrite on the caldera rim (right). 54
Fig. 6-8. Eutric Fluvisol(JJ048) 55
Fig. 6-9. Agricultural land on Fluvisols along the shores of the Lake Awasa (Awasa Caldera). 56
Fig. 7-1. Hydrology scheme of Leku area 61
Fig. 7-2. Discharge diagram of the Gidabo River at the Aposto River gauges 63
Fig. 7-3. Annual variability of the mean annual discharge of the Gidabo River and the Aposto River gauges 63
Fig. 7-4. Frequency of the yield of water points from porous aquifers of the Leku sheet 72
Fig. 7-5. Frequency of the yield of water points from fissured aquifers 73
Fig. 7-6. Conceptual hydrogeological model of the western plateau, escarpment and rift floor 75
Fig. 7-7. Piper diagram for the classification of natural waters 77
Fig. 7-8. Decrease in fluoride concentration with depth (Zenaw, 2003) 81
Fig. 8-1. Laboratory physical tests of samples from variably weathered basalt and ignimbrite lithologies in the study area (Leku map sheet) in the

northwestern escarpment. (a) porosity, water absorption and bulk density plots, (b) Point load index strength correct 88
Fig. 9-1. Gully system in the fault scarp, north of Yrba 95
Fig. 9-2. Piping in unconsolidated polygenetic sediments, south of Jara Dado 95
Fig. 9-3. Lateral erosion on a gully located in the lower part of an escarpment near Kube 96
Fig. 9-4. Ground fissure in polygenetic sediments near Jara Dado 96
Fig. 10-1. Beginning of collapse – wavy ground, Jara Dado 99
Fig. 10-2. Collapse of the land – rift direction, Jara Dado 99
Fig. 10-3. Collapse of the land – rift direction, Jara Dado 99
Fig. 10-4. Upper valley – landslides on both sides of gullies, south to Kuwe 100
Fig. 10-5. Beginning of the erosion in the upper part of a scarp, south to Kuwe 100
Fig. 10-6. Middle part of a gully with intensive deep erosion, south to Kuwe 100
Fig. 10-7. Lower part of a gully with lateral erosion, south to Kuwe 100

LIST OF TABLES

Tab. 1-1. Source of data used for base map preparation 15
Tab. 1-2. Summary of inventoried water points in the field....17
Tab. 2-1. Mean monthly precipitation in selected meteorological stations (source: Halcrow, 2008)....22
Tab. 2-2. Mean monthly precipitation at Belela in the period from 2006–2015....22
Tab. 2-3. Precipitation variability....23
Tab. 2-4. Summary of precipitation in sub-basins covering the Leku map sheet 23
Tab. 6-1. Soil particle distribution within the Luvisol profile (JJ041) and some diagnostic criteria....45
Tab. 6-2. Selected chemical characteristics of the sampled Luvisol profile (JJ041)....45
Tab. 6-3. Soil particle distribution within Nitisols profiles and some diagnostic criteria....47
Tab. 6-4. Selected chemical characteristics of the sampled Nitisol profiles....47
Tab. 6-5. Colour and textural characteristics of Vertisols in the mapped area 49
Tab. 6-6. Selected chemical characteristics of Vertisols in the mapped area....49
Tab. 6-7. Colour and textural characteristics of Andosols sampled in the study area 52
Tab. 6-8. Selected chemical characteristics of Andosols in the study area....53
Tab. 6-9. Colour and textural characteristics of the Cambisol profile....53
Tab. 6-10. Selected chemical characteristics of the Cambisol profile....54
Tab. 6-11. Textural characteristics of the Fluvisol profile....55
Tab. 6-12. Selected chemical characteristics of the Fluvisol profile....56
Tab. 7-1. Data at the river gauging stations 62
Tab. 7-2. Hydrological data....62
Tab. 7-3. Baseflow data for the Leku area....64
Tab. 7-4. Basic characteristics of the Lake Awasa 65
Tab. 7-5. Total surface water resources and total water resources (Halcrow, 2008) 66
Tab. 7-6. Impact of climate change on levels of lakes and the area (Halcrow, 2008) 67
Tab. 7-7. Representative aquifer parameters (Halcrow, 2008)....68
Tab. 7-8. Description of individual aquifer units encountered in the basin (JICA, 2012)....69
Tab. 7-9. Parameters determined for aquifers within the Ethiopian Rift by JICA (2012) 69
Tab. 7-10. Basic statistics of the yield of water points from porous aquifers in l/s....72
Tab. 7-11. Basic statistics of the yield of water points from fissured aquifers in l/s 73
Tab. 7-12. Basic statistics of the yield of water points from mixed aquifers in l/s....74
Tab. 7-13. Groundwater chemistry compared to drinking water standards and guidelines....79
Tab. 7-14. Aquifers of the area 82
Tab. 7-15. Assessment of water resources in the Leku area....83
Tab. 8-1. Index physical properties of soils from the Leku Map Sheet (Physical Laboratory test plots) 87

SUMMARY

The Leku map sheet is located within the middle part of the Main Ethiopian Rift System, on the border of its central and southern segment. Geologically, it is comprised of upper Miocene to Pleistocene volcanics. The predominant rocks represent the products of voluminous eruptions and pyroclastic deposits are associated with the Hawasa Caldera formation. Tectonic depressions and grabens located mainly in the northern part of the map sheet are filled by re-sedimented volcanoclastics, alluvial and lacustrine deposits of Pleistocene to Holocene ages.

Soil type classification was compiled based on the geological map, field survey, satellite image interpretation and digital elevation models. Four soil catena units have been identified as reference groups: Cambisols, Nitisols-Acrisols, Regosols-Cambisols, and Fluvisols in respective order from top of the escarpment to the rift floor. The soil classes have been identified based on chemical and physical properties.

Hydrogeological assessment has been made in accordance with the regional morphology, local geological and water points inventory from approximately 190 points in the area. Surface hydrological characteristics and groundwater dynamics have been addressed to develop water resource assessment in the region. The total volume of renewable groundwater resources of active aquifers in the area has been assessed to be 95 million m^3/ year. The quality of water resources available is also investigated showing transitional calcium bicarbonate and basic sodium-bicarbonate hydrochemical composition. Part of the groundwater has a high fluoride content that cause numerous serious public health problems. Distribution of the aquifers along with the hydrochemical compositions are combined in the created hydrogeological map at a scale of 1 : 50,000 of the Leku map sheet in this study.

Engineering geological assessment of the area indicates regions of rock mass ranging in strength classes as moderate (3–4 MPa) and low (the strength has almost been completely undermined). These correspond to the variation in lithological units, which on average show distinctly variable intact strength and variable susceptibility to weathering based on the field documentation and physiographic areal disposition. Genetic associations of soil in the area are also distinguished as volcaniclastic deposits, residual lateritic soil, colluvium and scree slope deposits.

Exogenous and endogenous hazards in the area have been defined based on existing studies and field documentation. In the case of endogenous hazards, seismicity has been found to be more critical as it has a higher probability of occurrence in addition to low preparedness and insufficient legislation to enforce precautionary measures, such as conservative design codes and emergency response systems as well as early warning systems. On the other hand, extensive exogenous processes posing danger to everyday life are extensively documented. Due to the morphological setup of the area, both erosion and suffusion-related hydrological hazards appear to be predominant, affecting farmlands as well as infrastructure. All the potential risk areas suffering from such exogenous hazards are shown in the hazard map.

SUMMARY IN AMHARIC

የለኩ ማፕ (0638-A2) 1 : 50,000 መስፈርት ሥነ-ምድር ካርታ አጭር መግለጫ

መግቢያ (Introduction)

ይህ ጥናት እና አባሪ 1፡50,000 መስፈርት ካርታዎች በቼክ ሪፑብሊክ የልማት ትብብር ኤጀንሲ (CZDA) እና በኢትዮጵያ ፌዴራላዊ ዲሞክራሲያዊ ሪፐብሊክ (ኢ.ፌ.ዲ.ሪ.) መካከል በተፈፀመ የመግባቢያ ሠነድ ማዕቀፍ ፤ በደቡብ ብሔር ብሔረሰቦች እና ህዝቦች ክልል በተመረጡ አካባቢዎች ዝርዝር የሥነ-ምድር ካርታ እና የተፈጥሮ አደጋ ተጋላጭነት እንዲሁም የከርሰ ምድር ውሃ ሃብት አለኝታ ግምገማ ላይ የሚያተኩር ነው፡፡ በዚህም መሰረት ጥናቱ በቼክ ሪፑብሊክ ጂኦሎጂካል ሠርቬይ (CGS) እና በኢትዮጵያ ጂኦሎጂካል ሠርቬይ (GSE) በጋራ ከ2007 ዓ.ም. ጀምሮ እስከ 2010 ዓ.ም. የተካሄደ ሲሆን ፤ በጥናቱ የተዳሰሱት አካባቢዎች በሲዳማ ዞን ሁለት ስፍራዎች ማለትም በለኩ እና በመጆ (በአቅራቢያው በሚገኙ አዋሳኝ የኦሮሚያ ክልል የቦረና ዞን ሰሜናዊ) አካባቢን ጨምሮ) ፤ በጌዲኦ ዞን በዲላ አካባቢ (በአቅራቢያው በሚገኙ አዋሰኝ የኦሮሚያ ክልል የጉጂ ዞን ሰሜናዊ አካባቢን ጨምሮ) ፤ እና በጋሞ ጎፋ ዞን የአርባ ምንጭ አካባቢን ያካተተ ነው፡፡

ጥናቱ በአራት የሥነ-ምድር ጥናት ዘርፎች ላይ በማትኮር የተካሄደ ሲሆን አነዚህም የመሰረታዊ ዝርዝር የጂኦሎጂ (የሥነ-ምድር) ካርታ ዝግጅት በ1፡50.000 መስፈርት ፤ የአፈር ሽፋን ካርታ ዝግጅት በ1፡50.000 መስፈርት ፤ የኃይድሮጂኦሎጂ (የከርሰ-ምድር ውሃ አለኝታ) ካርታ ዝግጅት በ1፡50.000 መስፈርት እና የጂኦሃዛር (የሥነ-ምድር አደጋ ክስተት አመላካች) ካርታ ዝግጅት በ1፡ 50.000 መስፈርት ናቸው፡፡ እነዚህን ተዛማጅ ጥናቶች ለማከናወን በመስክ የአፈር፤የአለት፤ የውሃ እንዲሁም ዝርዝር ቅኝትና የመስክ ላይ ልዩ ልዩ ሣይንሳዊ ልኬቶች የተደረጉ ሲሆን፤ እነዚህ መረጃዎች በሳተላይት ፎቶ እና የገጸ-ምድር ዲጂታል ሞዴል በዘመናዊ ጂኦግራፊያዊ መረጃ አያያዝ (GIS) ታግዞ በማቀነባበር ካርታዎቹ ተዘጋጅተዋል፡፡

የዚህ ጥናት መሰረተ ሃሳብ በገፀ-መሬት እና በከርሰ-ምድር አፈጣጠር መካከል ያለውን ትስስር በሣይንሳዊ ትንታኔ በመታገዝ ለሰው ልጆች ጥቅም የሚሰጡ ጠጣርና ፈሳሽ የማዕድን ሃብት ፤ እንዲሁም ለተፈጥሮ አደጋ ተጋላጭነትና ለአካባቢ ጥበቃ ወሳኝ የሆኑ መረጃዎች ማመንጨት ነው፡፡ ባጠቃላይ የተጠኑት ስፍራዎች የመሬት አወቃቀር ከእሳተ ጎሞራ (volcanic rocks) ጋር በተያያዘ የተፈጠሩ አለቶችና በከፍተኛ ሙቀትና ጭነት የተቀየሩ ልውጥ አለቶች (metamorphic rocks) የተመሰረተ ሲሆን ከአለቶቹ በላይ ሰፍረው የሚገኙት የቅርብ ጊዜ በደለል እና በናዳ የተከማቹ እንዲሁም ከበሰበሱ አለቶች የተፈጠሩ የበሃ የአፈር አይነቶች በሁሉም የተጠኑ ስፈራዎች ተዋቅረው የሚገኙባቸው ናቸው፡፡

ለኩ ማፕ (Leku map)

የሥነ-ምድር ይዘት (Geology)

በለኩ አካባቢ የተደረገው ጥናት 6° 45’ እና 7° 00’ ሰሜን ኬክሮስ እና 38° 15’ እና 38° 30’ ምስራቅ ኬንትሮስ (ለኩ ማፕ ሺት) ወሰን ውስጥ የሚገኝና የታላቁን የኢትዮጵ የስምጥ ሸለቆ መካከላዊ ስፍራን የያዘ ነው፡፡ በዚህ ስፍራ የሚገኘው ከርሰ-ምድር ይዘት ባጠቃላይ በእሳተ ጎሞራ አማካኝነት በተፈጠሩ አለቶች የተዋቀረ ሲሆን እነዚህም በአብዛኛው አሲዳዊ ይዘት ያላቸውና ከሃዋሳ እና ኮርቤቲ የእሳተ ጎሞራ ገደል በፍንጥርጣሪ ክምችትና ቀደምት የእሳተ ጎሞራ ክስተቶች የተፈጠሩ አለቶች ናቸው፡፡ አሲዳማ ይዘት ያላቸው አለቶች አፈጣጠራቸው ሁለት ሲሆን እነዚህም በእሳተ ጎሞራ ፍንዳታ ፍንጥርጣሪ የሚፈጠሩና በእሳተ ጎሞራ ቀልጦ ከፈሰሰ አለት የሚፈጠሩ ናቸው፡፡ በለኩ ማፕ ሺት ዉስጥ የሚገኙት የአፈር ሽፋን እና የአለት መዋቅር ከግንባታ ፤ ልማት እና ተፈጥሮ አደጋ ተጋላጭነት አንፃር የተቃኙ ሲሆን በአለቶቹ ባህርያት ከተካሄዱት የመስክ እና

የናሙና ውሱን ነጥብ ጭነት አለካክ መሰረት መካከለኛ (3–4 MPa) እና ዝቅተኛ (ከ 3 MPa በታች) ጥንካሬ ያላቸው ናቸው። በለኩ ማፕ ሺት ያሉ የአለትና የአፈር ሽፋኖች ተለይተው በካርታ የሰፈሩ ሲሆን እነዚህም በአፈጣጠራቸው እድሜ ቅደም ተከተል ፤ ከቀዳሚው ወደ ቀራቢው እንደሚከተለው ተዘርዝረዋል። የነዚህ አለቶች እና አፈር ስርጭት በተያያዘው አባሪ ካርታ ላይ የሰፈሩ ሲሆን በእንግሊዝኛ ቋንቋ ተገልፀው ይገኛሉ።የተዘረዘሩትን የስነ-ምድር አለቶችና ሽፋን በካርታው ላይ ለመለየት እንዲረዳ ከዝርዝሮቹ ፊት በቅንፍ የተመለከቱትን ቁጥሮች በማየት ከካርታው ላይ ማንበብ ይቻላል።

ከ23 እስከ 5 ሚሊዮን አመት በፊት ባለው ዘመን የተፈጠሩ የእሳተ ጎሞራ ውጤት አለቶች

(11) የእሳተ ጎሞራ ፍንጥቅጣቂ ጥብቅ እና ልል አለቶች ስብስብ ወይም በእንግሊዚኛው አጠራር Welded and non-welded ignimbrites and tuffs.

ከ2 ሚሊዮን ዓመት ገደማ ወዲህ የተፈጠሩ የእሳተ ጎሞራ ውጤት አለቶች

(10) የሃንታቱ የእሳተ ጎሞራ ፍንጥቅጣቂ ጥብቅ አለቶች ወይም በእንግሊዝኛው አጠራር Hantate welded ignimbrite.

(09) የዩብዶ ጥቁር ድንጋይ (ብረት ነክ ንጥረ ነገር አዘል አለት) ወይም በእንግሊዝኛው አጠራር Yubo basalt.

(08) የቦሪቻ አሲዳማ የእሳተ ጎሞራ ቅልጥ አለቶች ወይም በእንግሊዝኛው አጠራ Boricha Rhyolites.

(07) የሐዋሳ የእሳተ ጎሞራ ፍንጥቅጣቂ (ትፌ) ልል አለቶች ወይም በእንግሊዝኛው አጠራር Hawasa tuffs with minor ignimbrites.

(06) የሐዋሳ የእሳተ ጎሞራ ፍንጥቅጣቂ (ትፌ) ጥብቅ አለቶች ወይም በእንግሊዝኛው አጠራር Hawasa ignimbrites with subordinate tuffs.

(05) በናዳ የተከማቹ የአፈርና ስብርባሪ አለት ክምችት ወይም በእንግሊዝኛው አጠራር Colluvial sediments.

(04) በገፀ-ምድር ተንጉዘው የተከማቹ የእሳተ ጎሞራ ፍንጥቅጣቂ ክምችት ወይም በእንግሊዝኛው አጠራር Polygenetic sediments.

(03) የሐይቅ ዝቃጭ አፈር ክምችት ወይም በእንግሊዝኛው አጠራር Lacustrine sediments.

(02) የደለል አፈር ክምችት ወይም በእንግሊዝኛው አጠራር Alluvial sediments.

(01) የወንዝ ደለል (አሸዋ) ወይም በእንግሊዝኛው አጠራር Fluvial sediments.

በስፍራው በስፋት ተሰራጭቶ የሚገኘው የስነ-ምድር መዋቅር ከሰሜን-ምስራቅ ወደ ደቡብ-ምእራብ የተሰደሩ ሲሆን ዘግይተው በተፈጠሩ ከሰሜን ወደ ደቡብ የተሰደሩ የመሬት መዋቅሮች ተቆራርጠው ይገኛሉ።

ገፀ-ምድር (Geomorphology)

የለኩ አካባቢ ማፕ ሺት የገፀ-ምድር አቀማመጥ ሙሉ በሙሉ በታላቁ የኢትዮጵ ስምጥ ሸለቆና ተዛማጅ የእሳተ ጎሞራ ተዕእኖ ያረፈበት ሲሆን ምሥራቃዊው ክፍል በከፊል የምእራባዊ የኢትዮጵያ ክፍተኛ ስፍራ አምባ ግርጌ የተፈጠረ መልከአ ምድር ያለው ነው። በተቀረው የለኩ ማፕ ሺት (መካከለኛውና ምዕራባዊው ክፍል) የሚታየው መልካ-ምድር ከሰሜን ወደ ደቡብና ከሰሜናዊ ምስራቅ ወደ ደቡባዊ ምእራብ በተሰደሩ የመሬት መዋቅር (ስንጥቅ) የተከፋፈለ ሲሆን በነዚህ የመሬት መዋቅሮች አፈጣጠር የተነሳ በተፈጠሩ የመሬት ስርጉዶች (ውስጣዊ ስምጥ ሸለቆዎች) በቅርብ ዘመናት (ከ2 ሚሊዮን አስከ መቶ ሺህ አመታት በፊት) ተንጉዘው በተከማቹባቸው የደለልና የእሳተ ጎሞራ ፍንጥርጣሪ ውጤቶች ሙሊት የተዋቀረ መልካ-ምድር ነው። ስፍራውን የሚያዳርሰው የውሃ

ተፋሰስ የኢትዮጵያ ስምጥ ሸለቆ ሐይቆች ተፋሰስ ሲሆን ይህም በስተደቡብ ምእራብ የሚገኘው የጊዳቦ ወንዝ ንዑስ ተፋሰስ አካል ነው።

የአፈር ሁኔታ (Pedology)
በለኩ ማፕ ሺት ውስጥ በአፈር ሳይንስ መርሆ የተለዩት የአፈር አይነቶች ዋና ዋና ባህሪያት የሚከተሉት ሲሆኑ በዚህ ሪፖርት ያለውን አጭር መግለጫ ከተዘጋጀው አባሪ የአፈር ስርጭት አመልካች ካርታ ጋር ለማናበብ ስማቸው በእንግሊዝኛ ቋንቋ ጭምር ተገልጧል። በአጠቃላይ ከተወሰዱት ናሙናዎች አብዛኛዎቹ ከፍተኛ አሲዳማነት የሚያጠቃቸው ፤ መካከለኛ **"Cation Exchange Capacity"** (ጠቃሚ ንጥረ ነገሮችን አምቆ በመያዝ በውሃ መሸርሸርን የመቋቋም ባህሪ) ፤ ዝቅተኛ የአፈር ውስጥ ብስባሽ ፤ ዝቅተኛ የናይትሮጂን ይዘት ፤ መካከለኛ የካልሲየም ይዘት ፤ ዝቅተኛ የማግኒዝይም ይዘት እና በጣም ዝቅተኛ የፎሰፎረስ ይዘቶች ያሳያሉ።

አንዶሶል (Andosols) – በንጥረ ነገር የበለፀጉና ለማረስ አመቺ የሆነ ባህሪያ ያላቸው የአፈር አይነቶች ናቸው። በተጨማሪም ለበርካታ የተክል አይነቶች ተስማሚነት ያላቸው የአፈር አይነት ሲሆኑ፤ ነገር ግን ፎስፎረስን አምቆ በመያዝ ለእፅዋት እንዳይደርስ የሚያደርጉ የብረት ንጥረ ነገር በውስጣቸው በመያዛቸው ከፍተኛ የሆነ የማዳበሪያ ግብአት የሚፈልጉ ናቸው። በተጨማሪም በተዳፋት ስፍራ ላይ በሚፈጠሩበት ጊዜ ለአደገኛ ሸርሻሮ ስለሚጋለጡ በሰብል ወይም ልዩ ልዩ ዛፎች ሽፋን የሚፈልጉ ናቸው።

ካምቢሶል (Cambisols) ፡ ለእርሻ ተስማሚ የሆኑ የአፈር አይነቶች ሲሆኑ በአብዛኛው ለእፅዋት አስፈላጊ ንጥረ ነገር አሟልተው የያዙ ናቸው። ነገር ግን ለረጅም ጊዜ የውሃ እጥበት ሲጋለጡ የንጥረ ነገር ይዘታቸውን የሚያጡ በመሆኑ ለሸርሻሮና እጥበት እንዳይጋለጡ በተለይም በዝናባማ ወቅት በተክሎችና ዛፎች ሽፋን የሚሹ ናቸው። በተጨማሪም የናይትሮጅን ንጥረ-ነገር ታክሎባቸውና የተፈጥሮ ፍግ በመጠቀም እንዲሁም ተዳፋት መሬቶችን ባለማረስ ምርታማነታቸውን ለማስጠበቅ የሚቻል የአፈር አይነት ናቸው።

ፍሉቪሶል (Fluvisols) ፡ ታዳሽ የሆነ የንጥረ-ነገር አቅርቦት የሚያገኙ የአፈር አይነቶች ሲሆኑ እርጥበት በሚበዛባቸው ወይም በወንዞችና ውሃ አካላት አቅራቢያ በስፋት የሚገኙ ሲሆኑ ለአሲዳማነት የመጋለጥ እድል የሚስተዋልባቸው የአፈር አይነቶች ናቸው። በመሆኑም በአቅራቢያቸው ባሉ የውሃ አካላት እንዳይጥለቀለቁ ጥንቃቄ የሚሹ የአፈር አይነቶች ናቸው።

ሌፕቶሶል (Leptosols) ፡ በአብዛኛው ለግንባታ መሠረት አመቺ የሆኑ የአፈር አይነቶች ሲሆኑ ባጠቃላይ አነስተኛ የንጥረ-ነገር ይዘት ያላቸውና ውሃ ወይም እርጥበት የማዘል አቅማቸው ዝቅተኛ በመሆኑ ለእርሻ ምርት የማይፈለጉ የአፈር አይነት ናቸው።

ሉቪሶል (Luvisols) ፡ ለእርሻ ተስማሚ የሆኑ የአፈር አይነቶች ሲሆኑ የተሸለ የአየር እንቅስቃሴ በውስጣቸው የሚያስተናግዱና በአብዛኛው በንጥረ-ነገር ይዘት የዳበሩ ናቸው። በሌላ መልኩ ባላቸው የእርሻ ተስማሚነት ባህሪ ምክንያት ለረጅም ዘመናት ለእርሻ ተመረጭ በመሆናቸው በአብዛኛው አካባቢ የላይኛው የአፈር ክፍላቸው በመጥፋቱ የብስባሽ እና የናይትሮጂን እጥረት ያጠቃቸዋል። በተጨማሪም በተዳፋት መሬት ላይ ለከፋ ሸርሻሮ የተጋለጡ የአፈር አይነት ናቸው።

ኒቲሶል (Nitisols) ፡ ለልዩ ልዩ የሰብል ምርቶች ተስማሚ የሆኑ የአፈር አይነቶች ሲሆኑ በተለይም ለቡና ተክል ተመራጭ የአፈር አይነት ናቸው። ሆኖም በውስጣቸው ባለው የብረት ንጥረ ነገር ይዘት ባህሪ የተነሳ ፎስፌት የተባለዉን ጠቃሚ ንጥረ ነገር ለሰብል እንዳይውል አምቀው የመያዝ ባህሪ ያላቸው በመሆኑ በየአመቱ በፎስፌት የበለጸገ የማዳበሪያ ግብአት የሚፈልጉ ናቸው።

በተጨማሪም በአሉሚኒየም ንጥረ-ነገር መብዛት በሚከሰት የተክሎች መርዛማነት ተጽእኖ ለመቀነስ የኖራ ግብአት የሚስፈልጋቸው የአፈር አይነት ናቸው።

ቨርቲሶል (Vertisols) ፡ እነዚህ የአፈር አይነቶች በተለምዶው ጥቁር መረፌ አፈር ተብለው የሚታወቁ ሲሆን አስፈላጊው ጥንቃቄ ከተደረገላቸው ለእርሻ ምርት ከፍተኛ ተስማሚነት ያላቸው ናቸው። በተለይም ውሃ አቁሮ የመያዝ ባህሪ ስላላቸው በተለይም ለጤፍ ሰብል ተመራጭ ናቸው። ሆኖም ባላቸው ክፍተኛ የማጣበቅ ባህሪ ለእርሻ ስራ አዳጋች ከመሆናቸው በተጨማሪ እንደ ውሃ ይዘታቸው ሁኔታ ከፍተጫ የሆነ የመጠን መቀያየር ስለሚያሳዩ ለግንባታ መሰረትነት አደገኛ የአፈር አይነቶች ናቸው። በመሆኑም ለተሻለ አጠቃቀም የውሃ ይዘታቸውን የመቆጣጠር ቅድመ ሁኔታ የሚፈልጉ ናቸው።

የከርሰ-ምድር ውሃ (Groundwater)

የከርሰ-ምድር ውሃ አለኝታ ከተለዩባቸው የውሃ አዘል አካላት (aquifers) የመጀመሪውና በቀላሉ ጥቅም ላይ ሊውል የሚችለው ባልተጠቀጠቁ የአለትና የአፈር ውስጣዊ ክፍተቶች ሰርጎ የሚገኝ ውሃ ሲሆን በቀላሉ በሰው ኃይል ቁፋሮ ሊደረስባቸው የሚችሉ አለኝታዎች ናቸው። በሌላ መልኩ በጠጣር አለቶች ስንጥቅ እና አለቶች ውስጥ ባሉ ክፍተቶች የተጠራቀሙ የከርሰ-ምድር ውሃ ይዘቶች በሰፊው የሚገኙ ሲሆን በማሽን እገዛ በሚቆፈሩ ጥልቅ ጉድጓዶች (100 ሜትር ወይም በላይ) ውስጥ ፓምፖች በመግጠም ውሃውን ማውጣት የሚቻል አለኝታ ሲሆን ከፍተኛ ወጪ የሚጠይቁ ናቸው። ባጠቃላይ በአመት 95 ሚሊዮን ሜ. ኪዩብ የውሃ ሃብት ለመጠቀም የሚያስችል የከርሰ ምድር ውሃ ሃብት ሊገኝ እንደሚችል ተደረገው ጥናት አመላክቷል። በከርሰ-ምድር ውሃ ካርታ ላይ የሰፈሩ ዝርዝር የውሃ አለኝታ ቋቶች፡-

- ባልተጠቀጠቁ የአለት እና የአፈር ውስጥ ክፍተቶች በመካከለኛ መጠን ነገር ግን በስፋት ስርገው የሚገኙ (Extensive and moderately productive or locally developed and highly productive porous aquifers).
- በጠጣር አለቶች ስንጥቅ መካከል በመካከለኛ መጠን ነገር ግን በስፋት ስርገው የሚገኙ (Extensive and moderately productive fissured aquifer).
- በጠጣር አለቶች ስንጥቅ እና ባልተጠቀጠቁ የአለት ውስጥና የአፈር ውስጥ ክፍተቶች በመካከለኛ መጠን ነገር ግን በስፋት ስርገው የሚገኙ (Extensive and moderately or locally developed and highly productive mixed porous and fissured aquifers).

በአካቢው የሚገኙት የከርሰ-ምድር ውሃ ንጥረ-ነገር ይዘት ከተወሰዱት ናሙናዎች እንደታየው በከፍተኛ ቦታዎች በአብዛኛው ካልሲየም ባይካርቦኔት እና በዝቀተኛው የስምጥ ሸለቆ አካባቢ ሶድየም ባይካርቦኔት የከርሰ-ምድር ውሃ ይዘት አላቸው። በተጨማሪም ከአሳተ ጎሞራው አለት ተፅእኖ የተነሳ ከፍተኛ የፍሎራይድ መጠን በከርሰ-ምድሩ ውሃ ውስጥ የሚገኝ ሲሆን ይህም ውሃው ሳይታከም በቀጥታ ለመጠጥ እንዳይውሉ ያደርጋቸዋል።

የተፈጥሮ አደጋ (Geohazards)

የለኩ ካርታ ከተፈጥሮ አደጋ ተጋላጭነት አንፃር ገፀ-ምድራዊ (ውጪያዊ) እና ከርሰ-ምድራዊ (ውስጣዊ) ክስተቶች ጋር ተያይዞ የተገለፀ ሲሆን፤ በውጪያዊ የመሬት ላይ የተፈጥሮ ኡደት የሚፈጠሩ የተፈጥሮ አደጋ ስጋቶች በካርታ ላይ ሰፍረዋል። ከነዚህ የተፈጥሮ አደጋዎች በተለይም የርእደ-መሬት አደጋ እና የእሳተ-ጎሞራ ከርሰ-ምድራዊ ክስተት (ውስጣዊ) በስፍራው አሳሳቢ እና ዝግጁነት የሚያስፈልገው ሲሆን ከውጫዊ የተፈጥሮ አደጋዎች መካከል የእርሻ መሬትን እና መሰረተ ልማት ላይ አደጋ ሊያደርሱ የሚችሉ የጎርፍና ደለል ሙላት ችግሮች (aggradation, Suffusion) እንዲሁም የመሬት መሰንጠቅ (Ground fissure) በለኩ ማፕ በልዩ ልዩ ስፍራዎች በካርታው ሰፍረዋል (Geo-hazard map):: በተጨማሪም ለሚደርሱ ድንገተኛ የተፈጥሮ አደጋዎች ምላሽ እና ዝግጁነት አመላካች ትንተና በዝርዝር በሪፖርቱ ተካቷል።

1) INTRODUCTION

1.1 Background

A cooperation project on geological and applied mapping of selected areas in the South Nations, Nationalities and People's Region (SNNPR) were conducted in order to identify and assess the geo-hazards and vulnerability of the areas concerned. The project was implemented within the framework of the Memorandum of Understanding concluded between the Czech Development Agency (CZDA) and the Federal Democratic Republic of Ethiopia (FDRE) for cooperation on priority issues.

Four areas were studied within the project: Arba Minch, Leku, Dilla and Mejo. A part of the project was financially supported by the Czech Development Agency (CZDA) through the partner organization of the Czech Geological Survey (CGS) in response to the request of the Ethiopian counterpart, the Geological Survey of Ethiopia (GSE). In addition to the project outputs related to the areas investigated, training and strengthening of skills of the GSE staff and formulation of a representative methodology that can be used in other areas exposed to geo-hazards were all implemented.

The major objective of the project was to assess the vulnerability of the local population, farmlands and the natural environment to geo-hazard phenomena. The current sharp increase in population and settlements and demands for farmland have merged with adverse competition in search for or the existence of available natural resources, such as land for farming, groundwater, pastures, settlement areas and the likes resulting in increasing conflicts of interest. The extensive deforestation and endangering of indigenous vegetation due to the expansion of settlements and farmlands into outlying and empty areas is an example of such phenomena. Hence, the extension of agricultural land into often unsuitable areas is becoming a common practice increasing the risk of susceptibility to various forms of geo-hazards. Without reasonable land management, it is inevitable that the land expansion will soon result in accelerated erosion, formation of deep erosion furrows, and the overall degradation of farmland leading to falling long-term viability and productivity. These processes can lead to the formation of the so-called "bad lands", which are areas with no soil cover, without vegetation and with a high density of erosion furrows, which subsequently become unsuitable to keep the population in place if the area is not treated and managed appropriately. Some studies have shown losses of up to 42 tons of soil per ha of farmland each year, and the productivity of agricultural production going down by 2.2 % per year. Losses in agricultural production due to erosion have been estimated at ca. 600 million ETB (Ethiopian Birr) per year, which represent a significant economic loss for the country.

On the other hand, due to the setting of the natural environment where the great East African Rift Valley passes through the study area, serious threats are being noticed due to the creation of ground fissures and subsidence, leading to a substantial loss of property and land as well as being a potential threat to the safety of inhabitants.

Comprehensive research and investigation of geology and lithology, including the analysis of possible geological hazards in the tectonically active areas are hence

crucial for effective management and planning of development activities for sustainable agro-practice, improved quality and long-term protection of agricultural lands. The study also aids in directing and constraining the search for water resources and in the end leads to saving considerable financial costs associated with the remediation of negative phenomena arising from adverse geological processes. In connection with the current need for an analysis of possible geological hazards in vulnerable areas of southern Ethiopia, the GSE turned to the Czech Republic for assistance in improving its professionals capacity in the field of geological mapping, geological hazards risk assessment and hydrogeological investigation at a detailed scale (1 : 50,000).

Such level of information is envisaged to be practical enough to be implemented and therefore allowing a sufficient assessment of geological hazards risk and hydrogeological characterization in areas of strategic importance (e.g. current agglomerations, areas with rapidly growing population, areas susceptible to negative impacts of climate change, and areas with possible recent tectonic and seismic activity).

The GSE has chosen four areas exhibiting potential geological hazards to be defined, and to be comprehensively prioritized in terms of vulnerability to geo-hazards risk, and suitability for agriculture from a geological point of view. These areas also exhibit variability in geological structure and lithology, and consequently the variability in potential geological hazards. On the basis of findings and practices of study in the selected areas, GSE aims to develop practical methodologies in the form of a manual that will be crucial for subsequent similar tasks elsewhere in the country.

The Leku map sheet (0638-A2) is a part of Sidama Zone in the area with an extreme risk of sinks (fractures) in the context of recent tectonic activity and erosion of weathered products. This area is sensitive to recent climate change,as the geological structure consists of volcaniclastic sequences and unconsolidated sedimentary rocks.

The objectives of the study are to produce a set of geological and thematic geoscientific maps with explanatory notes for selected areas that are susceptible to geo-hazards. This includes large-scale geological maps at a scale of 1 : 50,000 showing the lithological, geochemical and structural characteristics of the area, then hydrogeological maps and geo-hazards risk maps, including maps indicating soil vulnerability. The maps and explanatory notes are also intended to be understood and informative for local authorities and even wider public, and can be used in land-use and development planning.

1.2 Objective

The objectives of the study are to produce a set of geological and thematic geoscientific maps with explanatory notes for the selected areas that are susceptible to various forms of geo-hazards. These include large-scale geological mapping at a scale of 1 : 50,000 showing the lithological, geochemical and structural characteristics of the area together with the hydrogeological map, geo-hazards risk map and soil types map of the area. The maps and explanatory notes are intended to be easily understood and be informative enough for local authorities and development officers. It is anticipated that the maps will aid the effort for natural resources management and planning of land-use practise and local development strategies.

1.3 Location and accessibility

The Leku map sheet and its surroundings are located in southern Ethiopia (Fig 1-1), defined by the geographic coordinates 6° 45' and 7° 00' N (northern latitude) and 38° 15' and 38° 30' E (eastern longitude). It is situated in the Main Ethiopian Rift Valley at the foot of the western Ethiopian volcanic plateau.

The area is accessible by a road from Addis Ababa to Dila either via – Butajira – Ziway – Awassa – Leku or Mojo – Ziway – Awassa – Leku. In general, the region is relatively poorly accessible due to fairly few dry weather roads, especially in the eastern part. The undulating landscape also makes the area difficult to be accessed, and the roads are occasionally affected by erosion, particularly during the rainy season.

1.4 Methods

The investigation was carried out in close cooperation of geologists and other specialists from CGS and those from GSE. The project began with reviewing and interpretation of published and archived data available from various sources. This includes the existing hydrometeorological data (precipitation, water discharge, etc.) from the Ethiopian National Meteorological Agency (NMA), topographic maps from the Ethiopian Mapping Authority (EMA), and a digital elevation model of the terrain from Global land cover data, optical Satellite imagery (Landsat 8) and ASTER imagery. These data

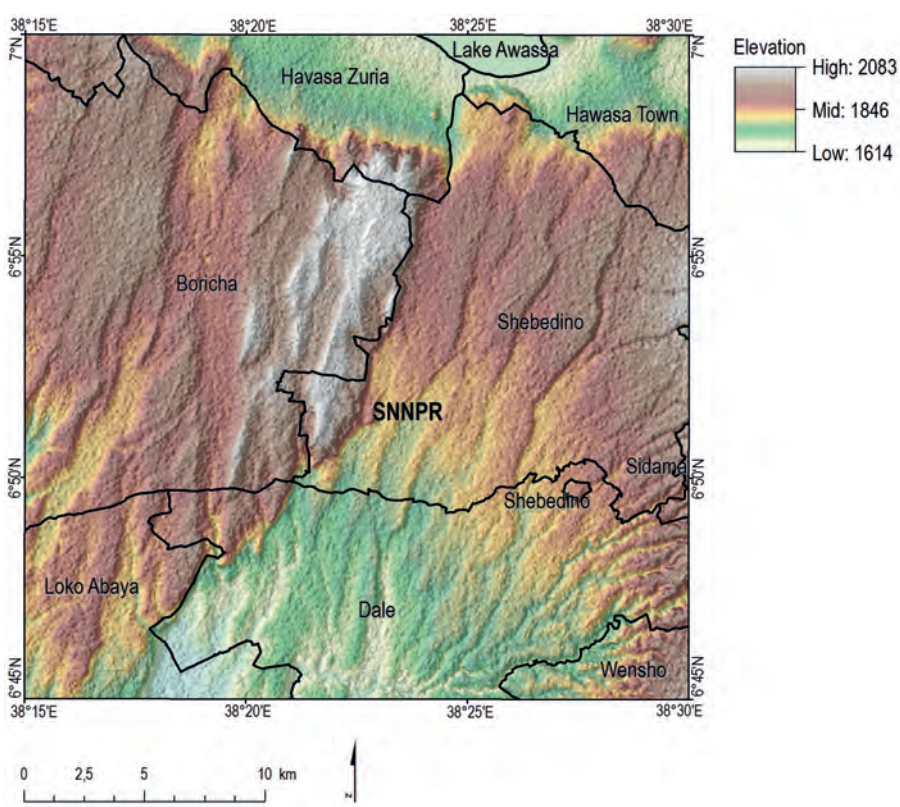

Figure 1-1. *Political subdivision of the studied map sheet.*

are summarized in Table 1-1. Other references to previously conducted studies and relevant reports and published articles were used as well. Base maps for the field survey were compiled by a combination of the topographic maps, digital elevation models and satellite images.

Table 1-1. Source of data used for base map preparation

Dataset	Source	Resolution
Land use and land cover	FAO (1984)	1 : 2 Million scale
Soil map	FAO (1984)	1 : 2 Million scale
Dem	USGS	30 m
Landsat images	USGS	28 m
ASTER	NASA	30 m
Topographic maps	EMA	1 : 50,000 scale

The approach adopted was to produce a set of geological and specialized maps of the investigated area. The set included hydrogeological, neotectonic, geochemical, geomorphological and soil maps compiled by respective specialists during the project implementation. These were intended to analyse and select the areas susceptible to geo-hazards risk.

For the unification and coherence in the collection of field data by multidisciplinary experts and different time periods, a unified methodology based on CGS experience and previous mapping work conducted on a regional scale in Ethiopia was established. An appropriate documentation and characterization of geological, hydrogeological and geo-hazards risk phenomena were all made in the field. Representative rock, soil and water samples were collected. Laboratory investigations and analyses of collected samples aimed to classify local lithology and to describe and establish geotechnical, geochemical and hydrochemical characteristics of the surveyed areas. These were used as a basis for geological interpretation of potential geo-hazards risks. Laboratory studies and analyses of collected samples were carried out by various organizations and institutes. Physical properties were determined in Ethiopia at the GSE Central Laboratory; geochemical analyses were carried out at Acme Labs in Canada, soil chemistry and the microanalysis of polished sections were carried out at CGS Laboratories in Prague, and K-Ar dating was conducted at ATOMKI , Institute for Nuclear Research Laboratory, Debrecen (Hungary). Moreover, the documentation and interpretation of historical and active geo-hazards phenomena were also executed.

The following text provides an overview of the topics that were used to compile the final results based on the integration analysis of the layers of geoscientific data in order to draw attention to the major geohazards risks and vulnerability of the study area to natural dangers. The field documentation is shown in Fig. 1-2.

Satellite data analysis

The interpretation of remote sensing data (Landsat Images) was used to identify and delineate the extent of tectonic patterns and lines and to establish lithological boundaries

followed by field reconnaissance and by a detailed survey later. The delineation of geomorphic features was also done using remote sensing data; aerial photographs and their analysis were combined with digital terrain models.

Geological mapping

The field work was carried out in order to compile a geological map of the area concerned, which at the same time serves as the basis for subsequent investigations. Therefore, sampling and field observations as well as the identification and brief characterization of geological units were undertaken in early stages of the project implementation. Tectonic pattern interpreted from the satellite images was compared and confronted with field observations, including the measurements of strike and inclination of geological units.

Geomorphological mapping

Geomorphological mapping appears to be one of the most effective tools or techniques to identify geo-hazards in the field. It was focused on the identification and recognition of fresh and recent characteristic landforms susceptible to geo-hazards and to assess the level of a potential risk. It also helps to trace neotectonic phenomena.

Soil mapping

Examination and mapping of major soil types and their parameters were done by the combination of selective field sampling and fusion of the geological map with land cover map, where the obtained data were subsequently compared to and confronted with the existing soil database of the country, which provides only regional distribution. Hence, in most cases, improvements in the available database have been made in terms of quality and detail. Soil sampling and site evaluation were performed by a CGS expert, where the local GSE geologists working alongside were given the opportunity to learn the methodology in the field. Representative soil samples collected in the field were analysed in the Czech Republic.

Hydrogeological Investigation

The potential role which the groundwater may play in the occurrence or formation of geo-hazards was assessed by hydrogeological research of lithological units, interpretation of tectonic pattern and analyses of the samples collected from existing water points. Local lithology, geological structure and tectonics were studied in order to find out the extent to which these phenomena may affect the quality of groundwater, and if a reasonable water management can also be established in selected areas. The hydrogeological study of the Leku area is based on the evaluation of data obtained from existing reports and maps and also from observations in the field. No previous hydrogeological mapping or investigation at a scale of 1: 50,000 were done, and the complete datasets needed for geometric configuration or distributions of an aquifer are scarce or missing. Nevertheless, the Dila map sheet at a scale of 1: 250,000 compiled by Agezew et al. (2014) provide an access to some scarce information. During the field operations, a total of 105 water points were identified and thoroughly documented, and 36 water samples were collected (see Table 1-3).

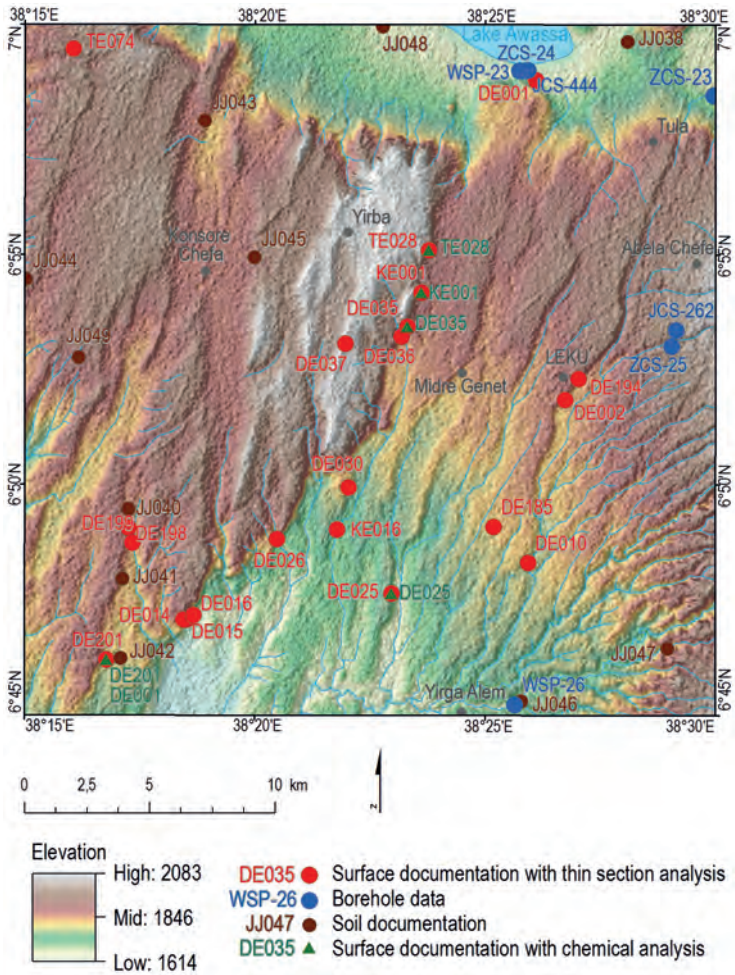

Figure 1-2. *Map of documentation points (location of analyzed samples).*

Table 1-2. Summary of inventoried water points in the field.

Water point type	Recorded water points	Sampled
Borehole (BH)	80	22
Dug well (DW)	1	9 (Zenaw, 2003)
Spring (CS, SP)	31	11
Surface water (RW)	3	3
Total	105	45

K-Ar dating

For the determination of the age of ignimbrites, the K-Ar method was used during the analysis carried out at the Institute for Nuclear Research of the Hungarian Academy of Sciences in Debrecen. The basic principles of the conventional K-Ar dating and applied

experimental techniques using the radioactive decay of the $_{40}K$ isotope were described by Dalrymple and Lanphere (1969). Approximately 0.05 g of illite grains separated from two rock samples were digested in acids (HF, HNO_3) in teflon beakers and finally dissolved in 0.2 M HCl. Potassium was determined by flame photometry with a Na buffer and Li internal standard using Industrial M420 type flame photometer. Multiple runs of interlaboratory standards (Asia1/95, LP-6, HD-B1, GL-0) indicated the accuracy and reproducibility of this method to be within 2%. Approximately 0.5 g of illite samples were wrapped in aluminium foil and copper sieve preheated for about 24 h at 150–180 °C in vacuum. Argon was extracted under ultra-high vacuum conditions by RF induction heating and the fusion of rock samples in Mo crucibles. The gas was purified by Ti sponge and SAES St 707 type getters in order to remove chemically active gas contaminants and some liquid nitrogen in a cold trap to remove condensable gases. The extraction line is linked directly to a mass spectrometer (90° magnetic sector type of 155 mm radius) being used in static mode. Argon isotope ratios were measured by a ^{38}Ar isotope dilution mass spectrometric method, previously calibrated with atmospheric argon and international rock standards. Experimental details of the K-Ar dating method were described in Balogh (1985). Age of the samples was calculated using the decay constants suggested by Steiger and Jäger (1977).

Mineral chemistry

Chemical analyses of minerals were obtained using a Camera SX-100 electron microprobe at the Joint Laboratory of the Department of Geological Sciences, Faculty of Science, Masaryk University in Brno and the Czech Geological Survey, Brno. The measurements were carried out in a wave-dispersion mode under the following conditions: acceleration voltage of 15 kV, beam diameter of 5 μm and probe current of 30 nA. The integration time was 20 s and the standards employed (Kα lines) were: augite (Si, Mg), orthoclase (K), jadeite (Na), chromite (Cr), almandine (Al), andradite (Fe, Ca), rhodonite (Mn) and TiO2 (Ti). Data were reduced on-line using the PAP routine procedure (Pouchou and Pichoir 1985). The empirical formulae of feldspars were recalculated to 8 oxygen atoms. The amphibole formulae were obtained on the basis of 23 oxygen atoms (Leake et al. 1997). The Fe^{2+}/Fe^{3+} ratios in amphiboles were estimated assuming the cation sum of 13 without Ca, Na and K (13 eCNK). Pyroxenes are classified according to Morimoto et al. (1988); the formulae were obtained on the basis of 4 cations and the ferric iron estimated after Droop (1987).

Whole-rock geochemistry

About 3–4 kg samples were crushed (jaw crusher) and homogenized in an agate planetary ball mill for the whole-rock chemical analyses. Major and trace elements were determined at Acme Analytical Laboratories, Ltd., Vancouver, Canada. Major oxides were analyzed by the ICP-OES method. Loss on ignition (LOI) was calculated from the weight difference after the ignition at 1000 ºC. The rare earth and other trace elements were analysed by ICP-MS following $LiBO_2$ fusion (analytic code: A4B4 – major oxides, Ba, Be, Co, Cr, Cs, Ga, Hf, Nb, Ni, Rb, Sc, Sr, Ta, Th, U, V, W, Y, Zr, REE; 1DX – Ag, As, Au, Bi, Cd, Cu, Hg, Mo, Ni, Pb, Sb, Se, Tl, Zn; 2ALeco – Ctot, Stot; for analytical details, reproducibility, and detection limits see http://acmelab.com). Geochemical data were handled and plotted using the GCDkit software package (Janoušek et al. 2006).

1.5 Previous studies

The studied area has been the focus of few studies because of its importance in terms of recent volcanism. The geological map of Kazmin (1972) is the first produced map covering the area at 1:2,000,000 scale; it was later improved by Mengesha et al. (1996). Later, the geological mapping by Di Paula (1971) was carried out at a 1:500,000 scale, focusing on the large Corbetti Caldera northwest of Lake Hawasa. Di Paula (1971) noted that the plateaux were very distinct in terms of the volcanics dominated by huge piles of basaltic lava, contrary to widespread acid ignimbrite volcanics within the Rift. The latter were associated with volcano-tectonic collapses, which produced large regional calderas such as Corbetti and even the bigger Hawasa Caldera. Di Paula (1971) also noted that a significant proportion of lacustrine sediments existed in the area. The prominent tectonic features of the area were also identified, being marked as a set of NNE–SSW normal faults arranged in asymmetrical open tensional fissures (Di Paula 1971). A recent detailed mapping in the neighbouring map sheets at a scale of 1 : 50,000 to the north revealed a number of distinct volcanic edifices with progressive age (Rapprich et al. 2014a).

Engineering geological and hydrogeological map at a scale of 1 : 75,000 have been compiled for the Lake Hawasa basin including the Leku area by the Geological Survey of Ethiopia (Tadesse and Zenaw 2003). The Leku map sheet also falls on the border of two regional maps at 1:250,000 scale, namely the Hosaina map sheet to the north (Basalifew et al. 2012) and the Dila map sheet to the south (Yismaw et al. 2015). The hydrogeological (Kefale and Šíma 2013; Agezew et al. 2014) and geo–hazard maps (Rapprich et al. 2014a; Rapprich et al. 2014b) were compiled for the two adjacent maps covering the Leku area with a similar scale. The geo-hazard maps identified the pertinent exogenous and endogenous hazards in the mapped area (Rapprich et al. 2014a; Rapprich et al. 2014b). The hydrogeological maps delineated extents of variably productive aquifers along with zoning of hydrochemical affinity (Kefale and Šíma 2013; Agezew et al. 2014).

Regional groundwater and surface water resources have been comprehensively studied (Halcrow 2008, JICA 2012). An earlier integrated master plan study for the Rift Valley Lakes Basin was carried out by Halcrow (2018) with broad spectrum and long-term forecast on the perspective of utilization of the water resources. In the study, the spring with records of both yield and temperature were evaluated, where high yields are noted to originate from thermal spring sources; although, a high variability was also noted, ranging between 1.5 l/s up to 75 l/s (Halcrow, 2008). JICA (2012) also carried out the assessment of the entire Main Ethiopian Rift valley groundwater resources, which generated vast baseline data for subsequent works (JICA, 2012). The study showed that a high variability exists among different aquifers in the area (2.8 l/s in alluviums to 6.3 l/s in basaltic tuff). Other studies have been conducted with emphasis on the utilization of Lake Hawassa, such as those by WWDSE (2001) where the lake level changes and bathymetric surveys were conducted for the assessment of irrigation potential. Some studies were also made focusing on the quality of groundwater from the Main Ethiopian Rift valley, which is often associated with high bicarbonate and fluoride concentrations (Gizaw 1976; Chernet et al. 2001). Chernet et al. (2001) asserted that the high content of fluoride reaches 300 mg/l and affects the health of people living in the area, while the alkaline and sodic characteristics of the water render the soil inadequate to support cultivation.

An area to the north of the Leku map sheet has been recently studied for the potential of developing a thermal spa site (Sima et al. 2012) with promising results. The Corbetti Caldera, which is superimposed on the bigger Hawasa Caldera, has been the focus of

a recent geothermal development which is underway. It has been studied both by deep wells and various geophysical surveys in addition to surface geochemical and geological exploration by the Geological Survey of Ethiopia (Kebede and Abdulkadir 1987, Gíslason et al. 2015).

Various prominent geological hazards are noted to occur in Leku and the surrounding area. Among these hazards, the most common are surface erosion and ground fissures. Geomorphological aspects of gully erosion in the area have been studied by Billi and Dramis (2003), while the occurrence of ground cracks (fissures) were investigated by several investigators (Asfaw 1998, Ayalew et al. 2004). Apart from the surficial hazards, endogenous hazards especially from volcanoes with signs of high recurrence recently got more attention. Tephrostratigraphic approach has been used in recent studies to reconstruct the first Holocene (~10 k.y.) record of explosive volcanism for the Corbetti caldera (Martin-Jones et al. 2017). The study found out that a future explosive event from the Corbetti caldera with a scale of decimeters in thickness and could potentially cover all of Hawassa and Shashamene by pumice and ash fallout, provided the eruption characteristics and wind direction are ‘favorable’ (Martin-Jones et al. 2017; Rapprich et al. 2016).

2) ENVIRONMENTAL SETTING OF THE STUDY AREA

2.1 Topography and Morphology

The study area lies in southern Ethiopia at the bottom of the Rift Valley, which forms an undulating plain that is penetrated and cut by river valleys. Relatively recent escarpments of fault origin, and young felsic and basaltic inactive volcanoes gave rise to the local hilly and undulating topography. In general, the elevation on average ranges from roughly 2,060 m a.s.l. in the north and northeast to 1,740 m a.s.l. in the southwest. The southern tip of the Corbetti Caldera and the Lake Hawassa form the northern boundary of the study area. The NW-SE running escarpment forming ridges represent the prominent physiographic features in the central and western parts of the area, while the dendritic structure and the landscape cut by an elevated volcanic land are characteristic for the eastern part of the area.

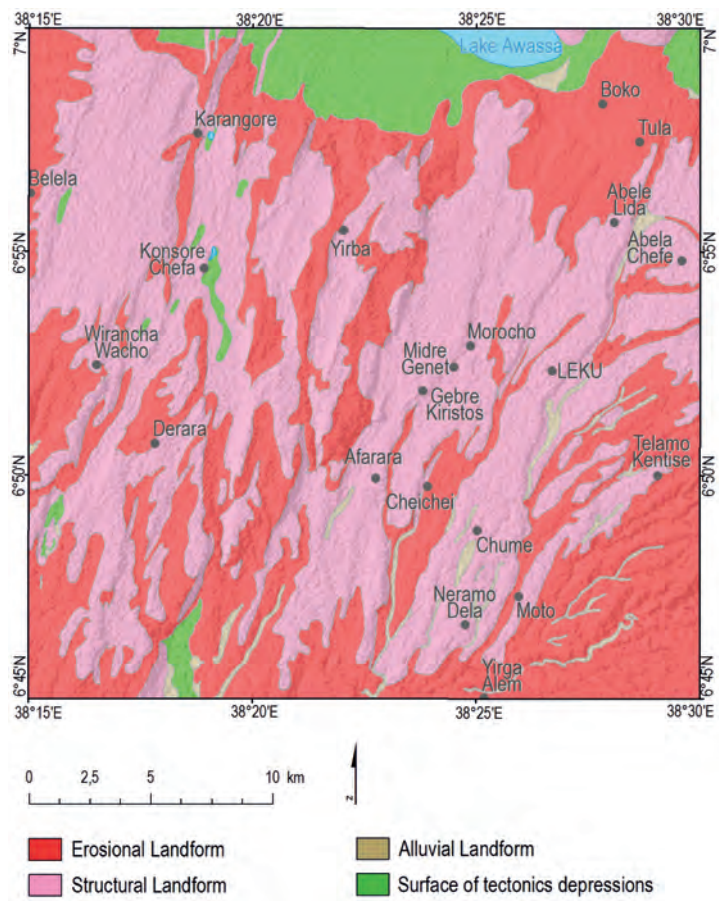

Figure 2-1. *Morphology of Leku area.*

The recent study shows the level or profile of a disaster risk in a district (woreda), in which the studied area extends between two agro-ecological zones of the Sidama Administrative Zone in the S.N.N.P Region. This area to the west falls into the Sidama Coffee Livelihood Zone of the Ethiopian Highlands (mid-highlands – 1,700 to 2,300 m a.s.l.), which include the administrative districts of Shebedino, Awassa, Hulla, Bensa and Aroresa (link to DPPC digital database profile of the Shebedino district). The eastern part of the studied area belongs to the Sidama-Gedeo Highland (2,100 to 3,200 m a.s.l.), which includes parts of the Awassa, Shebedino, Hulla, Arbegona, Bensa, Aroresa, Bule and Kochere districts (link to DPPC digital database of the Shebedino district). The farmland is mainly used for growing coffeeand fruit, including Ethiopian banana (enset) and food crops, while pastures are grazed by cattle. The surface is covered with sparse forest. The Sidama Coffee Livelihood Zone is exposed to a number of natural hazards, some of which endanger the economic growth of the area. The major hazards include the lack of rain and recurring droughts (cf. DPPC digital database of the Shebedino district).

2.2 Hydrometeorological characteristics

The area is climatically monotonous and is mainly characterized by a temperate Weina Dega zone, which is typical for the rift floor. Precipitation in the mapped area appears to be uniform and is characterized by four distinct seasons and bimodal precipitation patterns with two peaks, the first occurring in March–May and the second in September–November. There are three meteorological stations measuring and recording precipitation within the Leku sub-sheet. The differences in total precipitation within the stations located on the rift floor are small and this is supported by the annual average precipitation record at Awasa (north of the map sheet), Derara (10 km southwest of Leku), and Dila (south of the map sheet). The precipitation patterns at the Awasa and Dila weather stations are shown in Table 2-1 while precipitation data at the Dila, Awasa and Belela meteorological stations are summarized in Table 2-2.

Table 2-1. Mean monthly precipitation at selected meteorological stations (source: Halcrow, 2008)

	Jan	Feb	Mar	Apr	May	Jun	Jul	Aug	Sep	Oct	Nov	Dec
Dila	35.4	45.6	93.0	206.8	211.1	116.2	133.8	111.3	143.7	124.3	70.0	32.6
Awasa	29.1	41.2	80.5	111	119	105	121	118	123	72	30.8	22.1

Table 2-2. Mean monthly precipitation at Belela in the period from 2006–2015

	Jan	Feb	Mar	Apr	May	Jun	Jul	Aug	Sep	Oct	Nov	Dec
Belela	9.6	25.7	56.8	163.1	126.1	66.3	118.7	104.6	145.8	115.4	32.3	25.2

The difference between total precipitation and its variability during a measurement period in the Leku area and nearby located stations is shown in Table 2-3.

Table 2-3. Precipitation variability

Name	Average	Max	Year	Min	Year	Rainfall deficit [%]
Belela	1,039	1,612	2010	559	2009	46
Derara	1,222	2,579	1992	823	1999	33
Bilate Tena	927	1,344	1996	405	1984	56
Billate	793	1,111	2010	493	1999	38
Awasa	969	1,198	2006	704	2009	27
Dilla	1,319	1,755	1958	950	1961	28

Table 2-4 summarizes the annual average precipitation in sub-basins of the Rift Valley Lake Basin with respect to the Leku map sheet.

Table 2-4. Summary of precipitation in sub-basins covering the Leku map sheet

Sub-basin	Area [km^2]	A rain [mm]	T rain [Mm^3]
Awasa	1,295	1,135	1,470
Gidabo	3,491	1,244	4,343

A = annual average, T = annual total

2.3 Land use and Land cover

Poor land use practices and policy, improper management systems and lack of appropriate soil conservation measures have played a major role in causing land degradation problems in the country. Because of the rugged terrain, the rates of soil erosion and land degradation in Ethiopia are high. Setegn (2010) mentions the soil depth is already less than 35 cm on more than 34 % of the Ethiopian territory, indicating that Ethiopia loses a large volume of fertile soil every year and the degradation of land through soil erosion is increasing at a high rate. The highlands and some parts of the Rift Valley floor are now so seriously eroded that they will no longer be economically productive in the foreseeable future.

The land and water resources are in danger due to the rapid growth of population, deforestation and overgrazing, soil erosion, sediment deposition, storage capacity reduction, drainage and water logging, flooding and pollutant transport. In recent years, there has been an increased concern over climate change caused by increasing concentrations of CO_2 and other trace gases in the atmosphere. A major effect of climate change is represented by alterations in the hydrologic cycles and changes in water availability. Increased evaporation combined with changes in precipitation characteristics has the potential to affect runoff, frequency and intensity of floods and droughts, soil moisture, and water supplies for irrigation and generation of hydroelectric power.

Human interference in the physical environment is great due to the high population growth rate and migration of people resulted in people searching for additional farmlands by clearing the existing small patches of vegetation cover. Sheet and gully types of soil erosion are mainly observed. Cultivation and deforestation have considerably changed

the natural vegetation cover over much of the area, aggravating the rates of weathering and erosion; farming is also practiced on slopes, which can add to the erosion rate. Large areas have been totally devastated by sheet erosion of soil. Some areas to the north and west of Lake Abaya are protected to enable the soil to recover.

Land cover includes cultivated land (large-scale farms and family farms with a different intensity of cultivation), small vegetation (shrub lands and grassland, swamp), manmade features (urban or built-up areas), rocky outcrops, bare soil, and water bodies.

Land use information shows that the majority of the Leku area is moderately cultivated. The floor of the Rift Valley is used for irrigation to cultivate different types of vegetation and fruit. This land use classified as "Intensive Annual Crop Production" describes the areas where annual crops (cereals, pulses, oilseeds and vegetables) are cultivated.

2.4 Prominent natural features

Coffee, eucalyptus and fruit including enset (Ethiopian banana) plants around dwellings represent typical natural vegetation in the area. It is worth noting that the coffee plant reaches maturity to produce seeds about each 3–4 years, while enset takes about 4–6 years (DPPC digital database of the Shebedino district). The area is rich in sand and various rocks followed by streams and escarpments of fault origin.

Lake Awasa is bordering the study area. It is an endorheic basin located in the Main Rift Valley being 16 km long and 9 km wide with a surface area of 129 km^2. It is 10 meters deep at maximum and lies at an elevation of 1,708 m a.s.l.

3) REGIONAL GEOLOGICAL SETTING OF THE STUDY AREA

On a regional scale, the mapped area rests in the East African Rift System (EARS), which is an intra-continental rift separating the western African (Nubian), eastern Somalian and northern Arabian lithospheric plates. The axial zone of the rift consists of several depressions (rift valleys) separated by uplifted blocks. The EARS is comprised of three separated domains – the Western branch, the Eastern branch and the Main Ethiopian Rift (MER) to the north (Fig. 3-1). The latter extends to the north towards the Afar Depression, where it splits through a triple junction into NW– and ENE–trending oceanic ridges in the Red Sea and the Gulf of Aden, respectively. The rift separation is attributed to slips along transform faults, perpendicular to the rift axis. The orientation of these faults reflects the ~NW-SE direction of crustal spreading (see Chorowicz 2005, and references herein). A prominent feature of the EARS are highly elevated (3000–4000 m a.s.l) rift

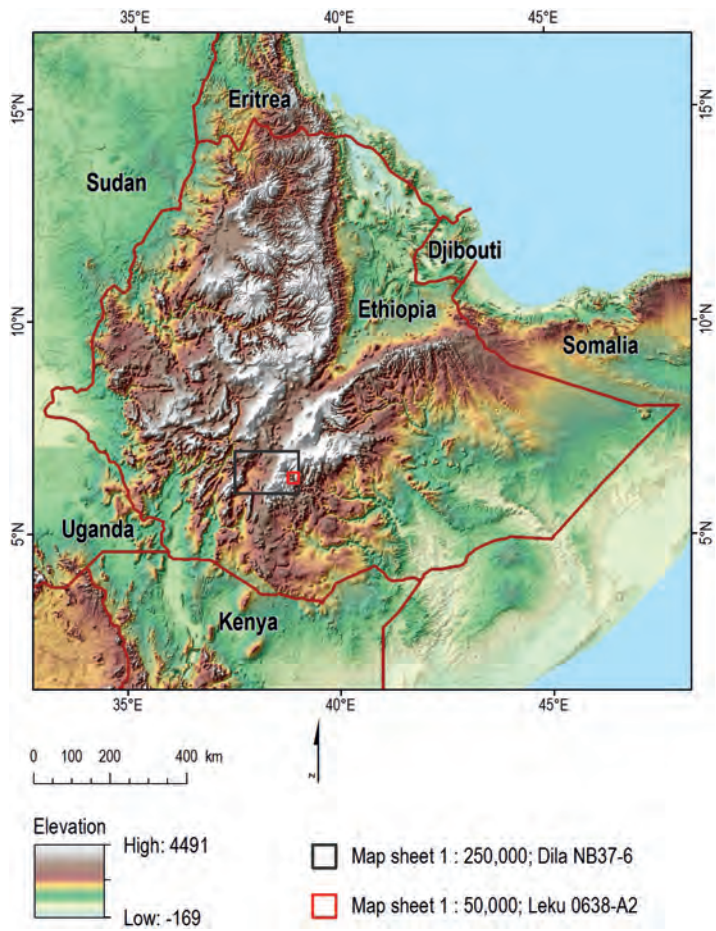

Figure 3-1. *Digital elevation model showing the East African Rift in Ethiopia and location of the studied area. Black rectangle is frame of the 1 : 250 000 scale map Dila, red rectangle for the map 1 : 50 000 Leku.*

shoulders and crustal domes, interpreted as being the result of an uplift by mantle plume (e.g. Chorowicz, 2005).

The MER is characterized by an active E–W– oriented extensional movement between the African and Somalian plates with a rate of 5.2+0.9 mm/yr (Saria et al., 2014) to 7 mm/yr (Stamps et al., 2008). Three parts of the MER, which are distinct in age, strain accommodation, volcanism and orientation of faults have been recognized (e.g. Kazmin et al., 1980; Hayward and Ebinger, 1996; Wolfenden et al., 2004).

The northern part of the MER is extending from the Afar Depression up to the Lake Koka region, which also forms the middle course of the Awash River. The main boundary faults in this region show an average N500 trend. This part of the MER was formed at around 10 to 11 Ma ago (Kazmin et al., 1980; Hayward and Ebinger, 1996; Wolfenden et al., 2004). The central MER includes most of the Lakes Region, and further southward up to the Lake Awasa area. Here, the major boundary faults exhibit roughly N300–350 trend, and the age of the faulting onset is estimated to be around 8.3–9.7 Ma. The southern MER extends south of the Lake Awasa into a ca 300 km wide system of basins and ranges, referred to as the broadly rifted zone or the Gofa Basin (Davidson and Rex, 1980; Ebinger et al., 2000). Faults in the southern MER show a dominant 00 to N200 trend and were active after ca 18 Ma (Woldegabriel et al. 1991; Ebinger et al. 1993).

These parts of the MER represent different stages of regional extension from early rifting in the southern MER to a more evolved crustal extension in the central and northern parts of the MER (Hayward and Ebinger 1996). The entire geodynamic evolution and tectonic pattern of the Main Ethiopian Rift has been summarized by Abbate et al. (2015). On the regional scale, the roughly ESE-WNW trending extension during the initial rifting has changed to the current ca ENE to WSW strike. A reactivation of earlier extensional faults resulting in left-lateral shearing following the change in orientation of the regional stress field was observed at several localities across the MER.

The southern MER extends south of Lake Awasa into the ~300-km wide system of basins and ranges also referred to as the broadly rifted zone or the Gofa basin and Range (Davidson and Rex, 1980; Ebinger et al., 2000) that characterizes the overlapping area between the Ethiopian and Kenyan Rifts (Emishaw et al., 2017, Davidson and Rex, 1980). Faults in the southern MER show a predominant N–S to NNE–SSW trend and were established well after ~18 Ma (Levitte et al., 1974; Zanettin et al., 1978; WoldeGabriel et al., 1991; Ebinger et al., 1993; Wolfenden et al. 2004). The southern segment is also the zone of an overlap between northern extensions of the Kenyan Rift, which typically has N–S trending faults and the southern extension of the MER has NE-trending faults. Around the Arba Minch area, the major structural control is represented by the Amaro Horst, which divides the rift into the eastern and western grabens. The western graben is called Ganjuli, which is more conspicuous further south in Kenya and runs up all the way up to Chamo and Abiyata Lakes basin, while the eastern graben is called Galana Basin and includes the area east of Amaro Horst up to the fault escarps at Dila.

In general, volcanism in the EARS is mainly concentrated in its northern part, which is interpreted as being a result of the Afar mantle plume impact (e.g. Schilling et al., 1992). Characteristic volcanic rocks are represented by alkaline to hyperalkaline types, which developed from continental tholeiites through alkaline to transitional magmas (Mohr et al., 1972). Recent geophysical survey revealed that volcanic activity in the MER is concentrated in magmatic segments localized along rift axis (e.g. Beutel et al., 2010; Keranen and Klemperer, 2008). The ages of volcanic rocks largely differ within the entire EARS. The volcanic activity in the MER started at around 45 Ma followed by more

extensive eruptions of tholeiitic to alkaline basalts between 31 and 28 Ma (Hofmann et al., 1997; WoldeGabriel et al. 1991). A second volcanic event of intermediate and felsic composition took place mainly between 17 and 11 Ma in the southern and central parts of the MER (Ebinger et al. 1993), and at around 12 Ma in its northern part (Wolfenden et al. 2004). Again, this followed after a hiatus by basaltic eruptions with ages ranging from 11 to 8 Ma. This was followed by a period of drastically low volcanism except for small eruptions of peralkaline pantelleritic ignimbrites intercalated with minor basaltic lava flows ca 7 Ma beyond the rift escarpment on the western plateau (Bonini et al., 2005).

By 1.8 Ma, volcanism and faulting were localized to the narrower magmatic segments within the rift (Keranen et al., 2004) with an oblique trend to north-northeast in comparison with the older overall northeast trend of the rift. The segments are separated from one another by shorter intervals in a right-lateral en echelon pattern. Therefore, the following types of volcanism had bimodal composition between acidic and basic. This late activity started with the eruption of widespread Pleistocene ignimbrites (1.6–0.5 Ma) that, although younger, may be correlated to the Nazret Group that largely characterizes the northern MER (Bonini et al., 2005). The volcanic succession is closed by the Nech Sar olivine basalts (1.34–0.77 Ma (Ebinger et al. 1993), and by few pumiceous tuffs and obsidian flows overlying the Quaternary basalts in the Bridge of God area (Bonini et al. 2005).

4) REMOTE SENSING ANALYSIS

Remote sensing techniques were used for a better understanding of lithologies on the Earth's surface, geological structures and to provide an overview of the regional context of study areas. The area of the Leku map sheet is extensively covered by vegetation, so that the spectral data from optical sensors (Landsat, Aster) provide mostly information on land use, but limited information on lithological variation. The main use of remote sensing data in this area has been the utilization of a digital elevation model (DEM) for an identification of geological structures using the morphotectonic analysis. Remotely sensed data (optical images, DEMs) were also used to identify and understand geomorphic processes and related potential natural hazards.

4.1 Data and methods

Remote sensing data used in this study comprise: Satellite images Landsat 7 ETM+, Digital Globe and digital elevation model (DEM). Landsat and subsequently the digital elevation model (DEM) have a spatial resolution of approximately 30 m. The ASTER DEM is derived from the optical stereoscopic coverage of ASTER satellite images. DEMs provide the key data for understanding the major geomorphological and tectonic features of the investigated area. We are also using optical satellite imagery like Landsat and ASTER to comprehend the lithology and land cover of poorly accessible areas. However, its use for geological applications is limited to the areas with poor vegetation.

The Landsat satellite images were used in order to better understand the surface lithology. The area is largely covered by vegetation, so that even the images taken during dry season show lots of vegetation cover, especially in the central and eastern parts of the map sheet. The vegetation was obscured and possible lithologies in the areas with rare vegetation were improved using the Principal Component Analysis (PCA). Different colours may correspond to different minerals, rocks and soil types on the surface, but the interpretation is still difficult in the areas partly covered by vegetation (Fig. 4-1). The comparison of interpretations using the Landsat Principal Component Analysis with those of field observations and mapping show that the volcaniclastic rocks in the NW part of the map sheet are quite distinctive appearing mostly in red-violet colours (in PCA 132 as RGB colour composite). Also, the NNE–SSW oriented bodies of rhyolites outcropping along the major normal faults in the central part of the map sheet can be recognized (violet colours). Ignimbrites correspond to mostly red-orange colours. High-resolution satellite imagery DigitalGlobe with a spatial resolution of up to 0.6 m was also used for selected areas where a detailed understanding of geomorphology is necessary (e.g. for the areas susceptible to landslides and other geo-hazards).

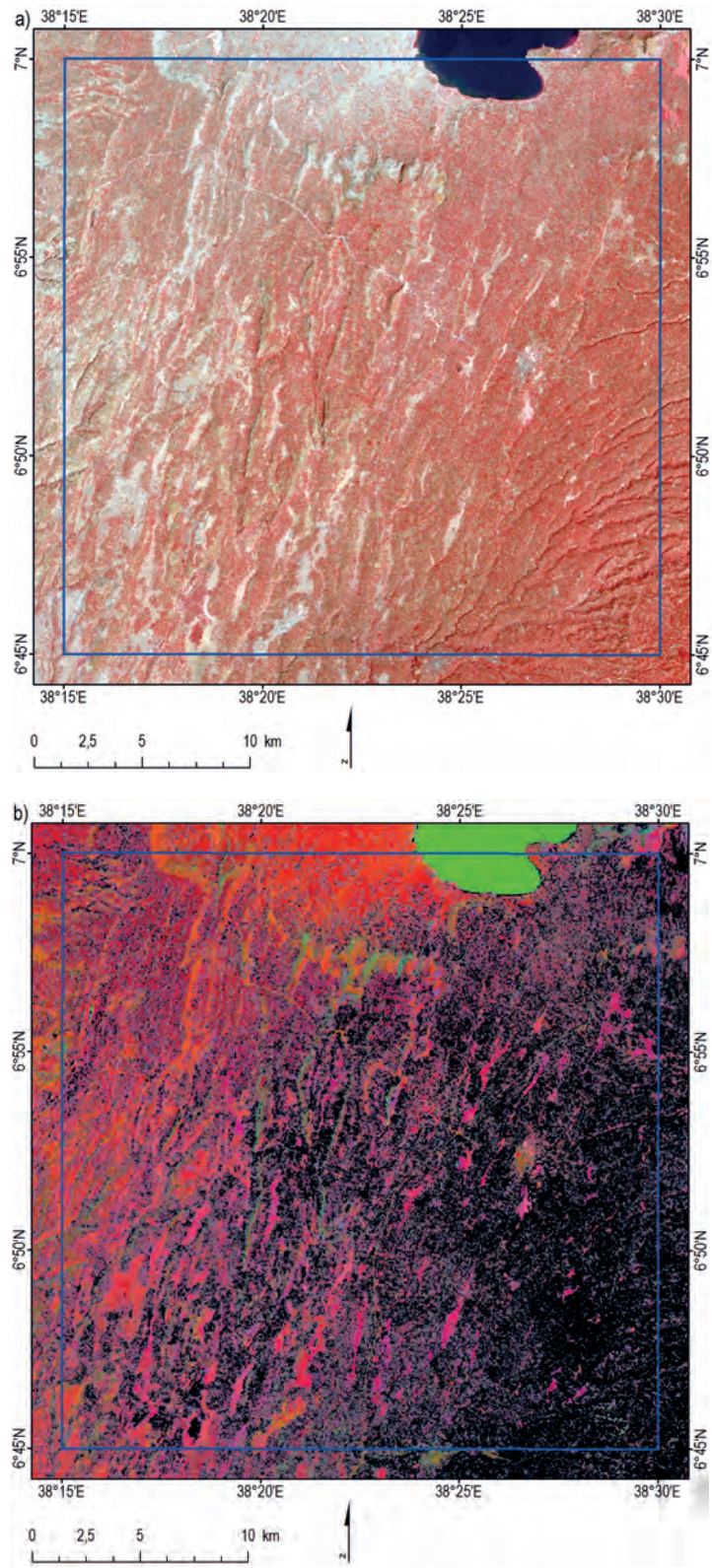

Figure 4-1. *Landsat image of the Leku map sheet. False colour image with the bands 432 displayed as RGB composite (up) is showing vegetation in red colours. Results of the principal component analysis (PCA) displayed as RGB composite of PCA1, PCA3 and PCA2 (down). Vegetation was obscured (black). Different colours represent different lithologies. For discussion see text.*

4.2 Morphotectonic analysis

Structural characteristics of an area can be revealed from the remotely sensed data by interpretation of linear features. It is the large synoptic view of satellite images that allows the recognition of features that are difficult to follow and interpret during field campaigns. The shape of the features is determined by their dip angles. Most faults dip steeply and form straight lineaments relatively unaffected by topography. There are, however, also other possibilities how the linear features can be interpreted in remotely sensed data from being actual faults, dykes, steep or vertical strata, to roads and data artifacts. Neotectonic faults can be identified by (1) their morphology, forming asymmetric ridges with one side corresponding to the breaks in slope or scarps, (2) the displacement of late Neogene lithological boundaries, structural or erosional surfaces, and (3) the occurrence of straight lines of several tens of kilometers in length (Dhont and Chorowitz 2006, Jordan et al. 2005, Snyder et al. 2000, Saintot et al. 1999). Satellite images and DEMs with geological maps have been systematically compared in order to carefully separate the scarps formed by fault planes (active) from those resulting from differential erosion of contrasted lithology (old faults or non-tectonic lithological boundaries). The active fault scarps, even eroded, are much higher and longer than the scarps formed by lithological contrasts. The identification of kinematic indicators is based on these features: Strike-slip faults have rectilinear traces and they locally bound push-up hills or extensional basins at step-over or bends of the fault trace. They can be associated with typical patterns such as tail-crack or horse-tail structures at fault ends. Reverse faults have sinuous traces and they are associated with half-cylindrical-shaped hills of the uplifted blocks due to drag folds deforming old planar erosion surface in the hanging wall. Normal faults are recognized by the following geomorphic characters: (1) they generally have a widely arched trace, mainly concave toward the footwall; in contrast to the strike-slip faults, whose trace is generally straighter; (2) they bound tilted plateaus or blocks; (3) as is also the case for the strike-slip faults, they are not related to half-cylindrical-shaped hills corresponding to recent drag folds, which accompany active reverse faulting. Mapping of recent folds, the synclines, forming lowlands filled with sediments, and the anticlines corresponding to regularly-shaped elongated hills is also possible. It is important to point out that this approach provides information on the finite strain, but not on its detailed history. Faults usually develop in conjugate sets where one direction is dominant. The recognition of conjugate fault systems allows an overall estimation of the orientation of maximum and minimum principal stress axes. Faults represent local weaknesses in the Earth's crust and become eroded easily so that they can form linear depressions often followed by streams, which is recognizable on digital terrain models and optical images. The higher water saturation of fault zones provides an excellent environment for plants that may grow along the fault line and enhance its discernment. However, as a rule, other geologically significant features such as truncations, displacements of lithological units, geophysical indicators or direct field checking should support the statement that a linear feature in an image represents a real fault structure. Active faulting in an area may be beneficial for the recognition of faults as it may produce specific landforms like headless valleys, facetted spurs, shutter ridges, offset streams or sag ponds (Snyder et al. 2000, Saintot et al. 1999).

Morphotectonic analysis on the Leku map sheet revealed prominent NNE–SSW to NE–SW (with minor N–S directions) linear indicators which have a clear expression in the present-day morphology. They mostly represent normal faults forming series of

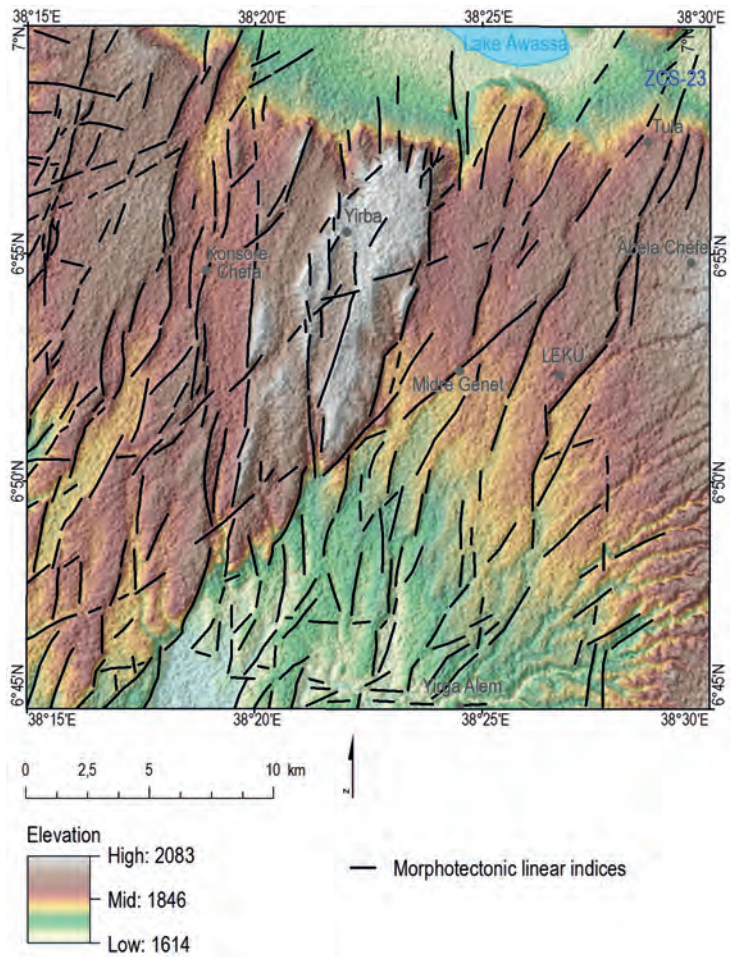

Figure 4-2.
Morphotectonic analysis of the Leku map sheet. Morphotectonic linear indicators are displayed on the color digital elevation model (ASTER DEM) combined with a shaded relief map.

grabens and horsts. Long linear indicators with large displacements are considered as regional faults. Linear indicators of the E–W directions occur rarely, especially in the northwesternmost and southern parts of the map sheet. They do not show significant vertical displacement, they may represent small strike-slip faults or fracture zones. Validation of the morphotectonic linear indicators with the field data and geological map eliminated several lines representing lithological boundaries. The results presented in Fig. 4-2 show linear indicators that are interpreted mainly as faults, fault zones and prominent joints.

The comparison of results of the morphotectonic analysis with a geological map shows certain concordance of the major morphotectonic linear indicators with those faults verified and inferred by geological mapping. Correlation is quite high, particularly regarding the NE and NNE-oriented structures, but some small or E–W oriented linear features were not identified during the field mapping as faults. They may represent only joint systems or were not verified by mapping due to the poorly exposed terrain.

5) GEOLOGY OF THE LEKU SHEET

5.1 Lithology and Petrology

The Leku map sheet is located within the middle part of the Main Ethiopian Rift System, on the border of its central and southern segments. Evolution of the southern segment of the Main Ethiopian Rift has been divided into three stages according to age (Stewart and Rogers, 1996): pre-rift (32–45 Ma), syn-rift (22–12 Ma) and post-rift (0–5 Ma). The Upper Miocene volcanic rocks belonging to the syn-rift stage are dominated by rhyolite ignimbrites cropping out in the quarry SW of Yirga Alem town. These rocks are covered by a relatively thick volcanosedimentary sequence (up to 1500 meters) of the post-rift stage being of Pleistocene age. The predominant rock types on the Leku map sheet are the products of voluminous post-rift eruptions called as the Dino Formation (Rapprich 2014b). The deposition of the predominant rhyolitic ignimbrites (Hawasa ignimbrites) and pyroclastic deposits are associated with the Hawasa Caldera formation (Rapprich et al. 2013). The pyroclastic deposits represent the later stages of caldera-forming eruptions. Within the Havasa ignimbrites and related pyroclastic deposits, a few metres thick massive basalt lava (Yubo Basalt), strongly welded, fine-grained rhyolitic ignimbrites up to 20 meters in thick (Hantate ignimbrites) and minor rhyolitic lavas (Boricha Rhyolite) forming the Boricha Ridge are all present. The tectonic depressions and grabens located mainly in the central part of the map sheet are filled by re-sedimented volcanoclastics, alluvial and lacustrine deposits of Pleistocene to Holocene ages.

Syn-rift volcanic deposite

Nazret Formation (Miocene age)

11. Ignimbrites only in geological cross-section and litostratigrafic scheme locally with intercalations of pyroclastic fall deposits and minor acidic lavas. The chemical composition of these rocks corresponds to alkaline rhyolites and trachytes (Rapprich et al. 2014a). The entire sequence belongs to the syn-rift stage, cropping out in footwall of the Yubo basalt along the NNE–SSW trending fault scarp, being exposed mainly in a quarry SW of the Yirga Alem town (Fig. 5-1). The thickness of the Miocene ignimbrite sequence reaches several hundreds of meters (Abebe 1984, Basalfew 2012).

Post-rift volcanic deposits

Pleistocene Dino Formation (Pleistocene age)

10. The Hantate Ignimbrite: welded to unwelded ignimbrites form a subhorizontally lying layer up to 20 m thick in the footwall of the Hawasa ignimbrites. The columnar-jointed Hantate ignimbrite sheet crops out on the cliffs (Fig. 5-4) near Danshe Sire and Sala Sire towns. The bluish-gray, dark gray to green, strongly welded, fine-grained

rhyolitic ignimbrite often contains feldspar phenocrysts (15-20 vol. %), dark fiamme (up to 8 cm long, 5-15 vol. %), basaltic and rhyolitic subangular to rounded fragments (2-25 vol. %). Elongated flattened fiamme have a glassy texture. The fine-grained groundmass exhibits an eutaxitic texture (Fig. 5-5) caused by the compaction and flattening of glass shards and pumice fragments. Common minerals include alkaline feldspar (Ab_{61-62} Or_{38-39}), quartz and Na-Ca amphibole (ferrowinchite, X_{Mg} 0.28 to 0.35, Si 7.58 to 7.68 apfu.) as crystal fragments up to 1 mm in size.

9. The Yubo Basalt consists mainly of dark gray to black massive basalt lava (Fig. 5-1) and scoria. Dark basalt lava flows are present in the footwall of the Hantate welded ignimbrite in a quarry SW of the town of Yirga Alem and in the escarpment SE of the Derara town. The Yubo basalt (Fig. 5-2) is a fine-grained, weakly porphyritic rock consisting of plagioclase (54 vol. %), clinopyroxene (41 vol. %) and olivine (5 vol. %). Polysynthetic phenocrysts of plagioclase occur as euhedral to subhedral tabular laths up to 1.5 mm long. Locally, up to 1 mm large phenocrysts of euhedral olivine (Fo_{65-75} Fa_{25-34}) occur as well. The groundmass is ophitic or poikilo-ophitic, and consists of subhedral plagioclase laths with weak normal compositional zoning (Fig. 5. 3a, An_{46-70} Ab_{28-51} Or_{2-3}), anhedral clinopyroxene (diopside, Fig. 5. 3b, X_{Mg} 0.69 to 0.71, Ca 0.85 to 0.88 apfu.), and subhedral to rounded olivine (Fo_{55-58} Fa_{41-44} Tp_1) crystals partially altered to iddingsite. The plagioclase is locally rimmed by alkali feldspar (An_{13} Ab_{65} Or_{22}). Magnetite and ilmenite represent typical accessory minerals.

8. Boricha Rhyolite usually occurs in the form of white to bluish-gray lava flows (Fig. 5-10) showing columnar jointing and also as glassy brecciated rhyolite lava, which is mostly confined to the Boricha dome. Locally, tuffs rich in fragments of pumice and obsidian can be observed as well. Rhyolites often show porphyritic texture with a fine-grained or glassy groundmass (Fig. 5-11). Subhedral phenocrysts of augite (X_{Mg} 0.62 to 0.64, Ca 0.75 to 0.77 apfu) and alkali feldspar (Ab_{61-62} Or_{38-39}) are up to 1 cm large; besides that, spherulites up to 2 cm in size originated by the devitrification of volcanic glass can be observed in some parts of the studied outcrops.

7. The Hawasa pyroclastic deposit with subordinate ignimbrite represents the last stage of caldera-forming eruptions in the studied area. The ignimbrites consist of welded as well as non-welded facies. The individual flow units are separated by pumice fall deposits of variable thickness (up to 8 m). The ignimbrite is made of slightly resorbed phenocrysts of alkali feldspar, oval crystals of quartz and small amphibole crystals enclosed in a groundmass composed of welded glass shards.

6. The Hawasa rhyolitic ignimbrite with subordinate pyroclastic deposit was produced by voluminous eruptions of rhyolitic magma ejected from the Hawasa Caldera (Rapprich et al. 2013). This unit on the map sheet consists of welded to non-welded rhyolitic ignimbrites (Figs. 5-6 and 5-7), and associated pyroclastic fall deposits (Fig. 5-8). The total thickness of this unit remains unclear (probably up to 30 m), but internally consists of numerous ignimbrite layers, usually 1-3 m thick, which are separated by tephra or paleosoil horizons (up to 1 m thick). Ignimbrite layers are usually moderately welded with pumiceous volcanic glass on the top. Poorly sorted ignimbrites consisting of rounded to sub-rounded pumice (2-40 vol. %) are typical, usually with sizes ranging from 0.5 to 3 cm (rarely up to 6 cm large). Lithic fragments (mainly rhyolite, trachyte) reach up to 10 vol. %,

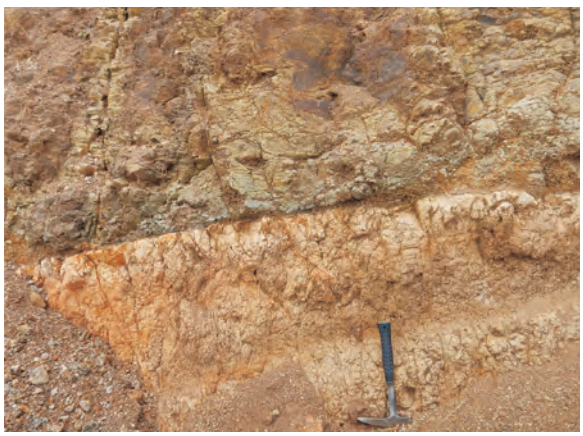

Figure 5-1. *Contact between greyish-yellow to reddish strongly weathered ignimbrite of the Nazret Formation and Yubo basalt flow cropping out in a quarry SW of the Yirga Alem town.*

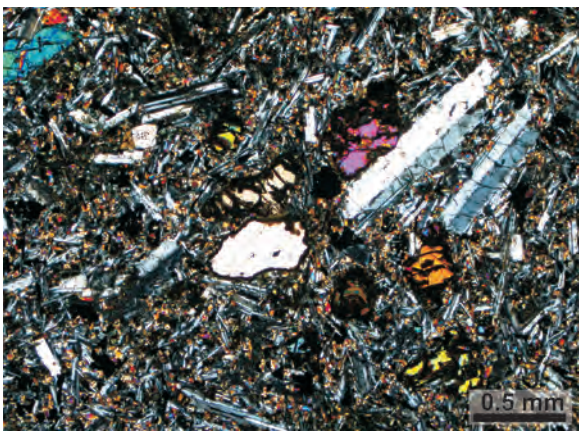

Figure 5-2. *Yubo basalt with plagioclase and olivine phenocrysts, amygdale fiilled with calcite is present in the central part of thin section, an outcrop on an escarpment located SE of the Derara town, XPL.*

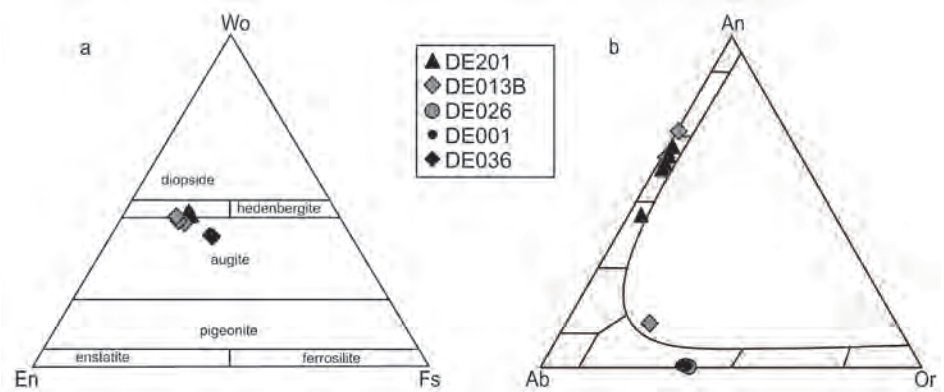

Figure 5-3. *Classification diagrams for Ca–Fe–Mg pyroxenes (a) and feldspars (b) from the Yubo basalt (DE201, DE013B), the Hantate welded ignimbrite (DE026), the Hawasa ignimbrite(s) (DE001) and rhyolite (DE036).*

and their size exceeds 1–3 cm in diameter. Obsidian fragments up to 0.8 cm in size are scarce (0-5 vol. %). Euhedral to subhedral crystals and fragments of quartz, Ca-Na amphibole (barroisite and winchite, X_{Mg} 0.57 to 1.00, Si 7.38 to 7.53 apfu.) and alkali feldspars (An_{0-1} Ab_{61-63} Or_{37-38}) are locally abundant (up to 15 vol. %) in the groundmass, which consists of moderately to intensely deformed volcanic glass shards. Ignimbrites with very slight compaction of glass shards are usually present in the top layers, and often are associated with ash to lapilli-size pumice fall deposits. A typical constituent of ash layers is represented by accretionary lapilliof 0.1 to 0.5 cm in size (Fig. 5-9). Locally, up to 3 m thick layers of gray to reddish welded ignimbrites occur with elongated fiamme of 1–3 cm in size.

Sedimentary deposits of Upper Pleistocene to Holocene

5. Colluvial sediments form rather thin deposits in the area of the Leku sub-sheet. Although steep slopes are frequent on fault scarps. Predominant sandy material and gully

Figure 5-4. *Outcrops of Hantate welded ignimbrite are distributed along an escarpment situated SE of the Derara town.*

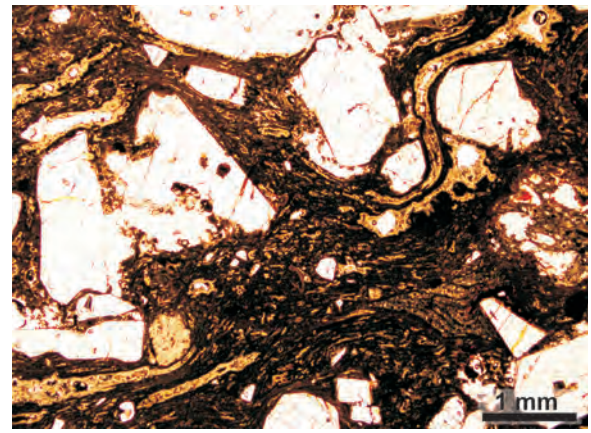

Figure 5-2. *Yubo basalt with plagioclase and olivine phenocrysts, amygdale fiilled with calcite is present in the central part of thin section, an outcrop on an escarpment located SE of the Derara town, XPL.*

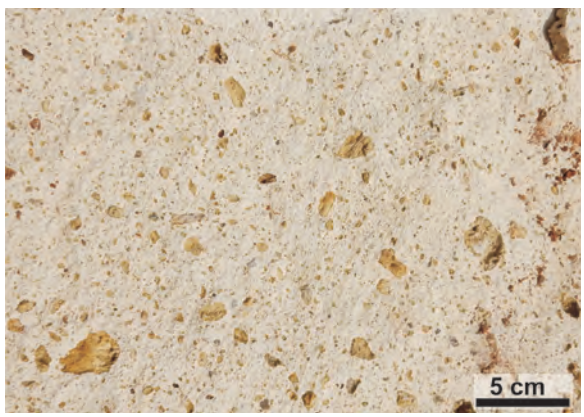

Figure 5-6. *Non-welded Hawasa ignimbrite from a quarry situated WNW of the Leku town.*

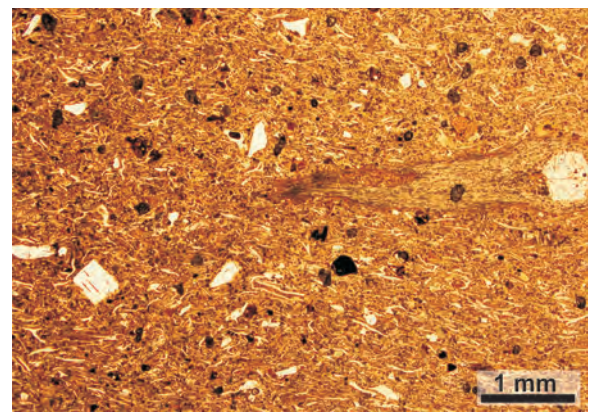

Figure 5-7. *Crystal fragments and fiamme in a fine-grained welded groundmass (slightly welded Hawasa ignimbrite), PPL.*

erosion on the scarp do not create favourable conditions for the formation of colluvial sediments. Colluvial sediments are related to the rather rare occurrences of accumulation zones of landslides and rock falls. The deposits usually consist of blocks of weathered ignimbrites and pyroclastic rocks. The thickness of colluvial sediments usually reaches several meters.

4. Polygenetic sediments (re-deposited pyroclastics, alluvial and lacustrine sediments) fill the bottom of the Hawasa depression. They are characterized by alternating beds composed of various sediments and changing lithology resulting from tectonic, volcanic and exogenous processes with fluctuating water levels in the lake. The reworked and re-deposited pyroclastics mainly consist of angular clasts of pumice or mixtures with a small amount of silt, sand or soil. Locally, they also contain clasts of weathered ignimbrites, fragments of tuffs and obsidian. Alluvial sediments are represented by loamy sands and silt with various portions of weathered volcanic rocks. Lenticular fillings of gravels were

observed in fissures and fractures. The lacustrine deposits are occasionally exposed on the surface. They comprise a heterogeneous sequence of silt with thin intercalations of sand and re-deposited pumice. Locally, some gastropod shells were observed in beds made of silt along the northern margin of the area. The thickness of the sedimentary filling exceeds 30 meters (Ayalew et al. 2004) or 40–50 meters elsewhere in the rift (Chernet 1982) is estimated based on drilling data.

3. Lacustrine sediments are exposed in narrow rims along the shores and adjacent swamps of Lake Hawasa and fill endorheic depressions of the tectonic grabens. The sediments consist of unconsolidated fine-grained deposits – mud, silt and sands. Lithology of these deposits is thought to be controlled by sediment transport and river flow rates of streams emptying into the lakes.

2. Alluvial sediments are associated with recent alluvial fans, which originate from the erosion of material accumulated on slopes. Afterwards, these were washed down during

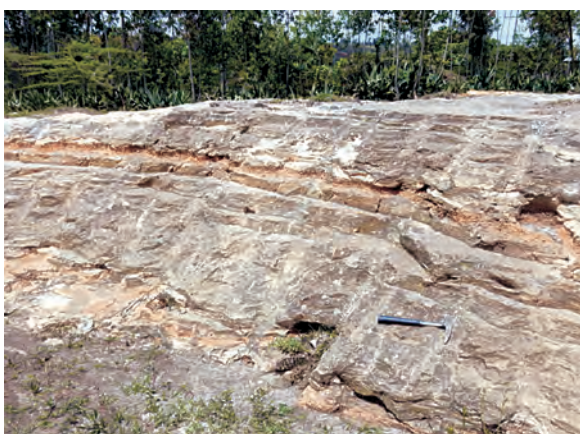

Figure 5-8. *Ash fall deposits with a layer of well-sorted pumice lapilli from the outcrop located N of the Moto village.*

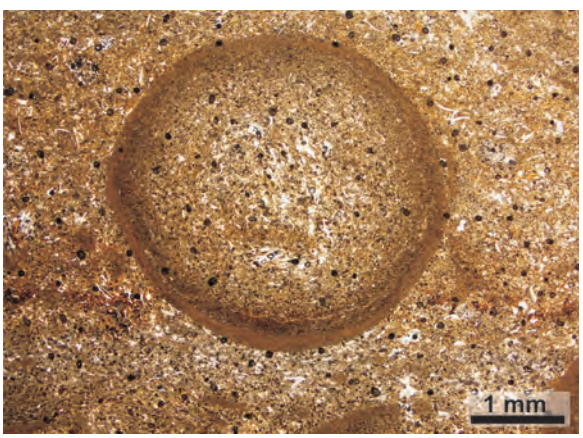

Figure 5-9. *Accretionary lapilli in ash fall deposits (an outcrop situated N of the Moto village, PPL.*

Figure 5-10. *Quarry situated in the southern part of the Boricha Dome.*

Figure 5-11. *Alkali feldspar phenocrysts in rhyolite from the Boricha Dome, XPL.*

rainfalls by sheet-flows or density currents. Alluvial fans are generally formed in the areas with an abrupt decrease in gradient. The sediments accumulate due to deceleration of flow at lower gradients. The alluvial fans occur at the mouths of valleys with streams emptying into lakes or in erosion valleys and gullies. Alluvial sediments comprise the re-deposited soil and fine- to medium-grained sands with a higher amount of weathered volcanic and volcaniclastic rocks. Angular clasts of pumice are common in sandy alluvial sediments. The thickness is estimated at several metres.

1. Fluvial sediments are preserved on floodplains along the river channels with a lower gradient. These sediments consist of silty and muddy unconsolidated material, locally with lenticular beds of gravel. The deposits are usually a few meters thick. Locally, wetlands formed on the surface of floodplains occur. The drainage pattern in the northern part of the area has a character of ephemeral streams due to erosion, resulting in a limited amount of fluvial sediments.

5.2 Geochemistry

TAS classification (diagram-Fig. 5-12a, total alkalis vs. SiO_2; LeBas et al., 1986) shows a bimodal basic–acid distribution of volcanic rocks based on relative proportions of alkalis and the silica content. Based on this diagram, the fiamme from Hantate is a welded ignimbrite that is subalkaline, being similar to that of the Hawasa ignimbrite. However, glass shards in groundmass of the Hawasa ignimbrites as well as the Chabi Rhyolites are alkaline to subalkaline. Ignimbrites and rhyolites straddle the subalkaline–alkaline boundary; however, all these samples exhibit a high Nb/Y ratio (Figure 5-12b; 1.19–1.87), which is typical for alkaline rocks (Pearce 1996). The Yubo basalt chemistry also corresponds to alkaline product. The K_2O contents in acid rocks are ranging from 4.6 to 5.2 wt. % (glass shards up to 6.0 wt. %), while the studied basalt has a relatively relatively low potassium content (0.9 wt. % K_2O). The basalt is enriched by Ti and depleted of Zr when compared to ignimbrite (Fig. 5-12b) and it is characterized by a high content of Na (K_2O/Na_2O = 0.3), whereas the studied ignimbrites are potassic (K_2O/Na_2O = 1.0–1.2; glass shards up to 1.4).

Chondrite-normalised REE patterns of basalt samples (Fig. 5-12c) display a gently decreasing trend from LREE to HREE (La_N/Yb_N = 7) and positive Eu anomalies (1.1). The distribution patterns of REE in the Hawasa ignimbrite and the Chabi rhyolites are characterized by the fractionation of LREE (La_N/Yb_N = 4–8), and a negative Eu anomaly (Eu/Eu*= 0.3–0.5). The total REE content of the basalt sample is low (121 ppm) in comparison to ignimbrite (512–660 ppm) and rhyolite (312–439 ppm).

Primitive mantle-normalised multi-element variation diagrams (Fig. 5-12d) for basalts show intraplate volcanic patterns with a decline in Pb and Th. The diagram for ignimbrite and rhyolite displays a marked decline in Ba, Sr, P and Ti, which is possibly caused by the fractionation of feldspars, apatite and/or Fe–Ti oxides.

5.3 K-Ar dating

The basic principles of the conventional K-Ar dating and applied experimental techniques using the radioactive decay of the ^{40}K isotope were described by Dalrymple and Lanphere

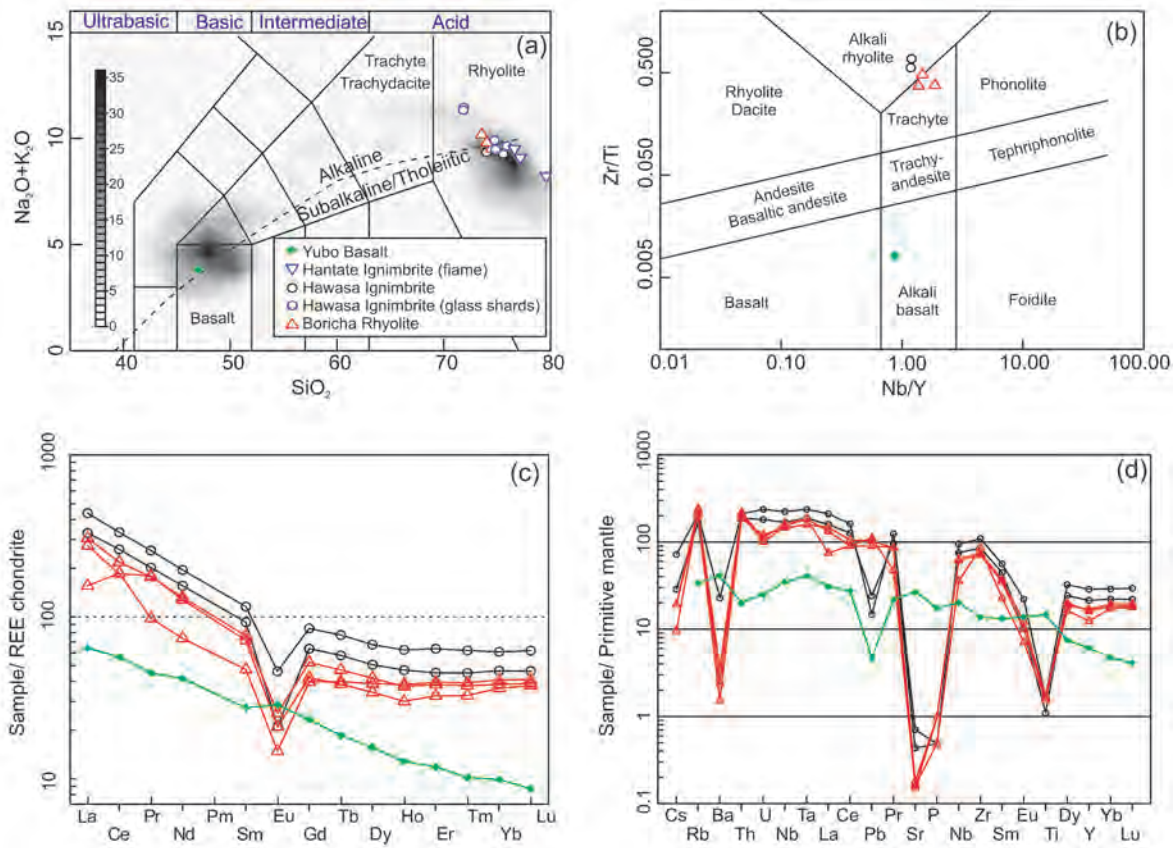

Figure 5-12. *Chemical composition of volcanic rocks: (a) Total alkalis ($Na_2O + K_2O$) vs. SiO_2 (TAS; LeBas et al., 1986); the filled contours in the background portray the frequency of other volcanic rocks in the southern MER (MacDonald and Gibson 1969; Brown and Carmichaeln 1969, 1971; Di Paola 1971, 1972; Bloomer et al. 1989; Hart et al. 1989; Asfaw et al. 1991; Zanettin et al. 1991; WoldeGabriel et al. 1991, 2005; Wolde and Widenfalk 1994; Stewart and Rogers 1996; Ayalew et al. 1999, 2002, 2006; George and Rogers 1999; Trua et al. 1999; Yemane et al. 1999; Katoh et al. 2000; Rogers et al. 2000; Furman et al. 2004; Haileab et al. 2004; Rooney 2010; Shinjo et al. 2011; Rooney et al. 2012; Wolela 2014; Rapprich et al. 2016); (b) Nb/Y vs. Ti/Zr discrimination diagram (Pearce 1996); (c) chondrite-normalised REE (rare earth element) patterns (values for normalization are based on Boynton 1984), (d) Primitive mantle-normalised multi-element variation diagrams (values for normalization are based on McDonough and Sun (1995).*

(1969). Approximately 0.05 g of finely grounded samples were digested in acids (HF, HNO_3) in teflon beakers and finally dissolved in 0.2 M HCl. Potassium was determined by flame photometry with a Na buffer and Li internal standard using Industrial M420 type flame photometer. Multiple runs of inter-laboratory standards (Asia1/95, LP-6, HD-B1, GL-0) indicated the accuracy and reproducibility of this method to be within 2%. Approximately 0.5 g of grounded samples were wrapped in aluminium foil and copper sieve preheated for about 24 h at 150-180 °C in vacuum. Argon was extracted under ultra-high vacuum conditions by RF induction heating and the fusion of rock samples in Mo crucibles. The gas was purified by Ti sponge and SAES St 707 type getters, to remove chemically active gas contaminants and some liquid nitrogen in a cold trap to remove condensable gases. The extraction line is linked directly to a mass spectrometer (90° magnetic sector type of 155 mm radius) using in static mode. Argon isotope ratios were measured by the ^{38}Ar isotope dilution mass spectrometric method, previously calibrated with atmospheric argon and international rock standards. Experimental details

of the K-Ar dating method were described in Balogh (1985). Age of the samples was calculated using the decay constants suggested by Steiger and Jäger (1977). Analytical error is given at 68% confidence level (1σ) using the equation of Cox and Dalrymple (1967).

The K-Ar dating result shows that the ignimbritic eruption occurred during at least three distinct phases in the central part of the MER, being of the Pleistocene-Holocene age (sample DE 159; Yerga Alem; 0.46 ± 0.05 Ma). The K-feldspar from the Hawasa ignimbrite (Mt. Kuwe SW of the Jara Damuwa town) has been dated using the K-Ar method (JICA 2012) at 1.28 Ma. Similar ages (1.1–1.85 Ma, K-Ar) are also given by Wolde-Gabriel et al. (1999). Rhyolites from the Boricha ridge were dated at 2.49 Ma (WoldeGabriel et al. 1990)

5.4 Structural and tectonic patterns

The Leku map sheet is localised at the border of the central and southern part of the NNE–SSW trending Main Ethiopian Rift (e. g. Hayward and Elbinger 1996; Bonini et al. 2005). The Main Ethiopian Rift (MER) underwent a typical evolution of continental rifting from continental extension (transtension) toward extensive bimodal volcanic activity and fault-dominated morphology during a break-up due to extension between the Nubian and Somalian plates (e. g. Agostini et al. 2011; Accocella 2013). The mapped area is built by post-rift effusive rocks and volcanoclastic deposits (rhyolites, ignimbrites and related pyroclastic deposits) of Pleistocene ages. A set of primary fabrics (flow foliation and bedding) and brittle rift-related structures (normal faults and extensional joints) were identified in the mapped area (Fig. 5-13).

Primary structures

Ignimbites and related volcaniclastic deposits (unwelded pyroclastic fall deposits and ash-flows) reveal a predominantly sub-horizontal to roughly NW–SE or NNE–SSW gently dipping bedding planes (Fig. 5-14) defined by the planar preferred orientation of high-porosity fragments of volcanic glass or pumice (fiamme) and gently elongated micro-vesicles or micro-crystals (Fig. 6-15). The origin of these planar structures is interpreted to be related to the flow-stretching of viscous lava or hot glass fragments formed during the flow of mainly clastic ignimbrites. The rare moderately to steeply dipping flow-foliation is likely to reflect minor morphological inequalities or represent marginal parts of partial volcanic flows. Contacts of individual flows, beds and lithological boundaries are mostly subparallel to the bedding planes. Original boundaries have been locally modified by normal faulting or related exodynamic processes (e.g. landslides and rock-falls). In the rhyolite dome (Boricha Rhyolite), a steeply to moderately WNW or ESE dipping flow-foliation defined by irregular compositional banding was identified (Fig. 5-14). Minor lacustrine sediments of Pleistocene to Holocene age cropping out around the Lake Awasa show scarce horizontal bedding.

Brittle structures

Several brittle structures such as extensional joints, normal faults and fault zones were observed in the mapped area. Predominant faults are mostly parallel to the axis of the rift, forming prominent morphological features of the rift system. These regional faults dip

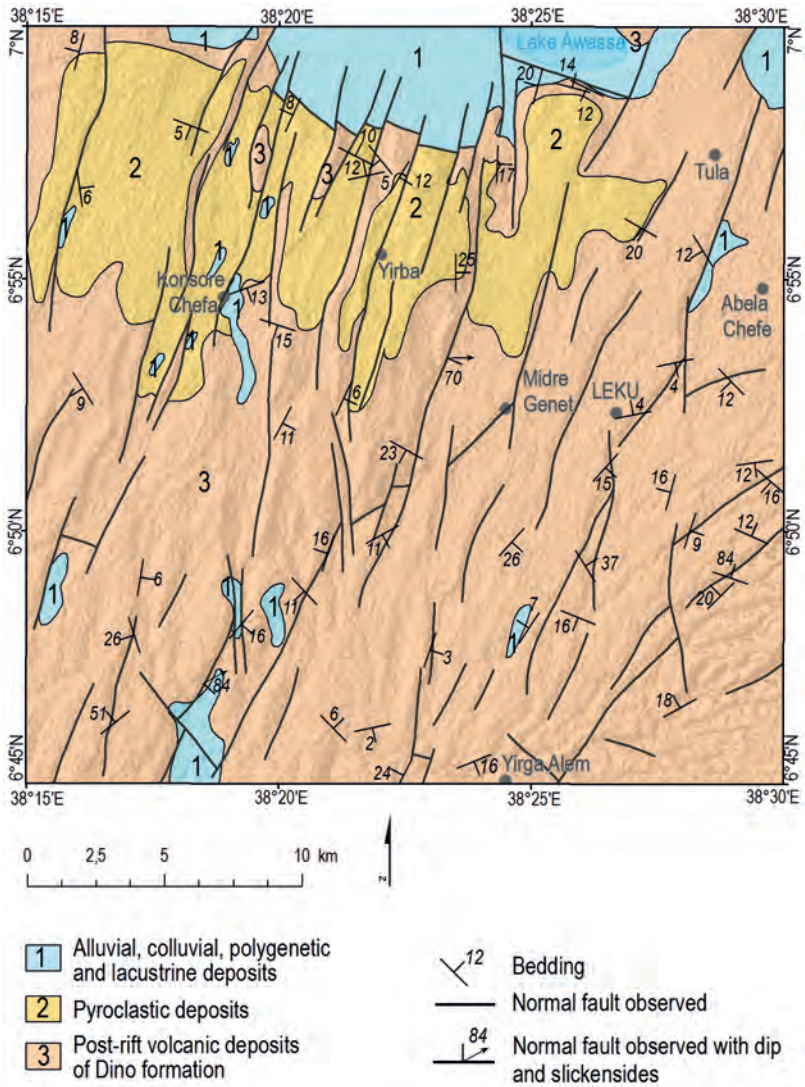

Figure 5-13. *Structural scheme of the Leku map sheet showing regional fault pattern and bedding in volcano-sedimentary rocks.*

steeply to ESE or WNW (Fig. 5-15). A relatively younger, sharply superimposed set of roughly N(NNW)–S(SSE) trending faults associated with the "Wonji Fault Belt" was identified in the central part of the mapped area. These younger faults have a fault lineation (slickensides) plunging steeply to moderately to ESE to NE bearing an evidence of normal kinematics. In addition, two subordinate sets of normal faults were identified in the area (Fig. 5-17): (a) steeply ~N(NNW) dipping faults with steeply plunging slickensides perpendicular to the regional faults, and (b) minor moderately to steeply dipping faults roughly of a NW–SE strike. A left-lateral strike-slip component was also observed at few localities. The frequency of each set of normal faults is shown in Fig. 5-17.

Three distinct sets of extensional joints similar in all mapped lithologies with no evidence of movement along the joint plane were identified across the mapped area (Fig 6-15). The most prominent joints run N(NNE)–S(SSW) and E(ESE)–W(WNW). Minor subvertical joints dip to the NE or SW. Their orientation is largely consistent with the fault pattern.

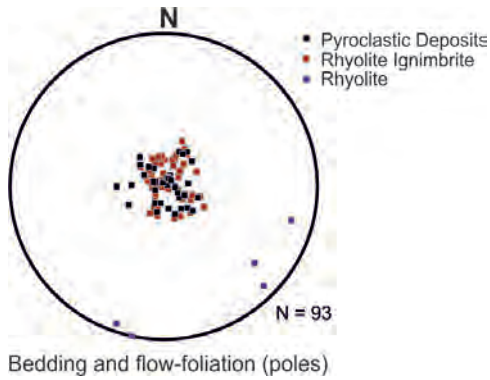

Figure 5-14. *Orientation diagram of the primary structures in post-rift volcano-sedimentary sequences of the Dino Formation – Bedding planes in rhyolite ignimbrites and pyroclastic deposits; flow-foliation in rhyolites. Equal projection to the lower hemisphere.*

Figure 5-15. *Bedding in unwelded pyroclastic fall deposits and minor ash-flows affected by NNE-SSE trending normal fault (west of Chirecha village).*

Figure 5-16. *Moderately dipping flow-foliation in rhyolite (Boricha Rhyolite Dome).*

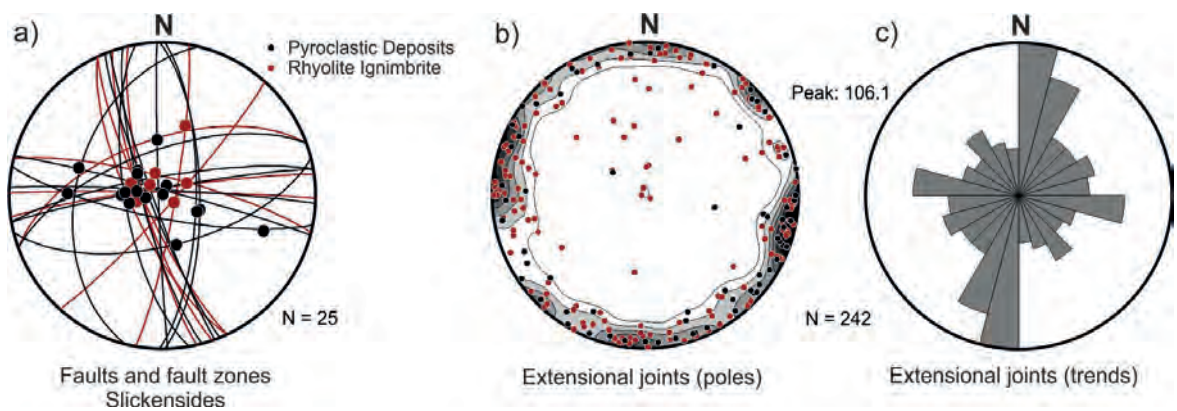

Figure 5-17. *Orientation diagrams of brittle structures in a post-rift sequence (red – rhyolite ignimbrites; black – unwelded pyroclastic fall deposits). (a) – normal faults and fault zones with steeply plunging slickensides; (b) – extensional joints and (c) – rose diagram showing trends in extensional joints in all units. Equal projection to the lower hemisphere.*

6) SOIL ENVIRONMENT

Soils are formed through the interaction of five major factors: time, climate, parent material, topography and organisms. The combination of all five factors determines the kind of soil development and soil distribution in the area. The relative influence of each factor varies from place to place, particularly in the areas with a great diversity of the soil-forming factors. Due to the very limited data available from the area, much effort has been made to obtain representative profiles and for the characterization of the soil environment in the current study. A detailed description of the soil-forming factors affecting the soil development in the study area is given in the second section.

6.1 Methods and samples

The soil survey was carried out randomly within the area of the map sheet. Various road cuts, dry river beds and other areas where a cross section of the soil profile is exposed, and other visible features (soil surface colour, rock outcrops) were used in the field work for the identification of major soil types. A soil core sampler was used on a flat terrain. Soil profiles were described according to the Guidelines for soil description (FAO 2006), photographed and documented using georeferencing by GPS at each site. A set of soil profiles was described and classified according to the latest update of the World Reference Base for Soil Resources system (IUSS Working Group WRB 2015). The classification of soils is based on soil properties defined in terms of diagnostic horizon, diagnostic properties and diagnostic materials, which should be measurable and observable in the field to the greatest extent possible. The WRB describes the soils by using two categorical details: the first level includes the Reference Soil Groups (RSG), the second level consists of the name of the RSG combined with a principal and supplementary qualifiers.

The disturbed soil samples of at least 1kg were taken from A horizons and B horizons (in the ABC soil profiles) or from A horizons (in the AC soil profiles), whose depths differ at various locations depending on the type of soil in order to complete the field observations of soil profiles with the necessary soil analytical data. The samples were delivered to the National Reference Laboratory of the Central Institute for Supervising and Testing in Agriculture in Brno for selected laboratory physico-chemical analyses. All samples from the profiles were dried, ground and sieved through a 2 mm sieve. The analyses have been done on the fine-earth (≤ 2 mm) fraction. The analytical procedures were conducted according to the Unified Working Procedures (Zbíral 2000) in order to analyze the following parameters:

- Particle size distribution (sand, silt, clay content) using the pipette method for the analysis of particle size fractions defined according to the Guidelines for soil description FAO (2000-63-2µm system),
- pH in H_2O and in 1M KCl,
- Cation exchange capacity (CEC) by the Mehlich method,
- Sum of base cations and base saturation (BS),

- Available nutrients P, K, Ca, Mg extracted by the Mehlich III method,
- Soil carbonates determination by the gravimetric method.

Total organic carbon (TOC) was determined in the laboratories of the Czech Geological Survey using an infrared analyzer.

A map of the spatial extent and distribution of the major reference soil groups was constructed. The final soil map is based on the geological map, results of the soil survey, aerial photos and topography. It can be said that if certain properties of soils from different parent materials under certain climate, vegetation, and topographic conditions are known, then the prediction of expected soil characteristics by looking only at the types of parent materials is possible (Gökbulak and Özcan, 2008). If the bedrock is identical, then the most important soil-forming factor is relief. This presumption permits the basic prediction of the soil spatial distribution and construction of a soil map in the case of limited resources for a systematic and detailed soil survey.

6.2 Reference Soil Groups in the study area

Soils are distributed over the landscape in relation to landforms, parent material and drainage pattern. The mapped area belongs to the rift floor zone near the Eastern Rift Valley escarpment. Its soil cover can be characterized by the following major Reference Soil Groups (RSG). *Fluvisols* cover polygenetic sediments (alluvial and resedimented pyroclastics) in the lowest part of the mapped area along the shores of the Lake Awasa (Awasa caldera) and fluvial and lacustrine sediments in the endorheic depressions and rare floodplains. The dissected plain forming the Rift valley floor in the mapped area is covered by various soils. *Chromic Luvisols* (and) are frequently encountered as well as *Nitisols*, while the occurrence of *Vertisols* depends on the position of relief and they are not distributed over larger areas. Nitisols occur predominantly in the SE part of the area, where the Rift escarpment is gradually rising. Many soils in the area are young soils developed on pyroclastic and strongly weathered layers, which have been deposited on top of former soils. These young soils (*Andosols, Regosolsand Cambisols)* often have a shallow depth. Severe erosion and land degradation occur in the mapped area. The gullies deeply incised into the soils and underlying layers and the barren and degraded badlands with a total soil loss (the soil is washed out). The highly eroded area and slopes with thin and stony soils are related to the occurrence of *Leptosols.*

Luvisols (LV)

Luvisols are moderately weathered soils and they occur on relatively young surfaces in the tropics. Luvisols have a higher clay content in the subsoil than in the topsoil as a result of pedogenetic processes (especially clay migration) leading to an *argic* subsoil horizon. An *argic* horizon is a subsurface horizon with distinctly higher clay content than the overlying horizon. Luvisols have high-activity clays throughout the *argic* horizon and a high base saturation at the 50–100 cm depth. Cation exchange capacity (CEC) equals to or more than 24 cmol per kg of clay throughout the argic horizon. The "*illuvial"* nature of the argic horizon may be established using a ×10 hand lens. If clay coatings occur on soil aggregate surfaces, in fissures, in pores and in channels – "illuvial" argic horizons show clay coatings on at least 5% of both horizontal and vertical aggregate faces, and

Figure 6-1. *Chromic Luvisol.*

in the pores. The "illuvial" character of an argic horizon can best be established using thin sections. Diagnostic "illuvial" argic horizons show areas with oriented clays that constitute on average ≥ 1% of the entire cross-section. Other tests involved are the particle-size distribution analysis to determine the increase in clay content over a specified depth, and the fine clay/total clay ratio. In the "illuvial" argic horizons, the fine clay to total clay ratio is larger than in the overlying horizons, due to the preferential eluviation of fine clay particles (IUSS Working Group WRB 2015).

Textural differentiation is the main feature for the recognition of argic horizons. An argic horizon has a texture class of loamy sand or finer and ≥ 8% clay. If the coarser textured horizon has ≥ 10 and < 50% clay in the fine earth fraction, the ratio of clay in the argic horizon to that of the coarser textured horizon is ≥ 1.4. (The fine earth fraction is obtained by sieving the dry sample with a 2mm sieve).

Luvisols have favourable physical properties. They have granular or crumb surface horizons that are porous and well aerated. The `available' moisture storage capacity is the highest in the argic horizon. The argic horizon has a well-developed stable blocky structure, which contributes to a good water-holding capacity. Nevertheless, the surface topsoils with high silt content may be susceptible to erosion.

The chemical properties of Luvisols vary with the parent material and pedogenetic history. Surface soils are usually wholly or partly decalcified and slightly acidic in reaction. Table 6-2 shows the soil reaction (pH/H_2O) neutral on the surface to moderately alkaline in the subsurface horizon, which corresponds to base saturation (from a moderately saturated surface to a completely saturated subsurface horizon). This is related to the high content of base cations (K, Ca, Mg) in a particular profile. The subsurface horizons of Luvisoils tend to have higher pH values.

Soil pH (KCl) values are less than pH (H_2O) and the ΔpH = pH(KCl) – pH(H_2O). This indicates a net negative charge of the soils (Yavitt and Wright 2002). Low negative ΔpH values are reported to indicate the presence of variable charge constituents in soils (Auxtero et al. 2003). The water dispersible clay contents of the soils are positively correlated with Δ pH values. The more negative the Δ pH values, the higher the amounts of water-dispersible clay. This indicates the association between surface charge condition and clay dispersion in soils. Luvisols contain a few percent of organic matter. The content of the total organic carbon (TOC) can be converted to the soil organic matter (SOM) by using a conversion factor of 1.724: SOM (%) = TOC (%) x 1.724. This conversion factor assumes that organic matter contains 58 % organic carbon (however, this can vary with the type of organic matter, soil type and soil depth). Luvisols are fertile soils, suitable for a wide range of agricultural uses if managed appropriately. They require erosion control measures on slopes.

Figure 6-2. *Rill erosion on a dirt road in Skeletic Luvisols.*

Luvisols share common properties with many other Reference Soil Groups. For example, Luvisols occurring together with *Vertisols* may have *slickensides* in the argic horizon, but do not meet the other criteria of a vertic horizon.

Table 6-1. Soil particle distribution within the Luvisol profile (JJ041) and some diagnostic criteria

Horizon	Sand (%)	Silt (%)	Clay (%)	clay B/ clay A	silt/clay	Texture
A	34.14	31.68	34.18	1.4	0.93	clay loam
Bt	16.27	37.21	46.52		0.80	Clay

Table 6-2. Selected chemical characteristics of the sampled Luvisol profile (JJ041)

Horizon	pH/ H_2O	pH/ KCl	Δ	P	K	Ca	Mg	TOC*	CEC	BS	$CaCO_3$
			pH	mg/kg	mg/kg	mg/kg	mg/kg	%	$cmol_c/kg$	%	%
Ap	6.70	5.40	–1.3	<3.5	529	1276	133	1.47	16.38	63.67	< 0.20
Bt	8.10	5.60	–2.5	<3.5	248	8616	708	1.86	30.07	100.00	< 0.20

Nitisols NT

Nitisols have developed from pyroclastic rocks in the mapped area. They are mostly found in the upper and middle slope position and they are classified as Vertisols or vertic units of other RSG towards the lower slope sections and/or bottom lands.

Nitisols are deep, well-drained, red tropical soils with diffuse horizon boundaries and a clayey *nitic* horizon that has a typical angular blocky structure breaking into polyhedral or flat-edged or nut-shaped elements with, in the moist state, shiny aggregate faces, which cannot or can only partially be attributed to clay illuviation. The nitic horizon is a clay-rich

subsurface horizon with at least 30 percent clay and the silt to clay ratio < 0.4. The difference in clay content between the overlying and underlying horizons is gradual or diffuse. Similarly, there is no abrupt colour difference within the horizons directly above and below. The colours are of a low value with hues often at 2.5YR, moist, but sometimes redder or yellower. These soils are predominantly derived from basic parent rocks by strong weathering (IUSS Working Group WRB 2015).

The rapid rate of weathering in the tropics is responsible for the leaching of basic cations and relative accumulation of Fe and Al oxides in soils. Iron oxides influence the physical and chemical properties of the highly weathered soils that contain kaolinite as the major clay mineral. Goethite and hematite are responsible for the yellow-brown and red pigment, respectively. Iron oxides are involved in the retention of anions such as phosphate due to their smaller crystal size and reactive surface sites (Singh and Gilkes 1992). In the sub-humid tropical climate, the alternating dry and wet seasons and the relatively drier environment may affect the composition of Fe-oxide and silicate clay species and the formation from various parent materials.

The exact origin of the shiny faces of the polyhedral, flat-sided or nutty elements typical for the nitic horizon is still under debate. The development of these typical nitic properties, or the nitidization process, is assumed to be related to the alternation of micro-swelling and shrinking (Driessen et al., 2001). The soil moisture regime plays an important role because it influences the degree of swell–shrink behaviour, which will be the strongest in a climate with contrasting wet and dry seasons. Contributing factors to Nitisol development are: (i) the presence of open 2/1 clays besides the dominant kaolinite, resulting in a relatively high water-dispersible clay content and a high swell-shrink potential, (ii) seasonal cycles of wetting and drying, contributing to a strong blocky soil structure development, (iii) recurrent conditions of weak temporary

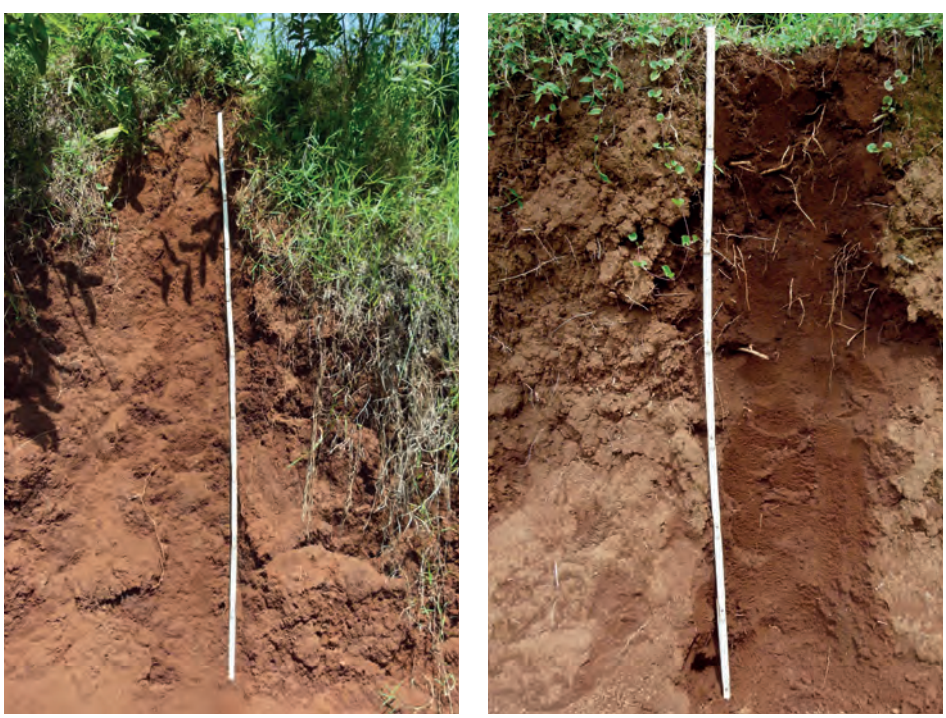

Figure 6-3. *Dystric Nitisols (JJ046 left and JJ047 right).*

hydromorphism, resulting in the redistribution of Fe-Mn oxides, and (iv) exceptional Fe oxide characteristics, particularly an extremely small particle size. Together with the presence of abundant clay coatings, these Fe oxide characteristics explain the shiny aspect of ped faces that is characteristic of nitic horizons (De Wispelaere 2015).

Table 6-3. Soil particle distribution within Nitisols profiles and some diagnostic criteria

Sample	Hor.	Munsell Colour	Sand (%)	Silt (%)	Clay (%)	clay B/ clay A	silt/clay	Texture
JJ046A	A	5 YR 2/4	21.10	37.33	41.57	1.5	0.90	Clay
JJ046B	Bt	5 YR 2/4	18.89	18.55	62.56		0.30	Clay
JJ047A	A	5 YR 2/4	19.38	34.43	46.19	1.2	0.75	Clay
JJ047B	Bt	5 YR 2/4	17.43	25.63	56.94		0.45	Clay

An important criterion used in the classification of tropical soils is the silt/clay ratio. It is also used in the evaluation of clay migration, degree of weathering and the age of parent material and soils. The more highly weathered a soil is, the lower the silt fraction. Therefore, soils with a silt/clay ratio of less than 0.15 are regarded as highly weathered (Van Wambeke, 1962). The silt to clay ratio < 0.4 is an important diagnostic criterion of *nitic* horizons.

Table 6-4. Selected chemical characteristics of the sampled Nitisol profiles

Sample	Hor.	pH/ H_2O	pH/ KCl	Δ	P	K	Ca	Mg	TOC	CEC	BS
				pH	mg/kg	mg/kg	mg/kg	mg/kg	%	$cmol_c/kg$	%
JJ046A	A	4.90	4.00	–0.9	< 3.5	205	1388	233	3.48	22.55	38.36
JJ046B	Bt	5.20	3.80	–1.4	< 3.5	176	645	148	0.83	21.33	25.22
JJ047A	A	4.50	3.90	–0.6	< 3.5	86	665	113	2.25	23.66	22.53
JJ047B	Bt	4.80	3.90	–0.9	< 3.5	174	571	85	0.86	16.23	17.88

Nitisols are strongly weathered soils, but far more productive than other red tropical soils. They are generally considered as fertile soils, in spite of their low level of available phosphorus and their normally low base status. The CEC is higher compared to other soils of the tropics (Ferralsols, Lixisols, Acrisols) due to the high clay content. Although the clay assemblage is dominated by low-activity clays, the clay content is high (more than 30 percent and not seldom more than 60 percent), and soil organic matter makes a considerable contribution to the overall CEC.

The deep and porous solum and the stable soil structure of Nitisols permit deep rooting and make these soils quite resistant to erosion. The good workability of Nitisols, their good internal drainage and fair water holding properties are complemented by chemical (fertility) properties that compare favourably to those of most other tropical soils.

Nitisols have relatively high contents of weathering minerals, and surface soils may contain several percent of organic matter, in particular under forest or tree crops. Nitisols are planted with plantation crops, such as coffee and are also widely used for food crop production on smallholdings.

Vertisols (VR)

Vertisols occurrence in the mapped area follows the common toposequences with Luvisols and/or Nitisols on slopes and Vertisols in low-lying positions in tropical regions. The typical configuration of "red-black" soil catena features red soils on crest and upper slopes (Luvisols, Nitisols), shallow or moderately deep red soils (Leptosols, Cambisols) on steeper sections of the slope and black Vertisol on lower positions. The combined processes of rock weathering, breakdown of primary and formation of secondary minerals, and transport of soil components produce the typically catenary differentiation with reddish well-drained soils on higher positions, and black, poorly drained soils in depressions. Leached soil components accumulate at poorly drained, lower terrain positions, where they precipitate and form new smectite clays that remain stable as long as the pH is above neutral (Driessen et al. 2001).

The environmental conditions that lead to the formation of a *vertic* soil structure: rainfall must be sufficient to enable weathering, but not so high that leaching of bases occurs; dry periods must allow the crystallization of clay minerals that form upon rock or sediment weathering, drainage must be impeded to the extent that leaching and loss of weathering products are curbedand finally, high temperatures promote weathering processes. Under such conditions, smectite clays can be formed in the presence of silica and basic cations – especially Ca^{2+} and Mg^{2+} – if the soil pH is above neutral.

Vertisols are recognised because of their clayey textures, dark colours and special physical properties. Vertisols are heavy clay soils with a high proportion of swelling clays. The alternate swelling and shrinking of expandable clays result in deep cracks in the dry season, and in the formation of slickensides and wedge-shaped structural elements in the subsoil. Shrink-swell behaviour may also cause gilgai microrelief to form, especially

Figure 6-4. *Pellic Vertisols.*

in drier climates. Vertic horizons are clayey and when dry, they often have a hard to very hard consistency. Polished, shiny surfaces (*slickensides*), often at sharp angles, are distinctive (IUSS Working Group WRB 2015).

Important morphological characteristics such as soil colour, texture, element composition, etc. are all uniform throughout the solum. There is hardly any movement of soluble or colloidal soil components.

Several other diagnostic horizons in the mapped area may also have high clay contents, e.g. the *argic* and *nitic* horizons. Although some of them may qualify as vertic horizons, most of them lack the characteristics typical of the vertic horizon. However, they may be laterally linked in the landscape with the vertic horizon, the latter usually taking up the lowest position.

Shrink-swell phenomena result from the interactions among mineralogical, physical and chemical properties of Vertisols (Tables 6-5 and 6-6).

Table 6-5. Colour and textural characteristics of Vertisols in the mapped area

Sample	Hor.	Munsell Colour	Sand (%)	Silt (%)	Clay (%)	silt/clay	Texture
JJ040	A	10 YR2/1	8.99	18.11	72.90	0.25	clay
DE198	A	10 YR2/1	14.78	29.98	55.24	0.54	clay

Table 6-6. Selected chemical characteristics of Vertisols in the mapped area

Sample	Hor.	pH/ H_2O	pH/ KCl	Δ	P	K	Ca	Mg	TOC	CEC	BS
				pH	mg/kg	mg/kg	mg/kg	mg/kg	%	$cmol_c/kg$	%
JJ040	A	7.40	5.90	–1.5	<3.5	380	2424	228	1.14	40.62	95.31
DE198	A	6.00	4.90	–2.0	<3.5	327	4574	359	1.80	37.27	76.37

Most Vertisols generally have a high cation exchange capacity (CEC) and a high base saturation (BS). The soil reaction varies from weakly acid to weakly alkaline; pH-values are in the range of 6.0 to 8.0. The CEC of the soil material is commonly between 30 and 80 cmol(+)/kg for a dry soil; the CEC of the clay is in the order of 50 to 100 cmol(+)/kg of clay. The base saturation percentage is greater than 50 and often close to 100% with Ca^{2+} and Mg^{2+} occupying more than 90% of the exchange sites.

Although their high natural fertility and positive response to management make Vertisols attractive for agriculture, some of their other properties impose critical limitations on low-input agriculture. The inherent limitations of Vertisols are largely a function of the moisture level of the soils and the narrow range of moisture conditions within which the mechanical operations can be conducted. Farmers using traditional methods of agriculture are aware of the high risks associated with the use of these soils.

The physical properties and the soil moisture regime of Vertisols represent serious management constraints. The heavy soil texture and domination of expanding clay minerals result in a narrow soil moisture range between moisture stress and water excess. Tillage is hindered by stickiness when the soil is wet and by hardness when it is dry. The susceptibility of Vertisols to waterlogging is the single most important factor that

Figure 6-5. *Surface drainage of Vertisols.*

reduces the actual growing period (below the estimates based on climatic data). Excess water during the rainy season must be stored for a post-rainy season use (water harvesting) on Vertisols with very slow infiltration rates.

Infiltration of water in dry (cracked) Vertisols with surface mulch or a fine tilth is initially rapid. However, once the surface soil is thoroughly wetted and cracks have closed, the rate of water infiltration becomes almost zero. (The very process of swell/shrink implies that pores are discontinuous and non-permanent.) If, at this stage, the rains continue (or irrigation is prolonged), Vertisols flood readily. The highest infiltration rates are measured on Vertisols that have a considerable shrink/swell capacity, but maintain a relatively fine class of structure. Not only the cracks transmit water from the (first) rains, but also they open spaces between slickensided ped surfaces that developed as the peds shrunk.

Data on the water holding capacity of Vertisols vary widely, which may be attributed to the complex pore space dynamics. Water is adsorbed on clay surfaces and retained between crystal lattice layers. Vertisols are soils with good water holding properties. However, large proportions of all water in Vertisols, and notably the water held between the basic crystal units, are not available to plants.

Vertisols in subhumid and humid areas have been put to a wide range of uses. A major part is still used as a pasture, because tillage constraints have prevented these soils from being cultivated. Under rainfed conditions, and depending on the temperature regime, Vertisols produce wheat, maize, sorghum, soybeans, cassava or pigeon peas. Under irrigation, Vertisols grow rice, sugarcane and cotton. Irrigation has to be adjusted to an initially fast infiltration through cracks and a subsequent slow and rather shallow uptake of water when the cracks are closed.

Andosols (AN)

The Reference Soil Group of the *Andosols* includes the soils developed in volcanic materials with andic properties. Volcanic rocks, especially pyroclastic, contain volcanic glass that weathers easily and accounts for the remarkable properties that the soils in most volcanic regions have in common. Translocations of weathering products and accumulation of short-range-order minerals and stable organo-mineral complexes are essential processes in the formation of the characteristic soils of volcanic regions: *Andosols*.

Andic properties result from the moderate weathering of mainly pyroclastic deposits. The presence of short-range-order minerals and/or organometallic complexes is characteristic of andic properties. These minerals and complexes are commonly a part of the weathering sequence in pyroclastic deposits (*tephric* soil material > *vitric* properties > andic properties).

Andic properties may be found at the soil surface or in the subsurface, commonly occurring as layers. Many surface layers with andic properties contain a high amount of organic matter (≥ 5%), are commonly very dark coloured (the Munsell colour value and chroma of ≤ 3 moist), have a fluffy macrostructure and a smeary consistence in some places. They have a low bulk density and commonly have a silt loam or finer texture. Andic surface layers rich in organic matter may be very thick, having a thickness of ≥ 50 cm in some soils. Andic subsurface layers are generally somewhat lighter coloured.

Andic layers may have different characteristics, depending on the type of the dominant weathering process acting upon the soil material. They may exhibit thixotropy, i.e. the soil material changes under pressure or by rubbing, from a plastic solid into a liquefied stage and back into the solid condition. Two major types of andic properties are recognized: one in which allophane, imogolite and similar minerals prevail (the *silandic* type); and one in which Al complexed by organic acids prevails (the *aluandic* type). The silandic property typically gives a strongly acid to neutral soil reaction and is a bit lighter coloured, while the aluandic property gives an extremely acid to acid reaction and a blackish colour (IUSS Working Group WRB 2015).

The genesis of Andosols is further complicated if there is a repeated deposition of fresh ash. Thin ash layers may just rejuvenate the surface soil material, but thicker layers bury the soil. A new profile will then develop in the fresh ash layer, while soil formation in the buried A-horizon takes a different course in response to the suddenly decreased organic matter supply and the different composition of the soil moisture.

The clay assemblage of Andosols changes over time; particularly that of the subsoil as allophane and imogolite are transformed to halloysite, kaolinite or gibbsite (depending on the silica concentration of the soil solution). Aluminium from the Al-humus complexes will gradually become available and ferrihydrite will eventually turn into goethite. All these processes are strongly influenced by such factors as the rate of rejuvenation, the depth and composition of the overburden, the composition of the remaining material and the moisture regime. Eventually, an Andosol may grade into a 'normal' soil, e.g. a soil with clay illuviation (Driessen et al. 2001).

Andosols occur together with almost any other RSG. A typical configuration on mountain slopes would place Andosols at the higher end of the slope, *Cambisols* and *Luvisols* at mid-slope positions and *Vertisols* (basic volcanic materials) or *Acrisols* (acidic materials) near the foot of the slope. In the Ethiopian Highlands, Andosols are often associated with *Nitisols*.

Figure 6-6. *Vitric Andosol (Thaptomollic) (left) and Mollic Andosol (Thaptovitric) from tuff (right).*

Many young soils developed on pyroclastic layers, which have been deposited on top of former soils in the studied part of the Rift Valley, are not Andosols but weakly developed Cambisols (according to discolouration and/or structure).

Andosols have highly variable exchange properties: the charge is strongly dependent on pH and electrolyte concentration. With charge properties variable, base saturation values are also variable. Base saturation values are generally low because of strong leaching, except for some very young Andosols and for Andosols in dry regions (Table 6.6).

Andosols have a high potential for agricultural production, but many of them are not used to their potential. Andosols are generally fertile soils, particularly those in intermediate or basic volcanic ash and the ones not exposed to excessive leaching. The strong phosphate fixation of Andosols (caused by active Al and Fe) is a problem. Ameliorative measures to reduce this effect include the application of lime, silica, organic matter and phosphate fertilizer.

Andosols have favourable properties for cultivation, plant roots and water storage. Strongly hydrated Andosols are difficult to till because of their low bearing capacity and

Table 6-7. Colour and textural characteristics of Andosols sampled in the study area

Sample	Hor.	Munsell Colour	Sand (%)	Silt (%)	Clay (%)	silt/clay	Texture
JJ043	A	7.5 YR 3/2.5	41.46	40.69	17.85	2.27	loam
JJ045A	A1	7.5 YR 2/3	48.56	27.99	23.45	1.19	sandy clay loam
JJ045B*	A2	7.5 YR 2/2	24.17	38.56	37.27	0.22	clay loam
JJ049	A	10 YR 2/2	27.79	53.21	19.00	2.8	silt loam

Table 6-8. Selected chemical characteristics of Andosols in the study area

Sample	Hor.	pH/ H_2O	pH/ KCl	Δ	P	K	Ca	Mg	TOC	CEC	BS
				pH	mg/kg	mg/kg	mg/kg	mg/kg	%	$cmol_c/kg$	%
JJ043	A	6.30	4.90	–1.4	< 3 .5	578	1854	275	1.88	16.89	76.04
JJ045A	A	6.90	5.80	–1.1	< 3.5	768	2103	256	1.47	15.58	74.02
JJ045B*	A2	6.00	4.50	–1.5	< 3.5	353	2589	332	1.69	21.11	53.47
JJ049	A	7.80	6.20	–1.6	< 3.5	1735	3085	434	1.57	16.99	52.40

their stickiness. Andosols are planted with a wide variety of crops including sugar cane, tobacco, sweet potato (tolerant to low phosphate levels), vegetables, wheat, and orchard crops. Andosols on steep slopes are perhaps best kept under forest. Paddy rice cultivation is a major land use of Andosols in lowlands with shallow groundwater.

Cambisols CM

The Reference Soil Group of Cambisols comprises soils with an incipient soil formation. The beginning transformation of soil material is evident from weak, mostly brownish discolouration and/or structure formation below the surface horizon. In the tropics, cambisols occur predominantly at medium altitudes in hilly and mountain regions, but also in deposition areas and in eroding lands at lower altitudes, where they occur alongside genetically mature residual soils.

Cambisols are soils having at least the beginnings of the development of a *cambic* horizon. The cambic horizon is a subsurface horizon showing the evidence of pedogenetic alteration that ranges from weak to relatively strong. The cambic horizon has lost, at least in half of the volume of the fine earth fraction, its original rock structure. If the underlying layer has the same parent material, the cambic horizon usually shows higher oxide and/or clay contents than this underlying layer. The pedogenetic alteration of a cambic horizon can also be established by comparison with one of the overlying mineral horizons that are generally richer in organic matter, and therefore have a darker and/or less intense colour. In this case, some soil structure development is needed to prove pedogenetic alteration. The cambic horizon can be considered as the predecessor of many other diagnostic horizons, which have specific properties that are not recognized in the cambic horizon – such as illuvial or residual accumulations or the development of a specific soil structure (IUSS Working Group WRB 2015).

Appreciable quantities of weatherable minerals and absence of any signs of advanced pedogenesis evidence the fact that Cambisols are in an early stage of the soil formation. There are, however, signs of incipient weathering/transformation of primary minerals in a situation of free internal and external drainage. Hydrolysis of iron-containing minerals (biotite, olivine, pyroxenes, amphiboles, etc.) in a weakly acidic environment produces ferrous iron that is oxidized to ferric oxides and hydroxides (e.g. goethite, hematite). This *`free iron'* coats sand and silt particles, and cements clay, silt and sand to aggregates. The soil becomes structured and yellowish brown to reddish in colour. Aluminium oxides and hydroxides, and silicate clays are formed in addition to ferric oxides. There may be some leaching of bases, but no clear migration of Fe, Al, organic matter or clay (Driessen et al. 2001).

Figure 6-7. *Chromic Cambisol from tuff deposited on top of a buried soil (left) and Eutric Cambisol from ignimbrite on the caldera rim (right).*

The processes that lead to the formation of a cambic subsurface horizon are fundamentally the same in all climate zones, but the intensities of chemical and biological transformations are considerably greater in the sub-humid and humid tropics than elsewhere. In the tropics, Cambisols can form in a few years.

Table 6-9. Colour and textural characteristics of the Cambisol profile

Sample	Horizon.	Munsell Colour	Sand (%)	Silt (%)	Clay (%)	Texture
JJ038A	A	7.5 YR 3/3,	14.18	43.56	42.26	silty clay
JJ038B	Bw	7.5 YR 3/4	10.48	60.12	29.40	silty clay loam
JJ039A	A	7.5 YR 3/3	24.92	32.48	42.60	clay
JJ039B	Bw	7.5 YR 3/4	17.33	46.64	36.03	silty clay loam

Table 6-10. Selected chemical characteristics of the Cambisol profile

Sample	Hor.	pH/ H_2O	pH/ KCl	Δ	P	K	Ca	Mg	TOC	CEC	BS
				pH	mg/kg	mg/kg	mg/kg	mg/kg	%	$cmol_c/kg$	%
JJ038A	A	5.40	4.00	–1.4	< 3.5	251	3288	557	1.83	32.94	76.15
JJ038B	Bw	6.20	4.70	–1.5	< 3.5	195	4457	608	2.30	35.20	87.15
JJ043A	A	6.20	4.80	–1.4	< 3.5	289	2178	332	2.30	21.04	58.14
JJ043B	A	6.30	4.50	–1.8	< 3.5	202	1496	262	0.80	17.11	69.39

The most Cambisols contain at least some weatherable minerals in the silt and sand fractions and most Cambisols are medium-textured and have a good structural stability, a high porosity, a good water holding capacity and good internal drainage.

Cambisols generally have a neutral to weakly acid soil reaction, a satisfactory chemical fertility and an active soil fauna. In the tropics, they are typically poor in nutrients, though they are still richer than the associated mature tropical soils and have a greater cation exchange capacity.

Fluvisols FL

Fluvisols occupy the lowest position of the mapped area, along the shores of the Lake Awassa in the Awassa caldera, and fluvial and lacustrine sediments in the endorheic depressions and very rare on floodplains. They are developed in the predominantly recent, fluvial and lacustrine deposits with an admixture of resedimented pyroclastics. Volcaniclastic lacustrine sediments cover mainly the floor of the caldera and are the only non-volcanic formations in the area. These sediments are dominantly distributed with large stretches at the sides of the lake and over the ignimbrites. Their formation is related to the recession of Lake Awassa, which occupied a larger part of the floor of the caldera in the past.

Figure 6-8. *Eutric Fluvisol (JJ048).*

Fluvisols represent genetically young soils with *fluvic material* without distinct horizon differentiation, only a distinct topsoil horizon resulting from cultivation is present. The texture of the parent material differs between river banks or lagoons and basins. Fluvic material refers to fluvial and lacustrine sediments that receive fresh material or received it in the past and still show stratification. Stratification may be reflected in different ways: Variation in texture and/or content or nature of coarse fragments, different colours related to the source materials or alternating lighter and darker coloured soil layers, indicating an irregular decrease in soil organic carbon content with depth. (IUSS Working Group WRB 2015).

Much of the Fluvisols of the Awasa caldera are cultivated, and a range of crops and farming systems are to be found. Small and medium-sized farms occur throughout the Awasa caldera, the majority being concentrated in the south and southwest.

Table 6-11. Textural characteristics of the Fluvisol profile

Sample	Horizon.	Sand (%)	Silt (%)	Clay (%)	Texture
JJ048	A	53.09	31.95	14.96	sandy loam

Table 6-12. Selected chemical characteristics of the Fluvisol profile

Sample	Hor.	pH/ H_2O	pH/ KCl	Δ pH	P mg/kg	K mg/kg	Ca mg/kg	Mg mg/kg	TOC %	CEC $cmol_c/kg$	BS %
JJ048	A	7.80	6.70	–1.1	< 3.5	968	2729	216	0.44	15.65	100.00

Figure 6-9. *Agricultural land on Fluvisols along the shores of the Lake Awasa (Awasa Caldera).*

The predominant crop is maize, but a variety of crops is grown, including haricot beans, teff, tobacco, peppers, enset and other.

6.3 Opportunities for and threats to the soils in the studied area

Soil is a natural resource that is not capable of being renewed on the human time scale. Sustaining soil and environmental features are the most effective methods for ensuring sufficient food supply to support life, reduce soil degradation and improve soil health (Soares et al. 2005). A short overview of strengths, weaknesses, opportunities and threats of the African soils was given by Jones at al. (2013) and a selection for the main soil groups in the mapped area is mentioned below.

Andosols

Strengths: Andosols are high in nutrients and easy to cultivate.

Weaknesses: High levels of phosphate fertiliser are needed to affect yields due to fixation by iron compounds in soil. The use of heavy machinery may pose problems because of their low bearing capacity, prone to smearing and stickiness.

Opportunities: They can be planted with a wide variety of crops such as sugar cane, tobacco, sweet potato (tolerant to low phosphate levels), vegetables, wheat and orchard crops.

Threats: Andosols are best kept under forest to prevent erosion on steep slopes.

Cambisols

Strengths: Cambisols belong among the better agricultural soils in Africa as they are less depleted in nutrients than other tropical soils and have a sufficiently high nutrient-holding capacity to retain fertilisers.

Weaknesses: Strongly weathered Cambisols contain limited amounts of nutrients.

Opportunities: Depending on their depth, their water-holding capacity can be high.

Threats: In hilly or mountainous areas, where Cambisols are the most frequent, care should be taken to prevent erosion when the surface is bare. Under such conditions, these soils are best kept under forest or perennial crops such as tea.

Fluvisols

Strengths: Fluvisols, except for the very acid ones, are fertile because of the regular supply of nutrients. Riverine Fluvisols are highly suitable for wetland rice because of the close proximity to fresh water.

Weaknesses: Flood control or drainage may be needed due to the proximity of rivers. Low-lying backswamps, if not suitable for wetland rice, are best left under the natural vegetation; these areas may be used for extensive grazing when they are accessible.

Opportunities: High agricultural potential.

Threats: Flooding and waterlogging. They are prone to urbanisation and sealing.

Luvisols

Strengths: Luvisols are productive soils; in northern Africa, they are planted with winter wheat and vegetables under irrigation during summer. They have a large mineral nutrient reserve and a good aeration. The rooting depth is normally unlimited unless they overlie a continuous hard rock or a petrified layer.

Weaknesses: Due to the long and continued cultivation in northern Africa since Roman times, most Luvisols have lost their topsoil; therefore, they are poor in organic matter and nitrogen-deficiency is quite common.

Opportunities: Productive soils if managed appropriately.

Threats: Prone to erosion on slopes.

Nitisols

Strengths: Nitisols are suited for a wide range of crops. Many Nitisols are used to grow coffee.

Weaknesses: In annual cropping, fertiliser application is necessary to make these soils productive. Due to the high amount of active iron, Nitisols suffer from phosphate-fixation. Retention rates of 80% or more are common.

Opportunities: Intensive liming can overcome the aluminium toxicity.

Threats: Erosion on slopes.

Vertisols

Strengths: Vertisols can be productive provided the right measures are taken.

Weaknesses: As most Vertisols occur in level areas, water movement in the soil is limited and water can stagnate on the surface during wet periods. Heavy to till when wet. Swelling and shrinkage may destroy the foundation of structures (e.g. roads, irrigation canals).

Opportunities: Raised beds made out of the surface layer, which is often crumbly, are good seed beds as the water drains quickly into the adjacent furrows.

Threats: Can be susceptible to droughts.

The large part floor of the Rift Valley in the mapped area is covered by the soils developed on recent volcanic deposits of ignimbrites, ash, lava and tuff, which form the dissected plain characteristic for the area. Generally, the soils are dark and free draining, while lacking distinct profile development. Although textures vary according to the parent material from clay and clay loam to sandy loam (Fig. 6-10), much of this land is now rather intensively cultivated, having recently been settled by farmers from the overpopulated highland areas. It should be emphasized that the low bulk density and weak structure of these soils make them vulnerable to erosion even on gentle slopes. Uncontrolled exploitation could lead to degradation. The soils on cultivated slopes towards and beyond the caldera rim are highly susceptible to gully erosion. Around the caldera rim, shallow soils, susceptible to erosion once the protective forest cover has been removed, occur over the weathered volcanic ash (Makin et al. 1975).

Recently, a large number of process-based soil erosion models have been used to assess the sheet and rill erosion in Ethiopia (Ali and Hagos 2016). The sheet, rill and inter-rill erosion has been estimated using the widely applied Universal Soil Loss Equation (USLE) (Wischmeier and Smith 1978) modified by Hurni (1985) for the Ethiopian Highlands. Despite the fact that disadvantages and uncertainties of the USLE are very well known, the USLE and its revised versions are widely used in the scientific and engineering world because of its relatively easy application.

Erosion rates are very sensitive to soil texture and moisture, vegetation cover, land use, slope and climate as well as to soil conservation practices at the field level. The USLE allows the prediction of annual soil loss based on the product of six factors. It is represented by **A = R ∗ K ∗ L ∗ S ∗ C ∗ P**; where A is the computed spatial average soil loss and temporal average soil loss per unit area, usually expressed in t ha^{-1} $year^{-1}$, **R** is the rainfall erosivity index, **K** is the soil erodibility factor. **SL** is the topographical factor (length and gradient of the slope), **C** is the plant cover factor and **P** is the factor of specific erosion control practices.

The USLE parameters predict only sheet, rill and inter-rill erosion; therefore, the overall soil erosion rate could be much higher than predicted by the USLE, especially in the areas where deep gullies are observed similarly to the mapped area.. However, other similar studies have calibrated the USLE model parameter for Ethiopian conditions (Nyssen et al. 2004; Nyssen et al. 2009; Gebremichael et al. 2005 and Haregeweyn et al. 2013).

The intensity of soil erosion is mainly influenced by three factors: erosivity of water, erodibility of soils and human activities. Infiltration rates of soils are also influenced by the morphometric characteristics of the land surface.

The erodibility of tropical soils is highly dependent on grain size distribution, clay content and organic carbon content, which influence the stability of soil aggregates. The soil with a high percentage of silt and clay particles has a greater erodibility than a sandy soil under the same conditions. The prevailing soil texture in the mapped area show textural triangles in Fig. 6-10.

The susceptibility to land degradation according to Stocking and Murnaghan (2000) differs within the major agricultural soils of the study area (Table 6-13).

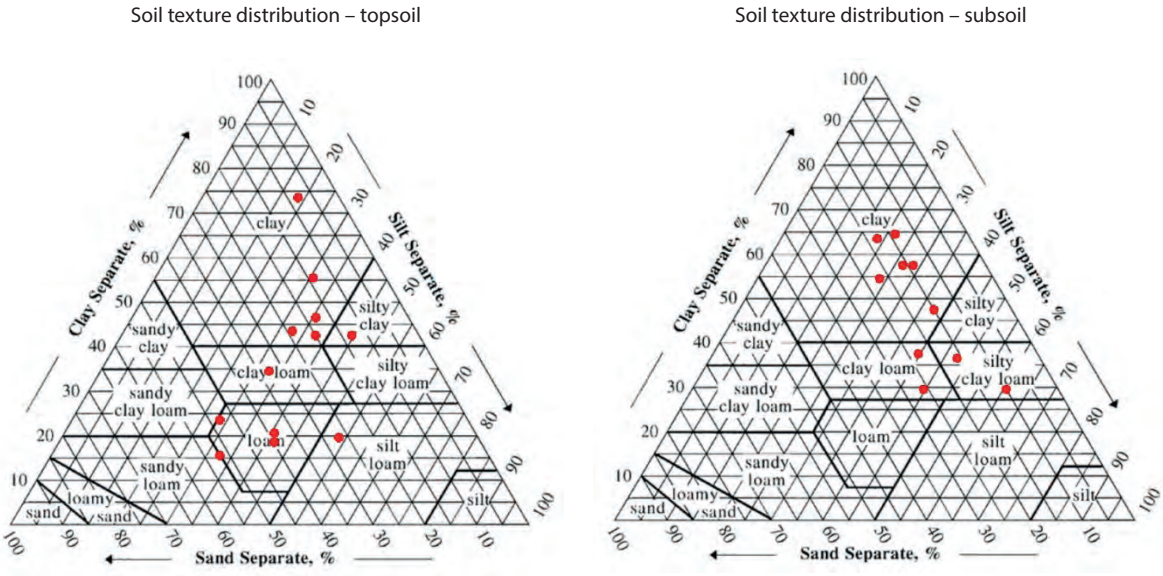

***Figure 6-10**. Soil texture distribution in topsoil and subsoil on the Leku map sheet.*

Table 6-13. Major cultivated soils of the mapped area and their susceptibility to land degradation

RSG*	Main Properties and Susceptibility to Land Degradation
Andosols	Soils developed from volcanic ash parent material; high in organic matter. Highly erodibleand limited in phosphorus. Chemical fertility is variable, depending on the degree of weathering. Andosols have low resilience and variable sensitivity.
Cambisols	They have a relatively good structure and chemical properties; therefore, gthey are not greatly affected by degradation processes until these become large. Because of increasing clay with depth, they tend not to be greatly impacted by degradation. Cambisols have high resilience to degradation and moderate sensitivity to yield decline.
Fluvisols	Soils formed from unconsolidated water-borne materials. Highly variable, but much prized for intensive agriculture. Under most conditions, they have high resilience and low sensitivity. The big tropical exception includes acid sulphate soils, which have massive chemical degradation impacts when drained for agriculture.
Luvisols	Soils most used by small farmers because of their ease of cultivation and no great impediments. Base saturation > 50%. However, they are greatly affected by water erosion and loss in fertility. Nutrients are concentrated in topsoil and they have low levels of organic matter. Luvisols have moderate resilience to degradation and moderate to low sensitivity to yield decline.
Nitosols	One of the best and most fertile soils of the tropics. They can suffer from acidity and P-fixation and when organic carbon decreases, they become very erodible. However, erosion has only a slight effect on crops. Nitosols have moderate resilience and moderate to low sensitivity.
Vertisols	Soils with 30% or more clay. Clays are usually active, cracking when dry and swelling when wet. Extremely difficult to manage (hence easily degraded) but known for very high natural chemical fertility if physical problems are overcomed.

**) Reference Soil Groups according to the World Reference Base for Soil Resources*

7) HYDROGEOLOGY

7.1 Hydrometeorology and hydrology

The character of precipitation in the surveyed area is described in Chapter 2.2., and the precipitation patterns at the Dila, Awasa and Belela meteorological stations are shown in Fig. 3-2; the data are summarized in Tab. 3-1. The Leku area is located in the Rift Valley Lakes Basin (RVLB), specifically in the area of the Awasa and Gidabo sub-basins with a surface of 1,295 and 3,491 km^2, respectively. The structural setting, tectonics and variations in lithology of the area obviously control the local drainage pattern, either partly or completely. Most of the rivers discharge their water into lakes on the bottom of the rift (Fig 7-1).

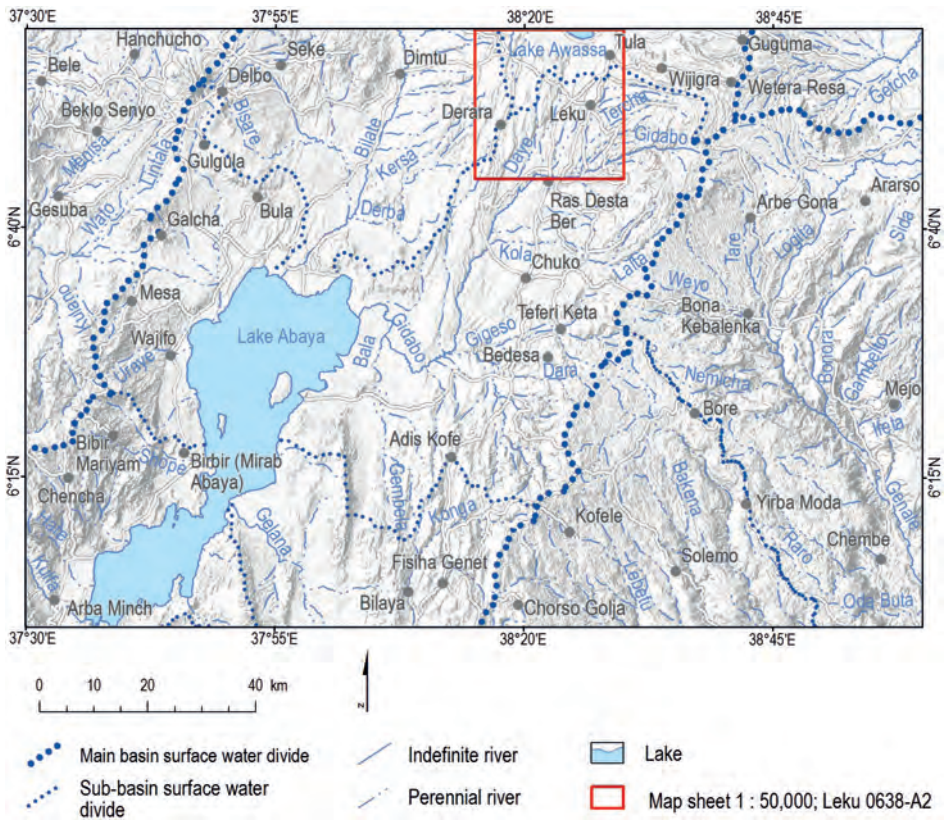

Figure 7-1. *Hydrology scheme of Leku area.*

River discharge and base flow

There are numerous river gauging stations across the RVLB, but only one station is located on the Gidabo River on the Leku map sheet. Other stations lie on the neighbouring sheets (see Tab. 7-1), and the data from these stations were also taken into consideration when assessing the surface flow and baseflow values, and likewise were used for the comparison and correction of data from the Leku area.

Table 7-1. Data at the river gauging stations

Map ID	Station number	River	Station	X UTM	Y UTM	Elevation [m a.s.l.]	Area [km^2]	Basin/ Sub-basin
1	82005	Bilate	Tena	403995	765960	1,486	3,881	Bilate
2	82016	Gidabo	Aposto	431294	746251	1,686	655	Gidabo
3	–	Gidabo	Meass	434731	713366	2,128	72	Gidabo
4	82028	Kolla	Aleta Wondo	436429	732022	1,894	166	Gidabo

The records from all stations show that the river discharge is directly proportional to the intensity of rainfall within the basin. There is a high discharge fluctuation between the wet and dry seasons during the year. The first high flow period is usually from April to May, the highest flow period lasts from July to October, and the peak flow for most of the rivers is usually recorded in September. The period from December to February is characterized by a low flow when most of the smaller streams are completely dry. Hydrological data are summarized in Tab. 7-2.

The measured and recorded discharge data of the Gidabo River at the Aposto River gauges in the period from 1979 to 2008 are given in Fig. 7-2. The diagram shows that the flow is relatively regular, but the total value of annual flow and particularly the maximum monthly flow can vary substantially from year to year. The lowest daily discharge usually occurs in the period from November to April, but the river dried up during November to January in the years 1987–1989. The highest daily discharge of 92 m^3/s was recorded at the river gauge on July 30, 1996. The calculated mean annual discharge of 6.4 m^3/s for the Aposto station represents the flow generated mainly in the eastern escarpment where the Gidabo River originates and in the eastern part of the rift floor, which the river is flowing through. This part of the surveyed area is relatively affected the most by atmospheric precipitation.

Table 7-2. Hydrological data

Map ID	River	Station	Mean flow [m^3/s]	Annual flow [mm]	Annual precip. [mm]	Area [km^2]	Specific runoff [l/s.km^2]	Dominant Aquifer
1	Bilate	Tena	20.5	117.2	1,165	5518	3.72	Volcanic/floor
2	Gidabo	Aposto	6.4	312.6	1,244	646	9.91	Volcanic/floor
3	Gidabo	Meass	–	–	1,244	72	ND	Volcanic/floor
4	Kolla	Aleta Wondo	2.9	443.6	1,244	206.3	14.08	Volcanic/floor

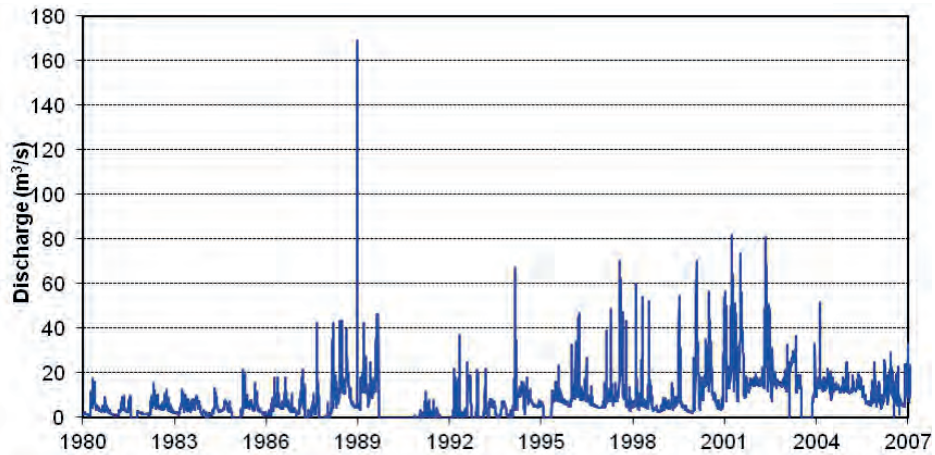

Figure 7-2. *Discharge diagram of the Gidabo River at the Aposto River gauges.*

Annual variability of the mean annual discharge of the Gidabo River at the Aposto River gauges is shown in Fig. 7-3.

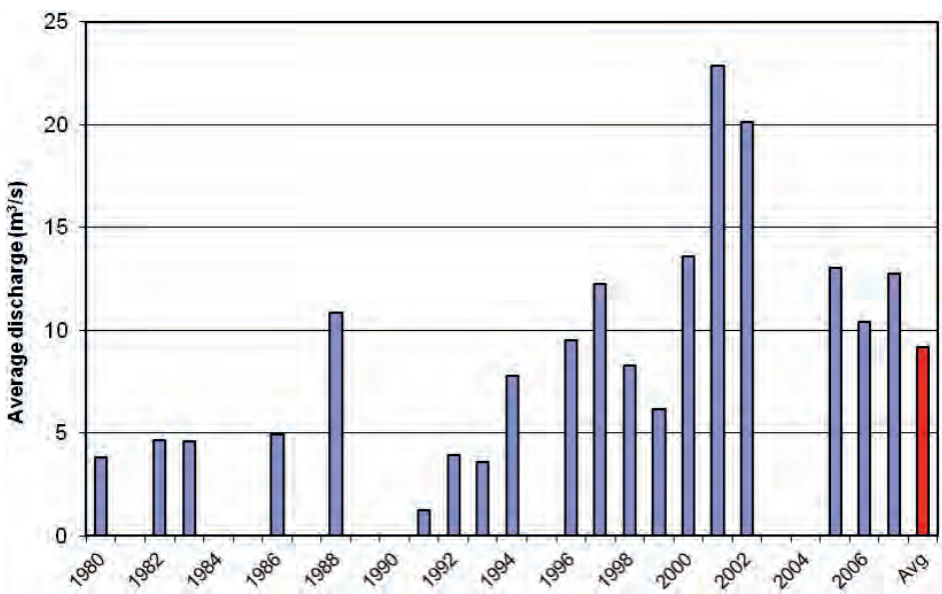

Figure 7-3. *Annual variability of the mean annual discharge of the Gidabo River at the Aposto River gauges.*

The assessment and interpretation of specific runoff based on the data from flow measurements and calculated specific runoff at the gauging stations is shown in Tab. 7-2, including the pertinent river basin within the Leku sheet also taking into consideration the altitudes and lithology of the area.

The **specific runoff** for the Leku sheet used for further calculations and considerations was assumed to be **4.0 l/s.km^2**.

Baseflow represents one of the most essential parameters and information on groundwater resources in a given basin. Some baseflow separation methods for analyzing individual rainfall-runoff events were introduced by Bogena al. (2005), also taking into consideration the correlation analysis and daily river discharge in order to determine the appropriate baseflow data.

The Kille's method for the calculation of baseflow was used in the study together with the separation of hydrographs, where baseflow data are derived from the discharge record of a stream by separating the baseflow component from the total discharge. The Kille's method was applied despite the fact that the data series are relatively shortand timewise. The data for baseflow assessed/established by this procedure are shown in Tab. 8-3 together with baseflow data assessed by the hydrograph separation method that was used for the assessment of this component. The baseflow separation techniques use the time-series record of stream flow to derive the baseflow signature. The common separation methods are either graphical, which focus on defining the points where baseflow intersects the rising and falling limbs of the quickflow response or involve filtering, where data processing of the entire stream hydrograph derives a baseflow component.

The graphical method was employed for the assessment of baseflow in rivers of the surveyed area. The daily flow data were used to plot the baseflow component of a flood hydrograph event, including the point where the baseflow intersects the falling limb. Stream flow subsequent to this point was assumed to be entirely baseflow, until the onset of the hydrographic response to the next significant rainfall event. These graphical approaches to partitioning the baseflow vary in complexity (Linsley, 1958).

A comparison of the assessment of baseflow using the Kille's method and hydrograph separation is shown in Tab. 7-3. The results show very small differences between the baseflow using the Kille's method and hydrograph separation.

The assessment of specific baseflow is based on the data from hydrograph separation and also using the Kille's method.

The specific baseflow of 2.0 l/s.km^2 (is) was established for the Leku sheet based on data from the river gauges.

Table 7-3. Baseflow data for the Leku area

Map ID	River	Area [km^2]	Specific runoff [l/s.km^2]	Kille's method [m^3/s]	Hydrograph separation [m^3/s]	Specific baseflow [l/s.km^2]	Aquifer
	Bilate	2,009	5.5	2.30	6.76	1.1/3.4	Volcanic/floor
3	Bilate Tena	5518	3.72	3.10	8.67	0.56/1.6	Volcanic/escarp.
5	Upper Gelana	95	2.63	0.22	0.23	2.3/2.4	Volcanic/escarp.
8	Gelana	376,2	18.88	2.62	–	7.0/–	Volcanic/escarp.
14	Gidabo (Aposto)	646	9.91	2.65	4.20	4.1/6.5	Volcanic/escarp.
16	Kolla	206.3	14.08	1.00	1.50	4.9/7.3	Volcanic/escarp.
17	Sala	67.5	62.22	1.74	1.81	25.8/26.8	Volcanic/escarp.

Lakes

There is one lake in the study area. The Lake Awasa covers only a very small part of the map sheet in the north and it was described in detail in the explanatory notes for the Hosaina map sheet (Kefale, Sima, 2013). Monthly measurements of lake levels were carried out at the Awasa station and started in the late 1960s or early 1970s. The basic descriptive data on the lake and the results of water level observations are given in Tab. 7-4.

Table 7-4. Basic characteristics of the Lake Awasa

Lake	Elevation [m a.s.l.]	Max. depth [m]	Mean depth [m]	Surface area [km^2]	Storage volume [Mm^3]	Level fluctuation [m]	Salinity [g/l]
Awasa	1,500	20 (32.2)	10.7	130	1,300	3.49	0.6

Aquifers Recharge in the Leku Area

There is a lot of information available in various reports concerning the recharge of aquifers. However, the information capability of these data varies considerably. The regional mechanism of aquifer recharge in the area has been described above. Similarly to other areas, the groundwater is recharged from atmospheric precipitation depending on its intensity and annual and areal distribution, topographical gradient of the area as well as the lithological composition (particularly in the vertical profile) of outcropping rocks and their tectonic pattern and disturbances, tectonic-climatic interactions, earthquakes, et cetera. A substantial part of the groundwater is recharged directly from precipitation. There is also a seasonal, but less significant recharging of some aquifers from most of the permanent and intermittent streams and lakes after the rains when the surface water levels are above the groundwater level in the surrounding aquifers. This type of recharging is important on the rift floor, where evapotranspiration is much higher and rainfall is lower than in the highlands.

Groundwater recharge assessment was performed based on rainfall infiltration (recharge from rainfall) according to the rainfall infiltration factor (RIF), and is about 6% using the criteria defined by WWDST (2003). The recharge areas of outcropping lithological units were considered only if the slope of the terrain was less than 20%.

Tesfaye (1993) characterized the groundwater recharge to be between 150 and 250 mm in the highlands and between 50 to 150 mm in the rift basin. Zenaw (2003) assessed the recharge for the Awasa basin to be about 5% of the rainfall (67 Mm^3/year). WABCO (1990) in the Water Resources Development Master Plan for Ethiopia refers to 5% recharge of the aquifers in the RVLB, representing about 57 mm of the annual recharge.

Groundwater recharge calculated from the mean values of baseflow shows the possibility of recharge variability from 10 mm/year to 100 mm/year with an average of 70 to 90 mm/year depending on precipitation depth variations in different years. When applying an adopted average baseflow value for the rivers in the rift floor, the recharge is about 50 mm. Compared to the adopted average depth of precipitation at 1,100 mm, the calculated infiltration (recharge) can be assessed as being 7% of the precipitation depth.

Water balance of the RVLB and irrigation potential

The Rift Valley floor is dominated by Lake Abaya and Lake Chamo with a basin area of 18,118 km^2. Relatively large basins of the rivers Bilate (5,900 km^2) to the north, Gidabo (3,447 km^2) and Gelana (3463 km^2) to the east drain the western and eastern highlands. Their flows contribute significantly to the water level of Lake Abaya. The rivers flowing from the western escarpment contribute less but they bring a large amount of sediments particularly to the Lake Abaya.

Currently, three large-scale irrigation schemes are planned by the Ministry of Water Resources, Energy and Irrigation for the rivers emptying into Lake Abaya. On the Gelana River, there are plans for a net irrigation command area of 5,356 ha. The command area currently being considered for the Gidabo River covers a net area of 9,215 ha, and there are plans for a rehabilitation scheme for the existing state farms on the Lower Bilate River, providing a net area of 7,715 ha.

The total surface water resources of the RVLB are estimated by Halcrow (2008) at just over 5,300 Mm^3/year, calculated from the total annual average river flow into the lake systems under 'natural' conditions – without human intervention as shown in Tab. 8-5. This determined the water availability of 597 m^3 per capita, which is below the threshold of 'water scarcity' of 1,000 m^3/capita/annum. This will decrease to 232 m^3/capita/annum by the end of 2034 because of population growth – a situation of extreme water scarcity.

The water resource analysis by Halcrow (2008) shows about 18,350 ha of land for new irrigation development may be 'allowable' from a water resources perspective in the Awassa-Abaya-Chamo basin. For the Lake Awasa, the sustainable limit is estimated to be about 500 ha. When 'allowable' irrigation is phased in with other water demands, the surface water resources are further depleted to a maximum of 5,057 Mm^3/year, a decrease by 2.4 %. Also, as the RVLB lakes are already either in a state of decline or in a very precarious balance, caution must be used when undertaking any future development.

Table 7-5. Total surface water resources and total water resources (Halcrow, 2008)

Lake system	Total surface water resources [Mm^3]	Total water resources [%]
Ziway	755	14
Abijata	200	4
Langano	258	5
Shalla	340	6
Awasa	143	3
Abaya	2,512	47
Chamo	506	10
Chew Bahir	598	11
Total	**5,312**	

Drought and Climate Change

Some parts of Ethiopia are often affected by recurrent drought causing famine. The impact of drought is severe both in the arid lowlands as well as in the highlands of Ethiopia. The existence of drought and desertification is well known from geological and archeological evidence as well as from the historical documents and on-going measurements. It is no wonder that the centre of the Ethiopian civilization was shifted about 1,000 km from the Axum town in the dry north to Addis Ababa located in the more humid centre of the modern Ethiopia over the last 2,000 years. The northern and eastern parts of the country appeared to be highly vulnerable to recurrent drought and famine.

Despite the fact that the central part of the Rift Valley is not considered as a drought prone region, Halcrow (2008) delineated and classified the areas of high variability of rainfall and considered these areas as being drought prone. These medium drought prone areas are found in the western part of the map sheet, along the water divide between the RVLB and the Omo-Gibe Basin. The highly drought prone areas are along the western bank of the Lake Abaya and cover parts of the Mirab Abaya and Chencha weredas (districts).

Table 7-6. Impact of climate change on the levels of lakes and the area (Halcrow 2008)

Lake	Lake level change [m]	Lake area change [%]
Ziway	–0.60	–12.2
Abijata	–1.26	–28.9
Langano	–2.05	–10.0
Shalla	–3.20	–2.9
Awasa	–2.07	–8.2
Abaya	–2.76	–14.4
Chamo	–12.11	–38.4

The impact of climate change on water resources of the RVLB has been assessed by Halcrow (2008) using a climate change scenario based on the outputs from the Global Circulation Models (GCMs) and scenarios used in other climate change studies for Ethiopia. This study used a hypothetical increase in temperature of +2 °C resulting in a 10% increase of evapotranspiration, but a 10% decrease of rainfall over the period of 30 years; a relatively high impact scenario. For this climate change scenario, the results from the regional flow model show a 24% reduction in the total annual flow in rivers compared to the present day runoff. The impact of climate change will be more serious in the lakes Ziway, Abijata and Langano, and the total average annual inflow into the Lake Ziway is predicted to decrease by 19% to 27%, due to decreasing inflows during the main rainy season (Tab. 7-6).

7.2 Hydrogeological surveys

Hydrogeology of the Leku map sheet is compiled based on the assessment and interpretation of data acquired from the existing reports and maps and additional field documentation. There is no previous hydrogeological work at a scale of 1 : 50,000 and full data sets required for geometrical aquifer configuration are scarce; however, the sheet of Dila at a scale of 1 : 250,000 was compiled by Agezew, Regassa and Sima (2014). The hydrogeological system of the Leku map sheet is similar to those in the adjacent areas; in particular to the highland area in the western sector of the map sheet, although some lithological units show different productivity characteristics or they are completely missing. The hydrogeological map of Ethiopia at a scale of 1 : 2,000,000 was published by Tesfaye Chernet (1993). He classified the geological units of Ethiopia

into four major groups, depending on the type of permeability and the extent of pertinent aquifer. The latest assessment of groundwater resources in the Lakes Region was done by Halcrow (2008) and by the Japanese International Cooperation Agency (JICA, 2012). The Master Plan Study by Halcrow (2008) compiled the studies of both the geology and hydrogeological conditions in the RVLB.

The borehole yield in l/s was assessed for various lithologies to be as follows:
- Lacustrine sediments 4.03
- Ignimbrite 2.81
- Basalt 2.67
- Volcanic sand 2.06
- Pyroclastic and sedimentary rocks 1.5

The spring yield in l/s was assessed for various lithologies to be as follows:
- Aglomerate 6.7
- Basalt 4.46
- Ignimbrite 17.17
- Lacustrine sediment 36.7
- Rhyolite 22.5
- Fluvial and alluvial gravel 2.0
- Scoria 13.25
- Soil 4.5
- Trachyte-rhyolite 1.5

Springs with the records of both yield and temperature were evaluated. The evaluation shows that most of the springs with high yields originate from thermal spring sources.

It can also be noted that the yields of thermal springs are highly variable (from 1.5 l/s up to 75 l/s). Representative aquifer parameters assessed by Halcrow (2008) are shown in Tab. 7-7 .

Table 7-7. Representative aquifer parameters (Halcrow, 2008)

Formation	Transmissivity [m^2/day]	Yield [l/s]
Ignimbrite	1–1,300	0.1–8.0
Basalt	39–130	2.7–3.0
Lacustrine deposits	10–2,800	1.0–6.6
Alluvium	40–345	1.0–6.0

For the purposes of the Master Plan, the adopted aquifer classification was broadly defined at 1 : 2,000,000 in the Hydrogeological Map of Ethiopia (1988). The following table (Tab. 7-8) gives a brief description of individual aquifer units encountered in the basin.

An assessment of the potential of various aquifers based on the discharge of wells and springs and the major lithology performed by JICA (2012) is shown in the following Tab. 7-9.

Table 7-8. Description of individual aquifer units encountered in the basin (JICA, 2012)

Aquifer	Permeability	Productivity
Alluvium (Qa; QHa)	Porous	Moderate, locally high
Fluvial sand and silt (QHr)	Porous	Moderate
Eluvium (Qe)	Porous	Low
Lacustrine sediments (Ql; QHl; NQl)	Porous	Moderate to low
Volcanic sedimentary rocks (Qvs;)	Porous	Moderate
Undivided sediments (Q; QH; NQ; NP)	Porous	Low
Pumice and non-welded tuffs (Qwpu)	Porous	Low
Extensive volcanic aquifers in basalts; rhyolites; trachytes; ignimbrites	Fracture	High to Low
Localized aquifers with permeability (basement)	Fracture and intergranular	Low to aquiclude

Table 7-9. Parameters determined for aquifers within the Ethiopian Rif t by JICA (2012)

Aquifer	Symbol	Lithology	Q [l/s]			Sp. cap [l/min/m]			T [m^2/day]		
			Ave	Max	Min	Ave	Max	Min	Ave	Max	Min
Pleistocene tuff, welded tuff and basalt	AL/Q	Alluvium	2.8	6.5	0.2	0.5	1.2	0.10	75.3	92.6	43.0
	Lac 1	Gravel, sand mud	4.6	7.3	1.5	0.3	0.7	0.01	69.0	137.0	1.0
	W	Tuffs and pumice	5.5	47.0	0.2	0.7	1.8	0.02	42.5	84.8	0.2
	G	Rhyolite welded tuff	4.6	18.5	0.2	0.5	1.5	0.01	65.3	173.9	0.0
	tb	Basaltic tuff	6.3	22.0	0.1	2.2	6.9	0.04	242.0	914.4	12.5
	ba	Basalt	2.9	7.7	0.2	0.3	0.9	0.05	77.7	211.7	2.7
Tertiary tuff and basalt	Rh, N2b	Rhyolite lava and tuff	4.9	19.6	0.6	0.2	0.4	0.10	9.3	24.8	0.1
	N1n N1ar	Rhyolitic tuff and basalt	3.9	6.0	2.0	0.2	0.2	0.20	12.6	12.6	12.6

Q – discharge, Sp. cap – specific capacity, T – transmissivity

In general, the highly productive water resources can be found in the area between the rift ridge slope and the flat lowlands. A high groundwater gradient is expected to be on the escarpment, while a high discharge is difficult to occur on the escarpment on the western ridge of the rift valley based on the conclusions of the JICA (2012) study. Geothermal studies consisting of geological, geochemical and geophysical investigations were carried out in the Rift Valley in order to determine the potential and to define feasible sites for geothermal power development (the Abaya geothermal field is located at the northern shore of the Lake Abaya).

The inventory of water points was based on a desktop study, during which the relevant materials such as geological and drilling reports and maps and aerial photographs were acquired from the Regional Geological Department of the GSE. Important climatic and gauging station data and topographic maps were obtained from various offices. The desktop study also included preliminary data interpretation and preparation of field maps using satellite images, aerial photographs and a digital elevation model (DEM) of the terrain with geology as a background.

7.3 Hydrogeological Classification/Characterization

The qualitative division of lithological units is based on hydrogeological characteristics of various rock types using water point inventory data and by an analogy with the adjacent map sheets and a regional assessment published for the Leku map sheet. The lithological units were divided into groups with dominant porous and fissured permeability. This division served for the definition of the aquifer/aquiclude system occurring on the map sheet. Since quantitative data such as permeability, aquifer thickness and yield are not adequate or evenly distributed enough to make a detailed quantitative classification of potential aquifers, an analogy was used for the characterization of rocks without the adequate number of water points. Hence, the hydrogeological characterization of the study area reveals the following aquifer/aquiclude systems:

- Units with porous permeability, where groundwater is accumulated in and flows through pores of an unconsolidated or semi-consolidated material. Porous materials of Quaternary age are represented either by lacustrine sediments with subordinate alluvial and colluvial sediments developed in depressions of lakes and/or along the foot of the eastern escarpment and along the valleys of former and existing rivers or by pumiceous pyroclastic sediments, redeposited pumice and non-welded tuff materials (polygenetic infill). The porous aquifers are widely developed over the study area. The unit with porous permeability forming aquifers is expressed in blue on the hydrogeological map.

- Units with fissured permeability, where groundwater is accumulating inside and flows through the weathered and fractured part of volcanic rocks. The porosity of lava flows may be high, but the permeability is largely a function of combination of the primary and secondary structures (joints and fissures) within the rock. In addition, the permeability of lava flows tends to decrease with geological time. The pyroclastic rocks between lava flows are generally porous, but usually less permeable due to poor sorting during transport and deposition. They can be represented by impermeable non-welded tuff in some parts of the volcanic sequence. Hence, extensive volcanic ash beds may form semi-horizontal barriers to the vertical water movement (infiltration), resulting in the lower productivity of basaltic units occurring at greater depths. They can have a confined or semi-confined character in some part of aquifers. The layers of paleosoil of various thicknesses in between lava flows are less permeable and usually consist of clayey material on the one hand, whereas the layers of fluvial and lacustrine sediments and pumiceous pyroclastic materials between various lava flows can enhance the well yield on the other hand.

- Neogene and Quaternary volcanic formations represented by basalts, rhyolite trachyte and ignimbrite form aquifers with good fissured porosity. The units with fissured permeability forming moderately productive aquifers are expressed on the hydrogeological map in green.

7.4 Elements of Hydrogeological System of the Area Surveyed (Aquifers)

The geological description and qualitative division of various geological units together with their topographical position in the surveyed area lead to the definition of elements of the hydrogeological system and its conceptual hydrogeological model. The system consists of a) a porous aquifer developed in lacustrine, alluvial and colluvial sediments and volcano-sedimentary type of rocks of Quaternary age along the rivers, lakes, at the foot of the western escarpment and as an infill of depressions on the rift floor, and b) a fissured aquifer developed in Tertiary and Quaternary basalts, trachytes, ignimbrites and rhyolites in the highlands, escarpments and rift floor areas. The hydrogeological map shows aquifers defined based on the character of the groundwater flow (pores, fissures), the discharge of springs and the hydraulic characteristics of wells. The following aquifers and aquicludes were defined:

- Extensive (39 km^2) and moderately productive or locally developed and highly productive porous aquifers (T = 1.1–10 m^2/d, q = 0.011–0.1 l/s.m, with spring discharge and well yield Q = 0.51–5 l/s). The aquifers consist of Quaternary alluvial and colluvial sediments, polygenetic infill of depressions and volcano-sedimentary rocks. The aquifers are shown in light blue.

- Extensive (366 km^2) and moderately productive fissured aquifers (T = 1.1–10 m^2/d, q = 0.011–0.1 l/s.m, with Q = 0.51–5 l/s). These aquifers consist of trachytes and basalts of the rift floor. The aquifers are shown in light green.

- Extensive (351 km^2) and moderately or locally developed and highly productive mixed porous and fissured aquifers (T = 1.1–10 m^2/d, q = 0.011–0.1 l/s.m, with spring and well yield Q = 0.51–5 l/s). These aquifers consist of volcanic, sedimentary and pyroclastic rocks of the central volcanic complexes and pumiceous pyroclastics of the Nazret Group. The aquifers are shown in light green with light blue horizontal hatching.

Extensive and moderately productive porous aquifers

The porous aquifers make up 39 km^2 altogether, accounting for about 5 % of the area (the bigger part of the aquifers is located on the northern adjacent sheet of Awasa) and consist of lacustrine sediments with subordinate alluvial, colluvial sediment, polygenetic infill of depressions and pumiceous pyroclastics of Quaternary age. These aquifers are shown in light blue.

Sedimentary and volcano-sedimentary rocks on the Leku map sheet are characterized by variable thickness and texture. The composition of sediments ranges from clay to sand and gravel, ash, tuff and diatomaceous materials. The dominant materials include

silts interbedded with tuffs. Lacustrine deposits reach a significant thickness, particularly around the Lake Awasa.

This porous aquifer with moderate and locally high productivity is often developed in the RVLB. Flowing rivers and high runoff from the escarpment transport the material (alluvial fans along the western escarpment) deposited in large lakes on the rift floor. This aquifer is a very good source of groundwater, depending on thickness, sorting and recharge conditions. The aquifers in unconsolidated sediments are mainly recharged from direct infiltration by percolating rain water, but can be also recharged by bank infiltration during floods with high levels of water in river channels as well as high levels of water in the Lake Awasa.

Volcano-sedimentary rocks generally form volcaniclastic strata associated with volcanic eruptions (the Corbetti volcano north of the Lake Awasa). These beds mostly consist of volcanic sand combined with pumice and are also mixed with alluvial and lacustrine sediments and tuff materials. Moderate yields of the local aquifer represent an important source and supply of water for the local population.

Sedimentary rocks are rather heterogeneous, consisting of alternating coarse and fine deposits. The yield of boreholes drilled in the aquifer varies from 1 to 5 l/s. The average thickness of the aquifer is about 50 m, but it varies from 40 m to more than 200 m. There are only several water points documented within the Leku map sheet; therefore, the yield of water points from this aquifer has been derived from the Dila sheet, being shown in Fig. 7-4, and their basic statistics are given in Table 7-10.

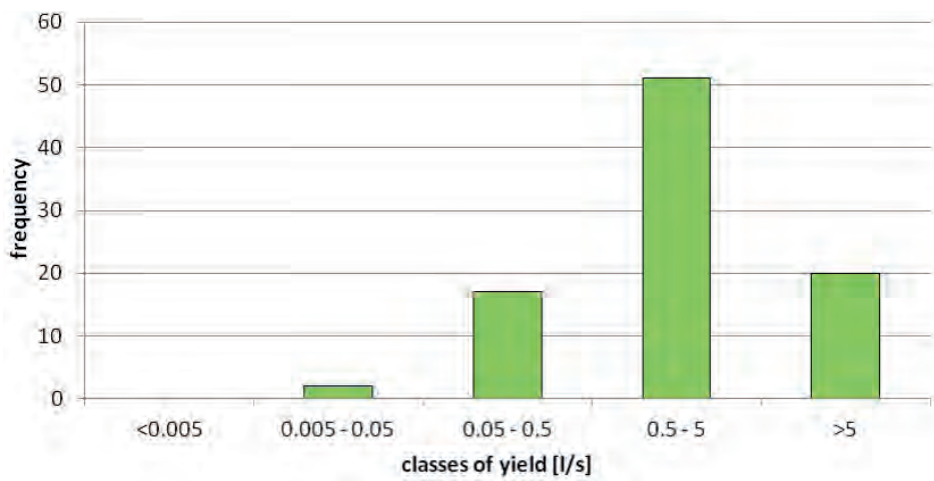

Figure 7-4. *Frequency of the yield of water points from porous aquifers of the Leku sheet.*

Table 7-10. Basic statistics of the yield of water points from porous aquifers in l/s

Number of data	Max	Min	Median	Average
90	75	0.029	2.5	4.61

Extensive and Moderately Productive Fissured Aquifers

Fissured aquifers of moderate productivity make up 366 km^2, accounting for 48 % of the area and mainly consist of trachytes with minor basalts of the rift floor and some

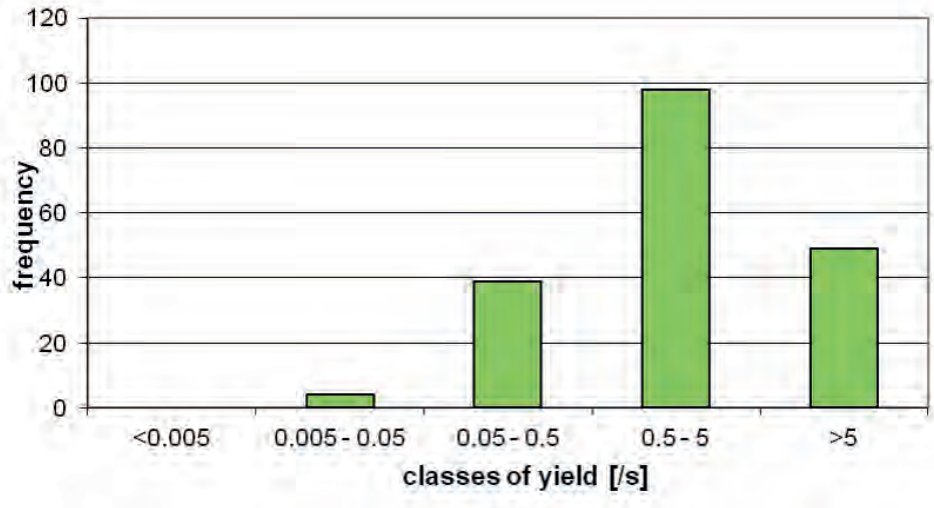

Figure 7-5. *Frequency of the yield of water points from fissured aquifers.*

tuffs, if not mapped separately. These aquifers mostly occur on the rift floor, but they are also present on the western escarpments, pediment slopes and adjacent western highlands. Their age, tectonic and geomorphological settings dictate their hydrogeological characteristics. Fissure flow is dominant.

Open faults and fault systems may also provide significant groundwater flow paths, which may allow the regional transfer of groundwater in places where they are extensive. The best example of the function of regional tectonic zones is documented by emerging big cold springs at the foot of the eastern escarpment. These fault systems can also be a source of hot springs (the Wondo Genet Group east of the Awasa town). There are only several water points inventoried within the map sheet in this aquifer. The frequency of the yield of water points from this aquifer, derived from the Dila sheet inventory, is shown in Figure 7-5 and basic statistics is given in Tab. 7-11.

Table 7-11. Basic statistics of the yield of water points from fissured aquifers in l/s

Number of water points	Max	Min	Median	Average
190	70	0.035	3	4.67

Trachyte and rhyolite lavas are more viscous and flows are often thicker than those of basalts, being less widespread and located closer to the centre of volcano or extrusion. Jointing, fissures and regional faulting represent the major source of secondary porosity. Where these flows are extensive, springs may occur and aquifers have potentially high yields, but the storage may be relatively limited because of the restricted extent of flows and/or domes.

Basalts usually form less viscous, thin lava flows and may be significantly affected by weathering, brecciation and interbedded with lacustrine or fluvial deposits. Groundwater flows through joints, fractures, scoria intercalations and scoriaceous horizons and interbedded sediments. The continuity of fractures in both horizontal and vertical planes provides the aquifers their hydraulic continuity within the adjacent units and aquifers.

Extensive and moderately productive mixed porous and fissured aquifers

The mixed porous and fissured aquifers of moderate productivity make up 351 km^2, accounting for 31 % of the area and consist of ignimbrites, rhyolite and trachyte lava flows mixed (intercalated) with tuffs, pumice, fluvial and lacustrine sediments.

The Nazret Group is exposed in the northeastern and northwestern part of the map sheet, where it is mainly composed of a thick succession of stratified silicic rocks, central volcanic complexes, ignimbrites, unwelded tuffs, ash flows, rhyolites, trachytes and minor basalts. The ignimbrite trachyte flows, basalt flows and rhyolites are columnar jointed and fractured.

The aquifer shows various types of permeability, specifically the intergranular and fractured/fracture permeability. The intercalated sediment does not function as an independent aquifer, but it rather contributes to a reliable yield of local wells. The aquifers are recharged directly by percolating rain water as well as indirectly from the overlying aquifers. The average yield of the aquifer is about 2 l/s and the median is 1.3 l/s; however, some cold springs have an extraordinary yield and discharge of several hundreds of litres, which serve as a water supply for small towns or settlements. Aquifers show both unconfined and confined water table conditions. The number of data on the yield of water points from fissured aquifers hosted by various volcanic rocks is shown in Tab. 7-12.

Table 7-12. Basic statistics of the yield of water points in mixed aquifers in l/s

Number of data	Max	Min	Median	Average
132	78	0.01	2	4.84

7.5 Hydrogeological Conceptual Model

Groundwater from the escarpment area recharges aquifers on the rift floor, in addition to the direct recharge from atmospheric precipitation, and finally discharges through lacustrine and alluvial sediments into lakes. On the other hand, the lacustrine sediments may also be recharged by water from lakes when their water level is higher than the adjacent groundwater level in the aquifers (see Fig. 7-6).

The ridges on the rift floor give rise to a local shallow groundwater flow. This shallow as well as deep groundwater flow appears in rivers as baseflow and recharges the lacustrine and alluvial sediments of lakes, which form the regional drainage pattern of the RVLB. Deep circulation of groundwater is evidenced by the existence of hot springs originating along the Gidabo and Bilate rivers with a high discharge (outside the map sheet). Unconfined groundwater is common, but artesian groundwaters are also known from the mixed volcano-sedimentary sequences of the rift floor.

The basic parameters of the general conceptual model for the Leku map sheet are based on or derived from the three main mechanisms of groundwater recharge as well as discharge and include the following:

- direct recharge of outcropping aquifers
- vertical recharge from the overlying aquifers into underlying aquifers
- horizontal recharge from the adjacent aquifers and rivers as well as the Lake Awasa

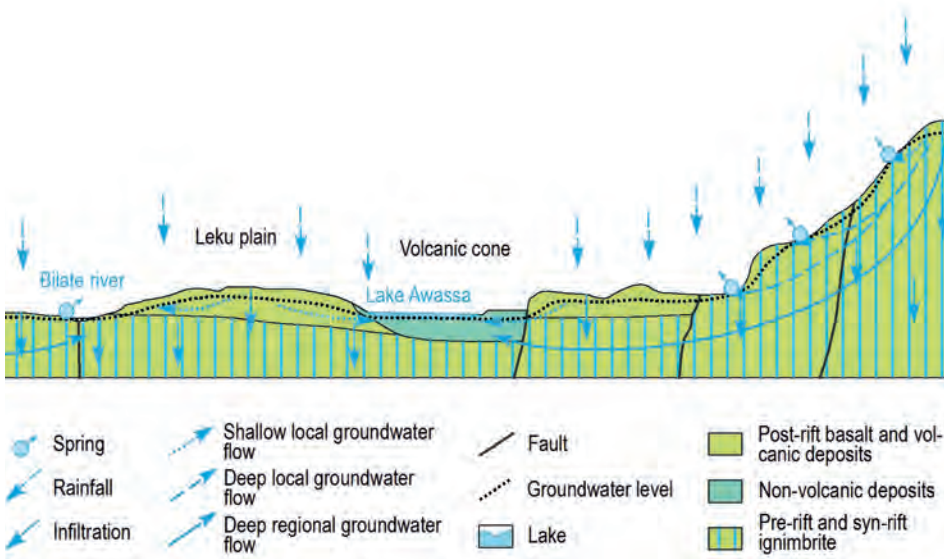

Figure 7-6. *Conceptual hydrogeological model of the western plateau, escarpment and rift floor.*

- direct discharge of springs originating from the outcropping aquifers
- direct discharge into rivers and lakes
- indirect discharge from one aquifer into another (both horizontal and vertical)

In general, the groundwater flow is parallel with the surface water flow system and comes in from the highlands through the escarpment to the rift floor. On the rift floor itself, the groundwater flow direction is governed by the relative elevations between the individual sub-basin lakes.

Groundwater (from boreholes and springs) represents the major source of water supply for towns and villages within the Leku map sheet; Halcrow (2008) estimates the groundwater to make up as much as 92 % of the water supply.

7.6 Hydrogeochemistry

One of the important tasks of the water point inventory and data collection was to investigate the groundwater chemistry and to assess the groundwater quality for its use within the mapped area. Therefore, a study of groundwater quality was carried out in different aquifers (geological formations) of the area as well as in various parts of the water circulation system (surface water and groundwater). The results of hydrochemical study can help to understand the groundwater circulation within the aquifers in addition to comparing the water quality according to various standards.

Tesfaye Chernet (1993) identified the hydrochemical characteristics of natural waters collected from different sources and the recharge/discharge conditions of the groundwater. According to Tesfaye Chernet:

- The water resources consist of a cold groundwater with TDS (total dissolved solids) below 1,000 mg/l and a hot water with TDS above 1,000 mg/l,
- The groundwater chemistry is characterized as being dominantly sodium-bicarbonate,

but some cold water is of the calcium-bicarbonate type. A part of the groundwater has a high fluoride content.

Hydrochemical characterization assessed by Halcrow (2008), JICA (2012), Zenaw (2003), Tesfay (1982) and other authors provide similar results to the previous characterization. Characterization of thermal groundwater was referred to in the UNDP report (1971).

A total of 45 water samples were collected from boreholes (22), dug wells (9), springs (11) around the Lake Awasa and from the Bedesa and Bilate rivers. All of the water samples collected for laboratory analyses were submitted to the Central Laboratory of the GSE and analysed to determine their chemical composition. The chemistry of analysed water is shown in Annex 4. Chemical analyses of the major constituents (Mg, Ca, Na, HCO_3, SO_4, Cl) and minor constituents (K, NO_3, F, HBO_2, CO_2, SiO_2), and measurements of electrical conductivity (EC) and pH at room temperature were performed in the same laboratory. Field measurements of pH, temperature and electrical conductivity were made at the time of sampling. The analytical results are presented graphically on a hydrochemical map to facilitate the visualization of water types and their relationships. The suitability of groundwater for drinking, industrial and agricultural purposes is assessed based on the pertinent quality standards.

The reliability of analyses was assessed using the cation-anion balance. The assessment showed that none of the samples exceeded the reliability level of 10 %.

Classification of natural waters

Classification of natural waters was used to express the groundwater chemistry on the hydrochemical map. Hydrochemical types are classified based on the Meq% representation of the main cations and anions by implementing the following scheme:

- Basic hydrochemical type, where the contents of the main cations and anions are higher than 50 Meq%. This chemical type is expressed on the hydrochemical map by a solid color.
- Transitional hydrochemical type, where the contents of the main cations and anions range between 35 and 50 Meq%, or exceed 50 % for one ion only. A dominant ion combination is expressed on hydrogeological map by the relevant colored horizontal hatching. The secondary ion within the type is expressed by an index (e.g. Mg^{2+}).
- Mixed hydrochemical type, where the contents of cations and anions do not exceed 50 Meq%, and only one ion has a concentration over 35 Meq%. This type is expressed on the hydrogeological map by the relevant colored vertical hatching.

Surface water is characterized or represented by the samples collected from rivers and lakes in order to establish their hydrochemistry. The Bilate and Bedesa rivers (flowing west of the Leku sheet) are endowed with water at the rift floor, and are characterized by a uniform chemistry of the basic sodium-bicarbonate type, but TDS vary at about 230 mg/l for Bilate and 530 mg/l for Bedesa, respectively.

The chemistry of **groundwate**r in the Leku area reflects the hydrological (aquifer) system, including the groundwater circulation and its variability in respect to the geology and hydrogeology of the area consisting of different sedimentary and volcanic rocks. The sodium-bicarbonate hydrochemical type of groundwater prevails in the studied area.

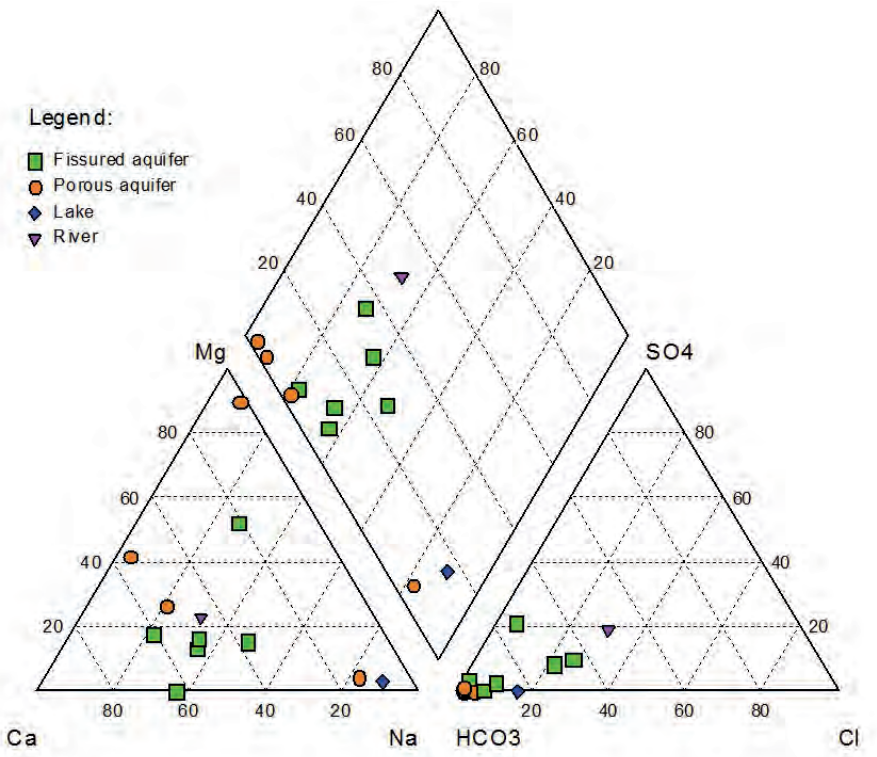

Figure 7-7. *Piper diagram for the classification of natural waters.*

The hydrochemistry of groundwater in the area is expressed on the hydrochemical map by the relevant coloured hatching (for transitional and mixed types). To facilitate the visualization of the classification of water types, the percentage of the major cations and anions of the analysed samples is plotted on the Piper diagram as shown in Fig. 7-7.

The high content of total dissolved solids (TDS) and the sodium-bicarbonate type of groundwater on the rift bottom generally reflect the impact of hot climate. Similarly, the groundwater circulation in lacustrine and volcaniclastic sediments shows higher solubility and its contact with volcanic rocks in geothermal systems also reflects climatic conditions in a closed basin, in which the drainage is represented mainly by medium saline lakes.

The low TDS and dominant calcium-bicarbonate type of groundwater indicate the fast hydrogeological regime of the area receiving a relatively high volume of precipitation where the groundwater flows in fractured volcanic rocks of plateaus and escarpment areas, which are also the main sources of aquifers recharge east of the Leku map sheet.

Groundwater residence time along flow paths, the length of water-rock interaction, lithology, ionic exchange and evaporation may play a significant role in the formation of groundwater composition. Major changes in the chemical composition of groundwater firstly occur in the soil zone during the deposition and concentration of salts by evaporation and evapotranspiration. The second most important correlation of water chemistry with its environment represents its contact with hot rocks, including the groundwater enrichment by carbon dioxide. This mechanism is believed to form the sodium bicarbonate groundwater chemistry of the majority of groundwaters on the rift valley bottom. The third most important interaction includes the leaching of fluoride from acid volcanic rocks, mainly from obsidian and rhyolite pumice.

Groundwater mainly infiltrates into aquifers in the highlands with a cold climate, receiving a high volume of precipitation and then flows to the west to the drainage areas formed by rivers of the highlands and continues through the escarpment to the Rift Valley. Groundwater flows in lithologilcally homogeneous fissured aquifers developed in various Tertiary volcanic rocks in the highlands and then proceeds in the lithologically heterogeneous fissured and mixed aquifers developed in various volcanic and volcaniclastic sedimentary rocks, and unconsolidated Quaternary lacustrine sediments in the Rift Valley. Finally, groundwater is drained by lakes of the Rift Valley (lakes Awasa and Abaya in the case of the Leku sheet) and evaporates. Gradual development in TDS in the highlands and escarpment areas is sharply changed when the groundwater flow reaches the rift valley floor, where the general trends in TDS as well as in groundwater hydrochemistry are highly affected by soluble material in variable volcano-sedimentary units of the rift valley floor and TDS are rapidly increasing together with a change of groundwater type from calcium-bicarbonate into sodium-bicarbonate. The groundwater is enriched by fluoride and its TDS increase from 200–300 mg/l to more than 1,000 mg/l. This increasing trend in TDS from east to west is shown by idealized isosalinity lines on the hydrochemical map.

Groundwater in aquifers of the surveyed area hosted by volcanic, volcaniclastic, volcano-sedimentary and lacustrine sediments is of the sodium-bicarbonate type. In general, the type of groundwater depends on the morphological position of the aquifer on the plateau, escarpment and/or rift floor.

The Rift Valley floor groundwater is characterized by high to very high TDS (particularly near lakes and in some hot springs), and represented by the basic sodium-bicarbonate type in the northwestern part of the sheet. The southeastern part of the sheet (close to the eastern escarpment) is characterized by the transitional sodium-bicarbonate type of groundwater, which has developed from the transient calcium-bicarbonate type occurring in the eastern escarpment and highlands. TDS increase from about 200 mg/l in the southeastern part of the map sheet to more than 1,000 mg/l near the Lake Awasa. The content of fluoride in groundwater, in addition to the higher TDS, exceeds the drinking water standard.

The hydrochemistry of groundwater is expressed on the hydrochemical map by a solid colour for the basic type, and by relevant coloured horizontal hatching for transitional types.

Water quality

The water quality in the surveyed area was assessed from the perspective of its use for drinking, agriculture/irrigation and industry. To assess the suitability of water for drinking purposes, the results of chemical analyses were compared to the Ethiopian standards for potable water (see Tab. 8-13) published in the Negarit Gazeta No. 12/1990 and The Guidelines of the Ministry of Water Resources (MoWR, 2002).

Table 7-13 shows that groundwater in the mapped area is not suitable for drinking in more than 60 % of the sampled water points. This situation reflects the fact that the majority of the groundwater dissolves fluoride and other components from volcano-sedimentary and lacustrine sediments, while also being in contact with the geothermal systems of the rift valley floor contributing to the higher mineralization of water. On the other hand, the groundwater of the highlands and escarpment areas is suitable for drinking.

Table 7-13. Groundwater chemistry compared to drinking water standards and guidelines

Property	Range (min–max) [mg/l]	Ethiopian standards (1) and MoWR Guidelines (2) [mg/l]		Number of exceeding values	
		Highest desirable level	Maximum permissible level	Highest desirable level	Maximum permissible level
Na (2)	2.3–475	–	358	NA	3
Ca (1)	2–88	75	200	1	0
Cl (1)	1.06–163	200	600	0	0
Cl (2)	1.06–163	–	533	NA	0
HBO_2	0.0–1.0	–	0.3	NA	1
(free) ammonia	NA	0.05	0.1	NA	wNA
Fe (1)	NA	0.1	1	NA	NA
Fe (2)	NA	0.4	–	NA	NA
Mg (1)	0.7–30	50	150	0	0
Mn (1)	NA	0.05	0.5	NA	NA
Mn (2)	NA	–	0.5	NA	NA
SO_4 (1)	0.05–82	200	400	0	0
SO_4 (2)	0.05–82	–	483	NA	0
TDS (1)	79–2084	500	1500	9	2
pH (1)	5.32–8.0	7.0–8.5	6.5–9.2	12	10
pH (2)	5.32–8.0	–	6.5–8.5	NA	10
NO_3 (1)	0.05–28	10	45	2	0
NO_3 (2)	0.05–28	–	50	NA	0
F (1)	0.11–10.46	1	1.5	17	6
F (2)	0.11–10.46	–	3	NA	4

In approximately 20% of the cases, the TDS content exceeds the maximum desirable level and poses a threat to the groundwater quality; however, such high TDS accompanied by high concentrations of fluoride (about 20% above the maximum permissible level) is related mainly to the area close to the Lake Awasa, where the surface is covered by fresh pumice fall deposits.

Particular attention was paid to the content of nitrates in groundwater. The content of nitrates is not related to the rock composition (type), but reflects the pollution of groundwater by human and/or animal waste. The background content of nitrates in groundwater is about 5 to 10 mg/l, depending on the relevant land cover. In forest areas, it can be even higher because of the decomposition of various plants and other organic material. The nitrate content in the Leku area varies from 0.05 mg/l to 28 mg/l.

Such nitrate pollution is an important factor to be considered, particularly in the areas where groundwater resources may be exposed to contamination. Such situation has to

be taken into account as well when planning the future development and protection of groundwater resources in the area. Proper location and distribution of water points and appropriate protective measures should be taken concerning the boreholes, springs and dug wells used for drinking water supply.

Agricultural standards for the quality of groundwater used for irrigation purposes are determined using the Sodium Adsorption Ratio (SAR), total dissolved solids (TDS), and the United States Salinity Criteria (USSC). The Sodium Adsorption Ratio (SAR) is used to study the suitability of groundwater for irrigation purposes. It is defined by SAR = Na/[(Ca+Mg)/2], where all concentrations are expressed in mg/l. The majority of water samples from the study area were found to be suitable for irrigation since they show the SAR value within the water quality class of excellent and/or good for agricultural purposes. Consequently, the water from the Bilate, Gelana and Gidabo Rivers is widely used for irrigation.

In general, groundwater from the mapped area can be used for industry, but some specific technologies require water treatment before the water is used for industrial purposes (particularly pH adjustment for brewing). There is a threat of incrustation or corrosion in about 15 % of the samples when such groundwater is transported in pipes for the public water supply or for the delivery of water for industry or agriculture.

The issue of fluorides in groundwater on the Rift floor

The issue of high contents of fluoride in water of the Ethiopian lowlands, including the Rift Valley, is very well known and has been described in many studies. The fluoride concentration in water in the Rift Valley frequently exceeds the Ethiopian and WHO guidelines level of 1.5mg/l. High fluoride concentrations in drinking water cause a range of serious public health problems. Concentration of fluoride exceeding 1.5 mg/l causes dental fluorosis characterized by hypomineralization of tooth enamel, a life-long handicap; 4 mg/l skeletal fluorosis resulting in thickening of the bone structure, thus contributing to impaired joint mobility accompanied by pains, eventual invalidity; 10 mg/l may cause crippling fluorosis, which can lead to deformity of the lower limbs in the areas with poor child nutrition. The treatment of fluoride in groundwater, if viable, could resolve a number of pressing water supply problems within the rift area.

Fluoride concentrations are particularly high in the areas with thermal waters or in those close to recent volcanism (e.g. around the Corbetti, Duguna-Fango and Hobitcha calderas – outside the map sheet). There is a direct correlation between acidic volcanic rocks, such as recent rhyolite, obsidian, pumiceous tuff and high concentrations of fluoride in groundwater. Chemical weathering of volcanic rocks is considered to be the most likely source of fluoride. Rhyolites containing volcanic glass and their products of weathering, which are extremely reactive, appear to be the major interacting materials. The interaction of these weathered and/or reworked volcanic materials with percolating groundwater and carbon dioxide with high pH causes the release of fluoride into groundwater. The fluoride content in groundwater is considered to be inversely related to the concentration of Ca (Tewodros, 2008). This allows a free mobility of the fluoride ion to enter the groundwater, exhibiting lower Ca concentrations. This effect of Ca deficiency is magnified where the cation exchange takes place, particularly in fluvio-lacustrine and volcano-sedimentary deposits, causing the removal of ions (mainly Ca^{2+}) from the solution and their replacement with Na^{+} ions released from the clay. Such hydrogeochemical processes

are responsible for the change of Ca (Mg)-HCO_3 type of groundwater in the highlands and escarpment areas into Na–HCO_3 types on the rift floor.

Thermal waters tend to have higher fluoride content than cold water as the water temperatures allow the greater dissolution of fluoride. This probably explains the predominance of high fluoride content in waters around the Awasa town. It has also been mentioned that closed terminal lakes attain high levels of fluoride, salinity and alkalinity as a result of evaporation and groundwater flow through acidic rocks. High concentrations can also be observed in a thermal zone along the Bilate River and in the geothermal area on the northern shore of Lake Abaya.

The reports of Zenaw (2003) and JICA (2012) showed that fluoride contents decrease with the depth of the water source (testing wells). This confirms that the main source of fluoride is related to the infiltration and percolation of rain water through the material derived from acidic volcanic rocks. Moreover, the concentrations of fluoride can increase in geothermal systems, and the same can be applied to the concentrations of chlorides and nitrates. Zenaw (2003) noted that the decrease in fluoride content with depth in the Awasa area indicates that the shallower lacustrine aquifer usually has higher fluoride content. The deeper aquifer hosted by ignimbrite is recharged from sources far in the eastern and western highlands with a very low content of fluoride (see Fig. 7-8). High fluoride concentrations in ignimbrite are related to thermal springs; their appearance on the surface is controlled by Quaternary fractures, particularly those confined to the Wonji and Bilate fault belts.

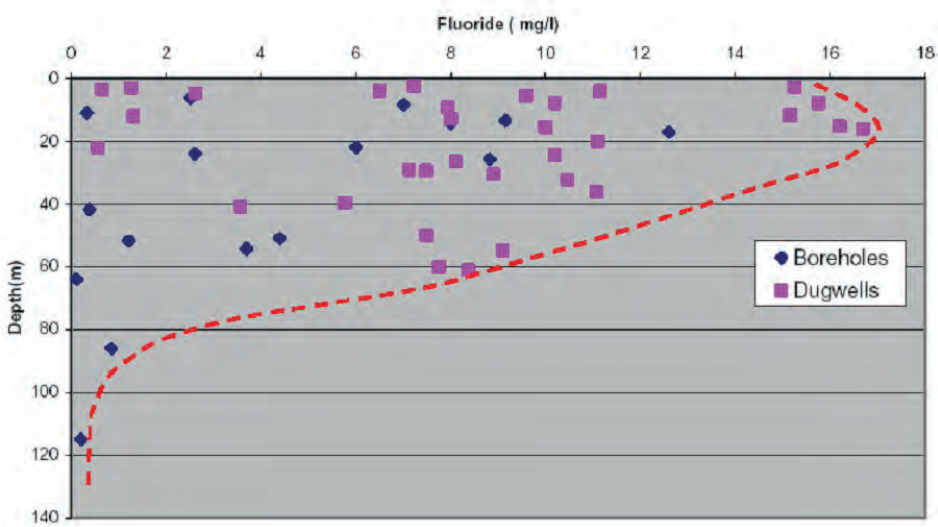

Figure 7-8. *Decrease in fluoride concentration with depth in Awassa Caldera (Zenaw, 2003).*

A number of fluoride removal methods are practiced in the basic water treatment plant designs. Thirteen common techniques can be listed under three groups: Precipitation, adsorption and ion exchange. Additional "special" methods are also in use. With regard to the special methods, the adding of gypsum to the artificial sand-pack filter of a borehole and mixing of hot water with cold water were successfully tested in a fluoride-rich groundwater in Mexico (Carrillo-Rivera, 2002).

7.7 Water resources

Water resources of the area mainly depend on rainfall and other climatic conditions and also on the hydrological, geological and topographical settings. The exploitation of surface and groundwater, as a part of the integrated water resources and development program, must be dealt with respect to the public interest, while addressing the acute problems of adequate and safe water supply schemes in the study area. In general, the ultimate source of all natural potable water is rain, but in an area where the atmospheric precipitation is scarce, some other ways should be suggested to meet the public demand. There are many meteorological stations operated by the National Meteorology Agency of Ethiopia in the surveyed area, and some of them with long-term measurements were selected to assess the rainfall intensity and duration (precipitation depth). The long-term mean annual rainfall of the area has been assessed to be about **1,100 mm/year**.

The areas of active aquifers that have the ability to store and provide water were selected and are depicted on the hydrogeological map. The active porous and fissured aquifers (see Tab. 7-14) cover an area of **763 km^2**.

Table 7-14. Aquifers of the area

Aquifers	Area [km^2]
Porous aquifers	39
Fissured aquifers in volcanic rocks	366
Mixed aquifers in volcanic and sedimentary rocks	351
Lake Awasa	7
Total of the area	763

The runoff characteristics vary widely because of the variability in climatic conditions and hydrogeological characteristics between different observation points. Surface river flow measurements are performed at many gauging stations in the Rift Valley, and river flow measurements were considered in the assessment of surface and baseflow values. The surface flow-baseflow assessment is highly affected by the quality of flow measurements, the effect of bank groundwater storage, difficulties in flow measurements in wide and unstable river channels and the unknown groundwater flow downstream the gauging stations. For further calculations, the values of **specific surface runoff of 4.0 l/s.km^2** and **specific baseflow of 2.0 l/s.km^2** for the Leku sheet were considered. The assessed water resources in the Leku area are shown in Tab. 7-15.

Water resources in the area are large, but their future utilization in the closed Rift Valley Lakes basin, covering the majority of the Leku map sheet, depends on climate change, human demands for water and water management practices.

Hydrogeological system in the rift has been in equilibrium between inflow and outflow and evaporation from lakes. The development and implementation of new irrigation schemes and the use of more surface as well as groundwater will cause a significant annual average decrease in water level of the Lake Awasa, and also drying up the marshy areas in the centre of the Rift Valley.

Table 7-15. Assessment of water resources in the Leku area

	Input	Area [km^2]	Total resources	Remarks
Precipitation	1,100 mm	763	839 Mm^3/year	
Total water resources – map	4.0 l/s.km^2	756	95 Mm^3/year	11 % of total rainfall
Renewable groundwater resources in active aquifers	2.0 l/s.km^2	756	48 Mm^3/year	5.7 % of total rainfall
Static groundwater resources in fissured and mixed aquifers	5 % porosity 100 m thickness	717	3,582 Mm^3	Not proved
Static groundwater resources in porous aquifers	15% 100 m thickness	39	585 Mm^3	Not proved

Surface water resources development

Despite the fact that the river stage measurements show relatively high but logical evapotranspiration when only 11 % of the total rainfall is drained as the total runoff from the area, there exist good water resources to be used for irrigation as well as the drinking water supply for the population of the studied area. The total water resources of the area were assessed to be 95 Mm^3/year.

The surface water of the area should be primarily used for irrigation. The irrigation plans and an assessment of potential and environmental impacts are discussed in detail by Halcrow (2008) for the Rift Valley Lakes Basin, by WWDSE (2004): Study and Design of Gelana, Gidabo and Bilate Irrigation Project, and in other studies.

Groundwater resources development

The river stage measurements show that nearly 5.7 % of the rainfall infiltrate and appear as baseflow. There exist reliable groundwater resources to be used for the supply of drinking water to the population living in the area. There is also a potential to use some volume of groundwater to support irrigation. The total volume of renewable groundwater resources of active aquifers in the area has been assessed to be 95 Mm^3/year.

The majority of people in the area live in small towns and villages, which are supplied with water mainly from drilled and dug wells. Moreover, the water from drilled wells represents the safest water for drinking, which should supply small towns as well as rural population. Therefore, drilling further wells for potable water would be preferable.

The data from regional and detailed surveys were evaluated in order to select appropriate areas and sites for the drilling of hydrogeological wells for water supply to the local population. The following criteria and lithologies were taken into account when selecting the most suitable areas and sites:

- Groundwater accumulated in volcano-sedimentary and volcaniclastic materials contains high concentrations of fluorine, which highly exceed the hygienic standards for potable water.
- Basalts, trachyte and ignimbrites contain groundwater, the quality of which mostly corresponds to the standards for potable water.
- The yields of the wells, which penetrate volcanic rocks, fluctuate between 2 and 10 l/s, and they are sufficient for the supply to as many as 8 000 to 40 000 inhabitants, the consumption being 20 l/day per person.

The strategy for the layout of wells, resulting from the above-mentioned presumptions, is as follows:

- To prefer the localization of the boreholes on outcrops of dark rocks (basalt, trachyte and ignimbrite).
- If there are only light coloured volcano-sedimentary rocks, a geophysical survey must be performed to determine the boundary between these rocks and the underlying volcanic rocks.
- To locate the boreholes in a fissured part of the volcanic rocks.
- To tighten the overlying volcano-sedimentary or volcaniclastic rocks in boreholes with a cement seal to avoid fast infiltration of water from these rocks along the borehole stem.

Some of the existing and documented water points do not provide safe water for drinking as they show an increasing content of nitrates, particularly in the shallow water-supply systems. Deeper wells currently represent a safe type of water supply, although they must be protected against pollution from local sources like human and animal waste (sources of pathogens and nitrates) as well as from potential industry (tanneries, textile industry, flower plantations, etc.). The minimum required distance of water supply wells and potential pollution sources should be maintained during the development of water resources in towns and villages. The same level of attention should also be paid to the development and protection of groundwater resources for rural communities. It should be necessary to start with relatively concentrated communities, where the feasibility and impact of developed schemes will be the most significant.

The development and protection of water resources of the area and the environment as a whole have a principal importance for the development of the infrastructure with subsequent impacts for the eradication of poverty (development of irrigated agriculture, maintaining livestock during drought). Access to safe drinking water improves the health level of the population (statistics show that 40 % of child death rates are related to diseases caused by insanitary water). About 15 % of the rural population have access to safe drinking water in the area, and about 70 % of infections are related to contaminated water resources. This is a serious problem for the creation of strong farm and pastoral as well as industrial communities capable of a full-time engagement in working activity. It is therefore important to provide safe drinking water to communities. Protection of the environment, particularly the prevention of soil erosion and degradation leading to food and water scarcity, is an important development aspect in the area. This aspect is based on the importance of water retention, which is of primary importance with regard to the increase in population numbers connected with rising demands on soil use.

Despite some local and regional environmental problems, the Leku area provides a potential for feasible and environmentally sound natural and human resource management. The same concerns the water resources requiring similarly sound water management.

8) ENGINEERING GEOLOGY OF THE LEKU AREA

8.1 Engineering geological characterization of the Leku area

The basic geotechnical characteristics of individual rock formations in the Leku sheet were assessed and are described in the following sections. The diverse lithological units in the terrain were characterized and categorized into engineering geological regions based on their occurrence in the terrain, geomorphic features and physical properties. The engineering properties of soils and rocks influence the formation of large-scale morphological features apart from other external factors or endogenous and exogenous processes. The method adopted in this study is based on the notion that a regional geomorphic and formational boundary supported the delineation of engineering geological units is a more practical and simpler approach than thousands of samplings and a lot of testing to achieve similar results. It can be regarded as reverse modelling, where the effect (the observed geomorphic features in this case) is used to derive the cause which, in this case, is represented by the engineering geological characteristics. A few examples of such approaches exist and are worth mentioning. For example, the Schmidt hammer rebound values were widely applied in the Polish Sudetes and used to reveal a strong correlation between variably weathered rocks and various elements of the relief (Placek and Migon 2007). Similar relations were reported in other studies (Day 1981; Aydin et al. 2005). This indicates that both the extraction of physical properties of the rocks from general morphological features of the terrain and vice versa can be achieved comparably. This can be considered an advantage as the engineering geological units can be identified and classified based on detailed morphological characteristics of the terrain, which are easier to delineate or categorize compared to intensive testing and sampling.

In the Leku area, two prominent volcanic edifices influence the engineering geological regions separated by a relatively flat land in between. From the north, a younger Caldera of Hawassa continues southward with related series of parallel sets of normal faults running N–S and cutting through pyroclastic ignimbrite rocks. To the east, an off–axis stratovolcano resting on a western rift escarpment forms ignimbritic rocks that are dissected by trellis-type dense stream networks with shallower valleys. The latter also resulted in the dense networks of low relief morphological features. The sampling of rocks for index physical properties was made in three regions: (1) in the western and eastern parts of the studied area with dissected topography (2) in the central flat to low undulating land, separating the western and eastern dissected terrains and (3) in the northern part of the map (the southern shore of Lake Hawassa) with a predominant formation of soft volcanoclastic sediments.

8.2 Engineering geological classification

The lithologies in the studied area generally have low to intermediate rock mass strength. Most of the rock units include pyroclastic ash, tuff and ignimbrite with a few subordinate basaltic rocks. Weathering is prominent in the eastern highlands that comprise the flanks

of the shield volcano on the eastern rift escarpment. Hence, the classification of the bedrock in the area was divided into two engineering geological rock mass classes. Most of the central area, which is a moderately undulating to plain area with a 0.5 to 1 meter thick eluvial soil cover, falls under the moderately strong rock mass category. The western high relief zones, with widely spaced typical N–S trending horst and graben structures, notably have the moderate rock mass strength as well. The eastern and southeastern parts of the studied area resting at the foot of the eastern shield volcano area are, for the most part, comprised of a densely dissected area with low relief and generally low rock mass strength.

The superficial younger Quaternary deposits, on the other hand, are classified into four genetic soil units. Such deposits with a considerable thickness mostly occur in the eastern and southeastern part of the map sheet on higher grounds, developing as residual soils. In addition, a few alluviumareas are found as well along stream segments with wide flood plains. The rest of the superficial Quaternary deposits (eluvium, diluvium and colluvium) occur in the western part of the area, which is tectonically highly dissected and forms the N–S trending sets of grabens and horst structures due to series of normal faults. These sediments are found filling various parts of such narrower basins. In the northern extremes near the shore of Lake Hawasa, predominantly ash fall deposits are found on and around the floor of the main Hawassa Caldera. Table 8-1 presents the results of laboratory physical tests conducted on representative soil samples from the area; in general, they show a moderate to low plastic silty soil nature. The physical tests on the rock samples are shown in Figure 8-2.

Genetic classification of soils in the area

Volcaniclastic deposits

These are pyroclastic fall deposits and reworked sediments that represent the southward continuation of the Hawasa Caldera. They cover a wider plain of mainly silty soil with a minor proportion of clay. They are dominated by tuff and ash interlayers with a higher degree of weathering. The soil has a dark brown to brown colour. The deposits are massive and stiff in competence when dry, and generally fine-grained with high plasticity and low dilatancy. According to the field observations, they have a clayey silt composition. A field test with a Pocket Penetrometer for the index compressive strength yielded 1.5 and 3 kg/cm^2. The thickness usually ranges from 0.5 to 1 meter.

A common problem associated with this soil is the occurrence of ground fissures. From the field observations, it appears that upon continued plastic deformation of the soil above the opening fissured rocks due to volcano-tectonic activity, the overlying soil suddenly yields and develops deep and longer cracks in the area following the general trend of structures on the floor of the Hawassa Crater. A geophysical survey implemented in the transverse direction by the seismic refraction method turned out to be unsuccessful. To get additional information, a more specialized and elaborate technique would be required. Nevertheless, it is still regarded as essential to map potential sites of the future occurrence of cracks based on the notion that the fissures are surficial expressions of the underlying bed rock fissures. The problem is further exacerbated by the occurrence of a rapidly developing deep gully, which requires extensive rehabilitation to retain the soil washed out. In general, the thickness of the soils is not more than 1 meter and hence, it poses no significant problem in terms of engineering applications as it can be easily excavated or replaced.

Weathering mantle (regolith)

Deeply weathered rocks are seen to be developing in the central and eastern part of the studied area, mainly on ignimbrite rocks. These soils composed of silty clay and sandy clay have a reddish-brown colour with firm to stiff consistency, are poorly sorted and well graded, boulder-free, having a fine-to-medium grain size with moderate plasticity and low dilatancy. The index compressive strength test from a field in the area performed with a Pocket Penetrometer gave values ranging from 1 to more than 3.5 kg/cm^2. From the engineering geological point of view, no significant problem is noticeable associated with this type of soil cover in the area, where its thickness reaches from 2 to 5 meters. Nevertheless, the proneness to erosion and gully formation is eminent in the area, requiring an early intervention.

Colluvial sediments

Granular and fine-grained soil mass units are noticeably accumulated through the gravitational process with moderate transportation by running water in the vicinity of the source region of the deposits. These are common in the foot escarpments and distal parts of the faults forming horst structures that bound the wide N-S running grabens in the area. As these are found in fewer patches and remain dry for most of the time throughout the year, no significant geological problems are anticipated with the exception of susceptibility to mass wasting hazards when saturated.

Slope scree sediments

Slope scree deposits are the result of a gravity-driven accumulation at the foot of steep fault scarps. They are mostly comprised of inhomogeneous fragments of rock and soil with minor silt. They may be problematic in the case of deep excavations in and around them, requiring permanent support for the construction of infrastructure.

Table 8-1. Index physical properties of soils from the Leku Map Sheet (Physical Laboratory test plots)

Soil sample	Gravel (%)	Sand (%)	Silt (%)	Clay (%)	Liquid limit (%)	Plastic limit (%)	specific gravity	USCS
SS-LK-01	9	38	53	–	34	30	2.57	MH
SS-LK-02	8	55	38	–	81	42	2.17	SM
SCL-LK-03	6	39	55	–	49	34	2.61	MH
SCL-LK-04	4	44	52	–	71	41	2.75	MH
SCL-LK-05	13	67	20	–	54	30	2.07	SM
SCL-LK-06	5	83	13	–	40	29	2.35	SM

Engineering geological rock mass classification

Moderate rock mass strength units

Tests on the rock samples collected from the area gave the point load index strength values ranging between 3–4 MPa with a very high porosity and water absorption ranging between 18–48 % (Figure 8-2).

Mostly, the weathered and decomposed ignimbrite rock is found which characteristically shows greyish colour when intact and dark grey and reddish brown

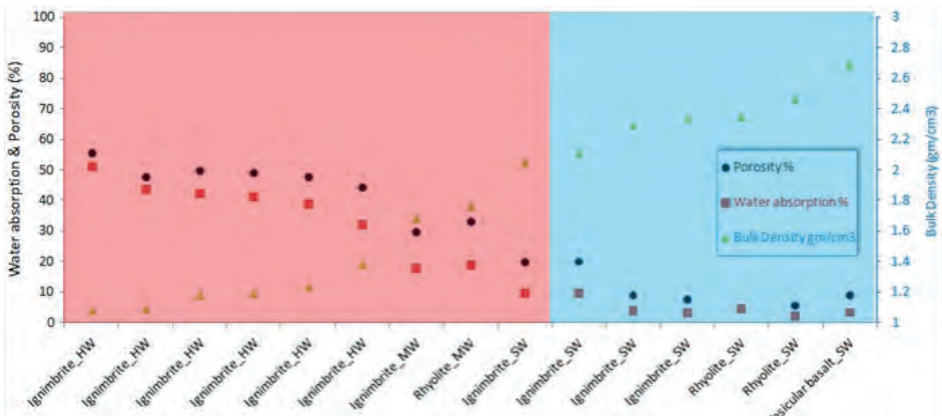

a)

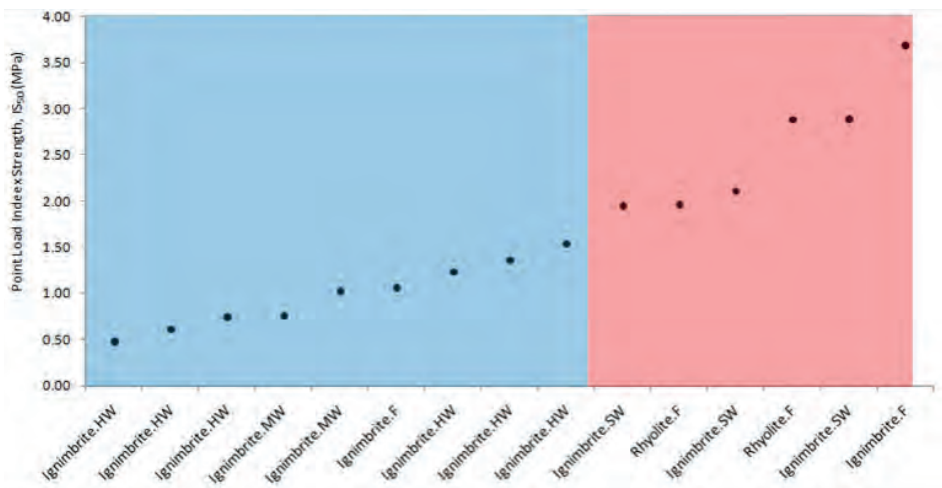

b)

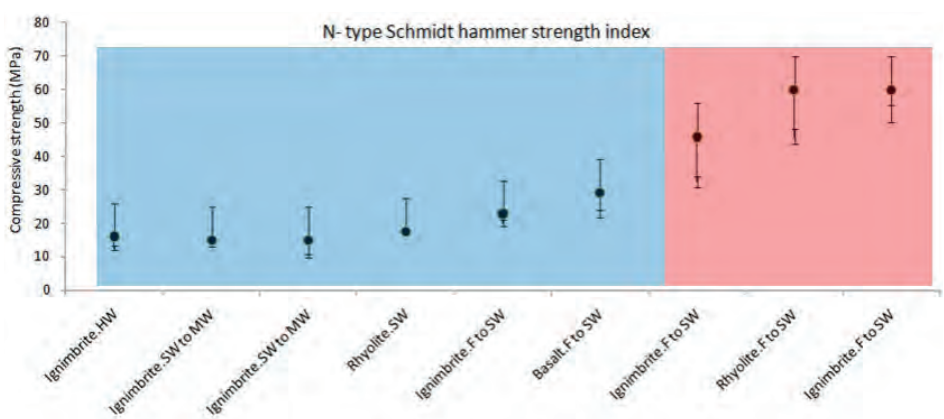

c)

Figure 8-1. *Laboratory physical tests of samples from variably weathered basalt and ignimbrite lithologies in the study area (Leku map sheet) in the northwestern escarpment. (a) porosity, water absorption and bulk density plots, (b) Point load index strength correct.*

colour when weathered. Occasionally, it occurs in a highly weathered state, usually containing lithic fragments. In some areas, manual excavation is practical due to low rock mass strength. In the escarpment of the horst, competent rock blocks are noted to be prone to rock fall hazard along the sub–vertical mega joints in the ignimbrites triggered by seismic activity. They are a very important source for dimension stones, such as cobble stones for pavements and buildings.

Low rock mass strength units

These rock units are comprised of lithological units that are soft and weak and often in a highly weathered state to the extent that their strength has been almost completely undermined. This can be seen from the laboratory physical test plots in Figure 9-2 (the left part of the plots). Pyroclastic ash and tuff fall deposits and highly jointed and weathered ignimbrites make up this class of rock units. Most of the vegetated areas in the southeastern part of the studied area are typical for such a low strength class of rock mass units.

9) GEOLOGICAL HAZARDS

The specific geological and climatic conditions in southern Ethiopia significantly affect the economic and socio-demographic development of this region. The geomorphological and geological character of the area creates favourable conditions for triggering geological processes that negatively influence human activities and the local environment. Surface erosion strongly affects the soil quality and causes an overall degradation of farmland. Expansion of urbanization could lead to the loss of settlements and human beings in the areas exposed to or suffering from seismicity. Risks associated with volcanic activity cannot be excluded either. Hazardous phenomena were derived and evaluated from the synthesis of geological, geomorphological and remote-sensing data, and are also based on geological and geomorphological mapping in the field and the multi-disciplinary analysis of the results obtained. A range of factors such as geomorphological features (landform origin, slope deformations, impact of head-ward erosion) as well as geological setting (lithology, degree and character of weathering, geotechnical and hydrogeological properties of rocks, data on historical earthquakes), and the age of volcanic rocks were taken into account and interpreted in order to identify and specify geological or natural hazards in general. The land-use and climate conditions were also considered.

The studied area morphologically belongs to the southern part of the MER; morphologically, it belongs to the central part of the whole territory located south of the Hawasa Caldera. The northern part of the area is drained by ephemeral streams into the Lake Hawasa, while streams in the southeastern part are emptied into the Lake Abaya. The western part is drained by the Bilate River, thus forming or copying the axial drainage pattern of the rift. The geomorphological character of the area is highly variable, generally being a result of the combination of volcanic and tectonic events as well as exogenous processes. The originally volcanic landforms of Pleistocene age were modified by tectonic processes. The vertical movements influenced the local topography, and hence the intensity of alluvial erosion, density and the character of drainage pattern in the area. The formation of the rift depression followed the development of the Main Ethiopian Rift (MER), and led to the lowering of base level that resulted in the head-ward erosion leading to intensive surface erosion and the formation of widespread badlands and subsequently, a large volume of sediment have been transported by streams into the Hawasa and Abaya lakes. These processes were accelerated by climatic conditions accompanied by torrential rains, by the local lithology inclined to strong weathering and also by deforestation of the landscape.

Structural landforms consist of fault scarps characterized by relatively steep and straight slopes that are inclined to form cliffs and escarpments. The majority fault scarps in the studied area are running N-S to NW-SE, forming a sub-parallel system of horsts and grabens separating the relatively flat volcanic plateaus. The exposed fault planes are often overprinted by intense surface erosion giving rise to badlands morphology. However, triangular facets or other morphological peculiarities have not developed.

Volcanic landforms are characterized by gently undulating to flat plateaus reflecting the dip of underlying gently inclined lava and pyroclastic flows or the more resistant ignimbrite strata. The volcanic plateau in the eastern part corresponds to the lowermost section of sloping flanks of the Dure Caldera located east, outside the surveyed map sheet (the Wijigra map sheet). Also, a rhyolite dome forming the Boricha ridge was identified in the central part of the Leku map sheet. The volcanic landforms in the central and western parts of the sheet are overprinted by younger tectonic features.

Denudation landforms are represented by erosion slopes and erosion valleys that result from the prolonged effect of erosion processes on the exposed fresh or weathered rocks. Erosion slopes are widespread landforms with a different gradient formed by alluvial erosion and deposition. Erosion slopes create scarps and V-shaped valleys, and frequently do not exactly follow or copy geological and tectonic structures. The parts of erosion slopes with poor vegetation cover and soft rock environment when affected by intense erosion are transformed into badlands.

Accumulation landforms consist of alluvial plains, alluvial fans and infillings of endorheic depressions. Most of the drainage pattern of the surveyed area has a character of erosional ephemeral streams so that the floodplains are rather rare having a limited extent. Alluvial plains are formed only in the parts where fluvial systems show lower gradient. Alluvial fans occur at the mouths of erosion valleys and gullies where steep, high-power channels enter a zone of reduced stream power. They dominantly form sheet-flood and relatively flat cone-shaped bodies with slopes radiating away from an apex located at the point where the feeder channel enters the fan. These alluvial fans are usually a few tens up to hundreds of meters large. Small endorheic depressions are formed in the axial parts of tectonic grabens and correspond to the occurrence of intermittent lakes originating during raining seasons. The most prominent endorheic depression is the bottom of the Hawasa Caldera, which coincides with lacustrine sediments of the Lake Hawasa.

9.1 Endogenous hazards

Seismic hazards in the study area are related to the extensional tectonics in the rift region. Continental rifts are characterized by a special type of seismicity – en dash earthquake swarms and volcanic earthquakes or the earthquakes related to volcanic activity. Geothermal phenomena related to the volcanic activity confined to rift regions represent another typical feature that can be observed in the surveyed area. Several types of earthquakes are documented in the area, for instance shallow seismic swarms related to the magmatic activity and magma-derived fluid intrusions. The swarms consist of many thousands of minor to moderate earthquakes with magnitudes less than 5 of the magnitude scale. The earthquakes accompanied by direct volcanic eruptions were observed and reported repeatedly in the past (Gouin 1979). The strong tectonic earthquakes are also recorded, being related to the displacements along active faults parallel to the rift valley. Historical earthquakes are poorly located and are difficult to be assigned to known faults; their hypocentral depths and distribution remain unclear.

Seismic hazard assessment has been usually based on a probabilistic approach in recent studies. For southern Ethiopia, there are only a few results presented by regional studies (Kebede and Eck 1997). The most important input data for seismic hazard

assessment include: the catalogue of historical earthquakes, seismograms of recent earthquakes recorded by seismic stations, paleoseismological observations, seismotectonic data, an attenuation model of seismic wave propagation and a local model of seismic velocities. The probabilistic method consists of three basic steps:

1) Definition of source zones and their parametres. This step has not been performed yet because of the lack of data due to the short history of the records. The most important parameter is the maximum magnitude assigned to a given source zone. It is clear that at least in some source zones, the maximum magnitude can exceed a value of 7. More accurate estimates are required.

2) Construction of attenuation curves. Southern Ethiopia represents a special geological structure (Rift Valley), which significantly influences attenuation curves. Therefore, standard attenuation curves are of a limited use. A large set of recorded seismograms is necessary for the construction of regional attenuation curves.

3) Computation of probabilistic seismic hazard curves. The result of the computation is an estimation of the probability exceeding the defined values of seismic acceleration or other characteristics of seismic motion. The resulting probability has to include local conditions. The effect of local conditions is very strong in southern Ethiopia due to the layers of thick sediments in the Rift Valley.

Volcanic hazards are associated with recent volcanic activity and post-volcanic features. A sub-recent volcanism was not identified in the mapped area, but the Quaternary Corbetti Caldera located 25 kilometres north of the Leku map sheet is associated with explosive volcanism. The age of pumice ejection during eruptions is dated at 400 BC, accompanied by widespread tephra deposits as a product of the Plinian style eruption (Rapprich et al. 2016). A question arises whether a new eruption within the Corbetti Caldera north of the Wendo Koshe volcano would or might endanger or destroy settlements by pyroclastic flows immediately with no time for evacuation (Rapprich et al. 2014a, 2016). The eruption would also emit a large amount of ash over a wider area, including the area of the map sheet (Jones et al. 2017). Systematic monitoring of this volcano is highly recommended to estimate the potential for early warning prior to a major eruption.

9.2 Exogenous hazards

Due to the nature of the landform in the southern segment of the rift, sets of noticeable exogenous processes that often lead to affect the normal activity of the livelihood are prevalent. These processes are a part of the natural phenomena that operated since the beginning of the present-day rift evolution set, which can be grossly in place approximately since 3 Ma (Bonini et al. 2005). Fault scarps and consequently the depression basin (grabens) are formed at the foot of the escarpment, which is the site of an intense depositional regime from the upland on the escarpment. The presence of the closed lake system (endorheic) in the case of the Lake Hawasa means that the huge sediment transported to the lakes leads to the level rise and continuous inundation of shores. This has caused escalation of infrastructure development costs on one hand and diminishing of land available for ever increasing population on the other hand. At the same time,

increasing threats of surface erosion as well as subsurface erosion, siltation, flooding and inundation are common. Landslides and rock fall do not represent a prominent hazard in this area.

The following part consists of texts describing the nature of delineated geo-hazards risk units in the accompanying geo-hazards risk map for the Leku sub-sheet.

Alluvial hazards

Alluvial hazards include dangerous exogenous processes associated with rivers and surface water streams, generally related and triggered by heavy rains and consequent flood events. During rainy season, the river banks are overflown by big discharge reverse, which are otherwise dry except the wet season. It often destroys farmlands and houses when occurring, while it also damages the major highway the middle of the flood plain, temporarily blocking traffic. No noticeable concrete and sustainable counter measures are in place concerning these hazards, despite their strong impact on the activity of the livelihood. The high sediment yielded and seasonal flooding of tributaries to the Lake Hawasa also could lead to a significant increase in lake level.

Alluvial erosion is one of the most common alluvial processes in the area as a natural exogenous process of the landscape. Tectonic processes creating high gradient relief, climatic characteristics with stormy rains producing rapid runoff, lithological setting with strongly weathered volcanic or volcano-clastic rock and unconsolidated sediments promote favourable conditions for surface erosion. Intensive deforestation and agriculture activity on steep slopes significantly accelerate erosional processes. It leads to a decrease of infiltration capacity of surface and runoff increase, at first as a non-erosive laminar flow, then it transforms into a turbulent sheet flow with erosive action. The erosion is associated with mass movement and high sediment load of the drainage system. The fault scarps and adjacent erosional and structure slopes created by weathered rocks as well as the areas with an occurrence of unconsolidated sediments are the most affected areas in general. The sheet erosion occurs in the uppermost part of slopes. Downward channelling of runoff water causes the creation of erosional rills at first, followed by V-shaped valleys, where the vertical component of erosion is prominent. In the foothill of slopes in a lower gradient setting, the lateral component of erosion leads to the formation of box-shaped walls with vertical sides (Fig. 8-1). The depth of gullies ranges from several meters to approximately 20 metres in depth and up to 30 metres in width; however, Moges and Holden (2008) reported 33 metres wide gullies. Thus, the surface flow is the most common mechanism of gully growth. However, piping is also documented south to the Jara Dado area (Fig. 8-2), being also reported (Morgan 1996, Bryan and Jones 1997) from this area. Piping associated with subsurface erosion (suffusion) represents one mechanism of gully development and growth. Lateral erosion is related to flood events and high discharge, mainly occurring in the outer bank of meandering channels and streams in general. Lateral erosion has been documented along brooks and rivers in floodplains in the southeastern part of the map sheet. Intensive lateral erosion is also reported from the gullies located in the lower part of slopes located south to the Lake Hawasa (Fig. 8-3). A lateral shift of streams in unconsolidated silty and sandy sediments and reworked tuffs leads to the collapse of edges of gullies and damages in the adjacent farmlands. The most affected area by the surface erosion is located in the erosional slopes of southern margin of the Hawasa Caldera (south to Jara Karera and Jara Dado, south and southwest to Unbulo

Walho), in erosional slopes south to Belela, in the fault scarps located south and southwest to Yirba, where the extend badland, characterized by an unvegetated surface dissected by a high density of rills and gullies and loss of soil, are created. Reforestation of the most vulnerable areas is necessary to decrease the negative impact of erosion. Planting of trees and diversified agriculture production can help slow down the erosional rates. The elimination of gullies is necessary to decelerate the runoff of water and sediment load; it should be carried out by planting rows of trees as well as by the construction of small dams and polders in the drainage system. Trees and deep-rooted bushes should also be planted on the boundaries of land plots to prevent soil erosion.

The expansion of the Lake Hawasa in the north affects the urbanized settlement around the lake and causes the *inundation* of the fertile and flat-lying adjacent tract of land, which is the basic means of subsistence for local dwellers. The lake level rise could be attributed to tectonic and hydrologic effects. Tectonic processes and consequently the vertical movements strongly influence the topography of the area as well as water level in the lake. Also, extreme soil erosion due to the deforestation and expansion of farmlands could contribute to an increase in sediment yield leading to the siltation of lakes. The endorheic (drainless) depressions related to tectonic subsidence in the central part of the sheet can be temporally inundated during the rainy season. Torrentional rains might cause flash floods in many ephemeral rivers systems and erosional valleys.

***T**he accumulation of sediments* is usually connected with floods as well as mass movement processes. The mass of silt and clay-sized particles to sand and gravel is often transported down narrow canyons and gullies from the upper parts of escarpments. The greatest risk of high accumulation occurs in the areas with an abrupt decrease in slope gradient. The loss of transporting medium power and carrying capacity result in rapid sedimentation of the material eroded and transported from the upper parts, leading to the creation of alluvial fans in the foothill of slopes, mouths of gullies as well as erosional and stream valleys, where a thick accumulation could be deposited. The sedimentation of material causes problems mainly in farmlands of the area (Moges and Holden 2008).

Ground fissures and suffusion were documented in various localities of the Ethiopian Rift Valley. Potential risk of the occurrence of fissures is associated with flat surface of the rift floor, where the volcanic bedrock is covered by unconsolidated or poorly consolidated sedimentary succession. In the sheet, the fissures are documented in the northern margin of the map sheet west and southwest of the Lake Hawasa (Fig. 9-4). Generally, the fissures create ground crack systems, lined parallel with the faults related to the Main Ethiopian Rift System, exhibiting a predominant N–S to NNE–SSW direction. In Jara Dado, the fissures are also bound to a WNW–ESE fault system. The mechanism of formation of ground cracks is uncertain and the occurrence of fissures is random and unexpected. The conformity of the youngest fault system and fissures promote the combination of tectonic origin and subsurface erosional processes of this phenomenon. The association of ground cracks and vertical displacement along normal faults in the depth are known in the world (e.g. Holzer 1984, Bell et al. 1992, Carpenter 1993). Another hypothesis is represented by the aquifer-system compaction and horizontal seepage stresses, which is connected to a decline in groundwater table (Ayalew at al. 2004). The fissure origin could also be caused by irregular topography (bedrock highs, scarps or buried pediment) at depth such

Figure 9-1. *Gully system in the fault scarp, north to Yrba.*

Figure 9-2. *Piping in unconsolidated polygenetic sediments, south to Jara Dado.*

as when compressible deposits overlie bedrocks (Schummann and Poland 1970, Carpenter 1993). The fissure development is accompanied by surface and shallow subsurface processes such as piping, hydrocompaction and changes in the volume of material. This processes cause a rapid and unexpected subsidence of surface and collapses of fissure side walls. The display of occurrence of fissures could be very discreet, in some cases only the hollows with a scale of several decimetres are developed in the surface. Ground cracks – en dash lines with up to 3 metres in width are common. Sometimes, gravitational collapse of fissure edges and the subsidence of blocks are present and the fissure system extends within a range of tens of meters. The visible depth is up to 10 metres approximately. The development of fissures and accompanying processes represents very dangerous geological hazards resulting to the loss of buildings, infrastructure and agriculture fields. A high risk of such processes impacts the areas with a high density of population and human activities. The destruction of houses and infrastructure as well as the loss of human lives and animals is documented in connection with the development of ground fissures.

Slope deformation hazards

Slope deformations occur rarely within the Leku map sheet. Several types of slope deformation – landslides, lateral spread and earth/debris flows – were documented. Most of the areas prone to slope movement are concentrated in the tectonic escarpments.

Fall and toppling are abrupt movements of masses of rocks and boulders that become detached from steep fault slopes or cliffs. The separation occurs along discontinuities such as fractures and movement occurs by free fall, bouncing, and rolling. Falls are strongly influenced by gravity, mechanical weathering and the presence of interstitial water. The large blocks of competent rocks with widely spaced tectonic indices and cooling contractional originated sub-vertical joints are well evident in the area. A high density of

Figure 9-3. *Lateral erosion on a gully located in the lower part of escarpment near Kube.*

Figure 9-4. *Ground fissure in polygenetic sediments near Jara Dado.*

tectonic and columnar jointing result from the cooling contraction of volcanic rocks and welded pyroclastic deposits (ignimbrites) and predispose rocks to decomposition and rock-fall. The endangered areas by rock fall and toppling are located on the steep fault scarps with extensive outcrops of welded ignimbrites. The main large-scale rock-fall triggering factors are seismic events, thus the foothills below the affected scarps are at a permanent risk of rock falls.

Small scale-fossil shallow seated *landslides* have been observed in the map sheet escarpment area from the image analysis of topographic disposition and field observation. Construction of houses is not recommended in the endarged areas. These failures are triggered by heavy rains, water saturation and loss of cohesion. Also, the deep excavation inappropriately changing the roadcut topography decreases the slope stability.

10) LOCAL PREVENTION AND MITIGATION MEASURES OF GEOLOGICAL HAZARDS

Geological hazards are the result of geodynamic processes taking place throughout the history of the Earth; hence, the application of measures to prevent or mitigate geological dangers should take this fact into consideration. Two measures or strategies should be adopted in the Leku area to cope with the above-mentioned issues. The first one is to reduce the geological hazards endangering the local population and infrastructure such as roads, farmlands and settlements. This requires appropriate planning whenever possible to avoid an unnecessary relocation of the infrastructure (roads or settlements) or even a complete abandonment of populated sites or the already built infrastructure. The second approach is to use mechanisms that control the local geological processes and dangers. This actually involves the rehabilitation of highlands with minimum human intervention.

It should also be noted that apart from these preventive and mitigation strategies, it is vital to maintain emergency preparedness and create a response plan based on the vulnerability of the area. This will ensure that the endangered population is safeguarded from the eminent hazards if such phenomena are identified. The Leku area situated in the active East African Rift indeed needs such preparedness (including the emergency response systems).

Some aspects of the encountered common problems caused by slope deformations and hydrologic processes and remedial measures taken thereof are discussed in the following paragraphs. They are followed by the recommended long-term preventive and rehabilitation strategies and succeeded by suggestions for the monitoring and preparedness (including the emergency response systems) for various potential disasters anticipated resulting from the geological setting of the area.

10.1 Manageable geomorphic hazards

Ground fissures and subsidence

In the plain situated west and southwest of the Lake Hawassa, ground fissures and the subsidence of surface occur. There are places where a segment of land suddenly subsides by as much as 16 m approximately. Witness accounts indicate that the collapses usually happen in just one day. The survey of some of these localities shows that in some places, the collapse is continuous at a lower rate after the initial collapse, as can be observed in the waviness of the ground. Sinkholes on the surface with approx. 1m in diameter and 6m in depth are encountered in places. At the time of the survey, no saturation or standing water was observed in the areas. Such disturbed sites obviously follow the local structural trends of the rift in the area. The material is comprised of unconsolidated sediments (silty-clay soil, sands, gravels). This phenomenon is very dangerous with regard to people's lives as the drops of land occur suddenly without a prior warning.

The cause of the fall is probably a long-term rifting movement, where tensile stress has accumulated in the soil and rock. The second influence is represented by subsurface erosion. Fine-grained particles are eroded and moved downward. This leads

to the formation of underground caverns that gradually increase over time and extend in the direction of the rift. When the underground cavern reaches such a size that the soil above is unable to carry the load, the top of the cavern collapses. The result of the collapse is the formation of a gully with vertical sides. In the long term, the vertical sides will collapse. To decelerate the impact of surface erosion, planting rows of trees as well as constructing small dams and polders in the drainage system and gullies is recommended. Trees and deep-rooted bushes should also be planted on the boundaries of land plots to prevent soil erosion.

Figure 10-1. *Beginning of collapse – wavy ground, Jara Dado.*

The risks pertaining to ground fissures are unavoidable. Nevertheless, precautionary measures and earlier exploration of suspected sites can help to delineate and mark such sites for any planned development work or safety consideration. Hence, as there are no technical possibilities to avoid the problem, the only possibility is to delineate problematic sites in the landscape and detect the sinking stage in time, and then mark the sites and make them non-accessible to humans and animals. These sites should be marked in the terrain by fencing off the areas where side collapses will subsequently propagate. It is estimated that the protective belt is approximately 30 m from the existing edge of fissures on either side.

Locating the fissures is done the best using a combination of geophysical and remote sensing methods. A geomorphological interpretation based on high-resolution remote sensing data can detect morpho-lineaments associated with potential ground fissures, the occurrence of linear depressions and areas with vertical movements of the surface including subsidence, while the multi-temporal analysis can contribute to information on the evolution of these failures. A suitable geophysical method is to use a Georadar (GPR-Ground Penetrating Radar) or electrical subsurface surveying methods. The Georadar could be used in the transverse direction to the direction of the local rift structural trends. It is advisable to perform measurements on large areas and carry out them repeatedly.

Figure 10-2. *Collapse of the land – rift direction, Jara Dado.*

Figure 10-3. *Collapse of the land – rift direction, Jara Dado.*

This would help to identify the development of fissures in the area clearly and thus to predict where the sinks will subsequently occur. This will provide time for the prediction of fissure occurrence and clearing out the area.

Surface erosion and gullying

Surface erosion leading to gullying presents a common risk in the area. Erosional structures are characterized by V-shaped rills and gullies approximately 1 to 12 m deep in silty clay soils ranging from 1m to 10m in thickness and resting on hard ignimbrites on the bottom, which prohibits deeper erosion. The lower part of slope box-shaped gullies in silty and clayey soils is underlain by tuffs or unwelded ignimbrites with a vertical height of 10–20 m, and the span of the gully width is approximately 30 m. Small-scale slumps and landslides occur in V-shaped gullies. In the lower part of the valley, which forms steep sides of 10 to 20 m in size, the side walls are subjected to lateral erosion of occasional streams and prone to collapse and the widening of the gullies.

Figure 10-4. *Upper valley – landslides on both sides of gullies, south to Kuwe.*

Figure 10-5. *Beginning of the erosion in the upper part of a scarp, south to Kuwe.*

Figure 10-6. *Middle part of a gully with intensive deep erosion, south to Kuwe.*

Figure 10-7. *Lower part of a gully with lateral erosion, south to Kuwe.*

Surface erosion is also a part of a natural process that cannot be altered by technical means and can be managed only. In the long run, the shape of a valley will change. In the upper part, the sides will slide until the inclination of the slope takes a stable configuration. It is therefore possible to define a zone along the edge of the current valley, where the probability of a landslide occurrence is high. This corresponds the most likely to the areas within ca 20 m from the current edge of the valley. In the lower part, where lateral erosion of the stream is already occurring, it is also possible to define a zone where access should be restricted and where the valley sides will gradually fail to produce a stable slope configuration in the long run. This zone can be estimated to cover around 40m from the edge of the existing gullies.

10.2 Preventive and mitigation measures for rehabilitation of natural environment

- The dangers that strongly affect the development of infrastructure and land-use in the studied area include tectonics, slope failures and alluvial processes. The greatest impact on land use is undoubtedly caused by alluvial processes associated with high precipitation during the rainy season.
- The main prerequisite for eliminating the negative impact of natural hazards is to obey natural processes that cause these dangers. It is important to note that any intervention in any natural system will induce an appropriate response often with adverse effects. Prior to each technical intervention into the development of the area, it is therefore important to carry out a study of possible impacts on both the planned project and the further decentralization of the concerned natural system.
- All structures closely associated with fluvial channels (buildings, bridges, culverts) must be designed to resist more than 100% of the maximum discharges. A simple reduction of the flow capacity with regard to its natural rate is only a short-term solution of the problem. Line constructions (roads, power lines, etc.), culverts and bridges should obey the topography of the area so that they would not be a barrier to the natural runoff during high discharges and rainy seasons.
- It is necessary to permanently maintain the same stream channel capacity by cleaning and removing the deposited material, particularly in the vicinity of bridges or other constructions, where the reduction of channel capacity may cause damage to or even the destruction of the whole structure.
- Active alluvial fans represent the areas of a high natural risk, especially in the lower-lying regions, where the zones along active and abandoned channels can be affected by floods.
- Reforestation is the primary choice of a natural way to tackle the issue of areas susceptible to erosion. Planting rows of trees, construction of small dams and polders in drainage pattern and gullies are recommended to decelerate the runoff and to reduce the transport of sediment.
- The sites affected by active and fossil slope failures represent the areas unsuitable for urban development. Also, it is advisable to avoid these places for road construction. In case of any construction, it is suggested to carry out an engineering geological survey to check the slope stability and to ensure drawing a design and implementation of useful drainage.

10.3 Suggested hazard monitoring and emergency response systems

The majority of natural hazards are derived from the landforms or geomorphology of the area so that detailed and high-resolution topographic data are necessary to be obtained to prevent natural hazards. The use of modern remote sensing methods (e.g. interferometry to measure small displacements) will allow identifying the changes in topography or morphology of the terrain that may indicate movements in fault zones and consequently even the prediction of seismic hazards, which may result in mass movements such as landslides or slope failures, etc. High resolution topography using new remote sensing techniques will enhance information on the terrain in order to better understand the processes taking place on the Earth's surface and to delineate the areas susceptible to geological hazards such as alluvial plains or flat areas generally prone to severe floods, et cetera.

The elaboration of quantitative models of fluvial processes associated with rivers and streams, runoff models of basins and the optimization of water management should be a part of the long-term strategy. The installation of gauging stations with remote data transmission and the design of flood hazards early warning systems are vital steps for the management and protection from potential risks in low-lying plains.

To eliminate the risks from seismic and volcanic hazards, which are also eminent in the area, it is recommended to reinforce and strengthen the already installed seismic monitoring stations network to precisely locate earthquake epicentres, mitigate the risks and plan for any emergency.

For the assessment of volcanic hazards, it is necessary to have comprehensive information on the wider volcanic, geological and tectonic context of the area, including the characteristics of individual volcanoes. The approach followed in the current study on geo-hazards phenomena and mapping of critical factors should be expanded to other areas. Age determinations provide fundamental information for the initial scoping assessment. Such age determinations may include historical information, stratigraphic relationships, radiometric dating and morphological considerations. In addition to the monitoring of seismic data, it is advisable to carry out continuous monitoring of accompanying volcanic phenomena, such as the activity of fumaroles and monitoring of changes in the physical and chemical properties of fumaroles and thermal waters. To eliminate the impact of volcano-seismic hazards, it is important to set up standards and strongly implement them in the construction of various civil infrastructure projects. In the zones with potential impacts of natural hazards, evacuation plans and evacuation paths should be identified in consultation with a multi-professional team composed at least of a law specialist, a medical team and geo-scientists to minimize the loss of human lives. Furthermore, an extensive campaign should be regularly held to increase the awareness of the wider public of the mechanisms and consequences of natural disasters to increase the resilience in all aspects.

REFERENCES

Abbate, E., Bruni, P., Sagri, M. (2015): Geology of Ethiopia: a review and geomorphological perspectives. In: Landscapes and Landforms of Ethiopia, Springer Netherlands, 33–64.

Agezew, T., Regassa, T., Šíma, J. (2014): Hydrogeological and hydrochemical maps of Dila NB 37-2. Explanatory notes. AQUATEST a.s., Prague. Czech Rep.

Agostini, A., Bonini, M., Corti, G., Sani, F., Mazzarini, F. (2011): Fault architecture in the Main Ethiopian Rift and comparison with experimental models: Implications for rift evolution and Nubia–Somalia kinematics. Earth and Planetary Science Letters 301(3), 479–492.

Asfaw, L. (1998): Environmental hazard from fissures in the Main Ethiopian Rift. Journal of African Earth Sciences 27(3-4), 481–490.

Asfaw, B., Beyene, Y., Semaw, S., Suwa, G., White, T., WoldeGabriel, G. (1991): Fejej: a new paleoanthropological research area in Ethiopia. J. Human. Evol. 21, 137–143.

Auxtero, E., Maderia, M., Sousa, E. (2003): Variable charge characteristics of selected Andisols from the Azores, Portugal. Catena 56(1-3), 111–125.

Awlachew, S.B. (2006): Investigation of physical and bathymetric characteristics of Lakes Abaya and Chamo, Ethiopia, and their management implications. Lakes and Reservoirs: Research and Management 11, 133–140.

Ayalew, L., Yamagishi, H., Reik, G. (2004): Ground cracks in Ethiopian rift valley: facts and uncertainties. Eng Geol 75, 309–324.

Ayalew, D., Yirgu, G., Pik, R. (1999): Geochemical and isotopic (Sr, Nd and Pb) characteristics of volcanic rocks from southwestern Ethiopia. Journal of African Earth Sciences 29(2), 381–391.

Ayalew, D., Barbey, P., Marty, B., Reisberg, L., Yirgu, G., Pik, R. (2002): Source, genesis, and timing of giant ignimbrite deposits associated with Ethiopian continental flood basalts. Geochim. Cosmochim. Acta 66, 1429–1448.

Ayalew, D., Marty, B., Barbey, P., Yirgu, G., Ketefo, E. (2006): Sub-lithospheric source for Quaternary alkaline Tepi shield, southwest Ethiopia. Geochem. J. 40, 47–56.

Aydin, A., Basu, A. (2005): The Schmidt Hammer in rock material characterization. Engineering Geology 81, 1–14.

Balogh, K. (1985): K/Ar dating of Neogene volcanic activity in Hungary: Experimental technique, experiences and methods of chronologic studies. ATOMKI Rep. D/1, 277–288.

Billi, P., Dramis, F. (2003): Geomorphological investigation on gullyerosion in the Rift Valley and northern highlands of Ethiopia. Catena 50(2-4), 353–368.

Bloomer, S.H., Curtis, P.C., Karson, J.A. (1989): Geochemical variation of Quaternary basaltic volcanics in the Turkana Rift, northern Kenya. J. Afr. Earth. Sci. 8, 511–532.

Bogena, H., Kunkel, R., Schrobel, T., Schrey, H.P., Wendland, F. (2005). Distributed modeling of groundwater recharge at the macroscale. Ecological Modeling 187, 15–26.

Bonini, M., Corti, G., Innocenti, F., Manetti, P., Mazzarini, F., Abebe, T. & Pecskay, Z. (2005): Evolution of the Main Ethiopian Rift in the frame of Afar and Kenya rifts propagation. Tectonics 24(1), 1–21.

Brown, F.H., Carmichael, I.S.E. (1969): Quaternary volcanoes of the Lake Rudolf region: 1. The basanite-tephrite series of the Korath Range. Lithos 2(2), 239–260.

Brown, F.H., Carmichael, I.S.E. (1971): Quaternary volcanoes of the Lake Rudolf region: II. The lavas of north island, south island and the Barrier. Lithos 4(3), 305–323.

Carpenter, M.C. (1993): Earth fissure movements associated with fluctuations in groundwater levelsnear the Picacho Mountains, South-central Arizona, 1980–84. US Geological Survey Professional Paper 497-H, Washington, 40 pp.

Carrillo-Rivera, J.J., Cardona, A., Edmunds, W.M. (2002): Use of abstraction regime and knowledge of hydrogeological conditions to control high-fluoride concentration in abstracted groundwater: San Luis Potosí basin, Mexico. Journal of Hydrology 261(1-4), 24–47.

Central Statistics Authority (2012): Statistical abstract.

CES 58 (2013): Compulsary Ethiopian Standard. Ethiopian Standard Agency.

Chernet, T. (1982): Hydrogeology of the Lakes region, Ethiopia. Ministry of Mines and Energy Ethiopian Institute of Geological Surveys. Addis Ababa. 222 pp.

Chernet, T. (1993): Hydrogeology of Ethiopia and Water Resources Development – MS EIGS. Ministry of Mines and energy, Addis Ababa.

Chernet, T. (2006): Geology and Geothermal Resources in the Northern Lake Abaya Area (Ethiopia). First East African Geothermal Conference, ARGeo – C1, November 24–29, Addis Ababa, Ethiopia.

Chernet, T., Travi, Y., Valles, V. (2001): Mechanism of degradation of the quality of natural water in the Lakes region of the Ethiopian Rift Valley. Water Research 35(12), 2819–2832.

Cox, A., Dalrymple, G.B. (1967): Statistical analysis of geomagnetic reversal data and the precision of potassium–argon dating. Journal of Geophysical Research 72(10), 2603–2614.

Dalrymple, G.B., Lanphere, M.A. (1969): Potassium-Argon Dating. Principles, Techniques and Applications to Geochronology. W.H. Freeman and Co., San Francisco. 258 pp.

Davidson, A., Rex, D.C. (1980): Age of volcanism and rifting in south-western Ethiopia, Nature 283, 654–658.

Day, M. (1981): Rock hardness and landform development in the Gunong Mulu National Park, Sarawak, E. Malaysia. Earth Surface Processes and Landforms 6, 165–172.

De Wispelaere, L., Marcelino, V., Regassa, A., De Grave, E., Dumon, M., Mees, F., Van Ranst, E. (2015): Revisiting nitic horizon properties of Nitisols in SW Ethiopia. Geoderma 243-244, 69–79.

Di Paola, G.M. (1971): Geology of the Corbetti Caldera area (Main Ethiopian Rift Valley). Bulletin Volcanologique 35(2), 497–506.

Di Paola, G.M. (1972): The Ethiopian Rift Valley (between 7 00′ and 8 40′ lat. north). Bulletin Volcanologique 36(4), 517–560.

Driessen, P., Deckers, J., Spaargaren, O., Nachtergaele, F. (2001): Lecture notes on the major soils of the world. World Soil Resources Reports No. 94. FAO, Rome.

Droop, G.T.R. (1987): A general equation for estimating Fe^{3+} concentrations in ferromagnesian silicates using stoichiometric criteria. Mineral Mag 51, 431–435.

Ebinger, C.J., Yemane, T., Harding, D.J., Tesfaye, S., Kelley, S., Rex, D.C. (2000): Rift deflection,migration, and propagation: Linkage of the Ethiopian and Eastern rifts. Africa, Geol. Soc. Am. Bull. 112, 163–176.

Ebinger, C.J., Yemane, T., WoldeGabriel, G., Aronson, J.L., Walter, R.C. (1993): Late Eocene-Recent volcanism and faulting in the southern main Ethiopian rift. J. Geol. Soc. London 150, 99–108.

Engdawork, A., Bork, H.R. (2014): Long-Term Indigenous Soil Conservation Technology in the Chencha Area, Southern Ethiopia: Origin, Characteristics, and Sustainability. Ambio 43(7), 932-942.

FAO-UNESCO (1978): FAO-UNESCO, Soil map of the World, 1 : 5,000,000 (download for ArcGis). *http://www. lib.berkeley.edu/EART/fao.html*

Furman, T., Bryce, J.G., Karson, J., Iotti, A. (2004): East African Rift System (EARS) plume structure: insights from Quaternary mafic lavas of Turkana, Kenya. Journal of Petrology 45(5), 1069–1088.

George, R., Rogers, N. (1999): The petrogenesis of Plio-Pleistocene alkaline volcanic rocks from the Tosa Sucha region, Arba Minch, southern Main Ethiopian Rift. Acta Vulcanol. 11, 121–130.

George, R., Rogers, N. (2002): Plume dynamics beneath the African plate inferred from the geochemistry of the tertiary basalts of southern Ethiopia. Contributions to Mineralogy and Petrology 144, 286–304.

Gíslason, G., Eysteinsson, H., Björnsson, G., Harðardóttir, V. (2015): Results of Surface Exploration in the Corbetti Geothermal Area, Ethiopia. Proceedings: World Geothermal Congress, Melbourne, Australia.

Gizaw, B. (1976): The origin of high bicarbonate and fluoride concentrations in water of the Main Ethiopian Rift Valley. East African Rift system, Journal of American Science 22(4), 391–402.

Gökbulak, F., Özcan, M. (2008): Hydro-physical properties of soils developed from different parent materials. Geoderma 145, 376–380.

Haileab, B., Brown, F.H., McDougall, I.A.N., Gathogo, P.N. (2004): Gombe Group basalts and initiation of Pliocene deposition in the Turkana depression, northern Kenya and southern Ethiopia. Geological Magazine 141(1), 41–53.

Halcrow (2008): Rift Valley Lakes Basin Integrated Resources Development Master Plan Study Project, Phase 2 Report, Part II Prefeasibility Studies. Halcrow Group Limited and Generation Integrated Rural Development Consultants. Addis Ababa.

Hart, W.K., WoldeGabriel, G., Walter, R.C., Mertzman, S.A. (1989): Basaltic volcanism in Ethiopia: constraints on continental rifting and mantle interactions. Journal of Geophysical Research: Solid Earth 94(B6), 7731–7748.

Hayward, N.J., Ebinger, C.J. (1996): Variations in the along-axis segmentation of the Afar Rift system, Tectonics 15, 244–257.

Hofmann, C., Courtillot, V., Féraud, G., Rochette, P., Yirgu, G., Ketefo, E., Pik, R. (1997): Timing of the Ethiopian flood basalts event and implications for plume birth and global change. Nature 389, 838–841.

HSDP (2008): Ministry of Health (MOH) [Ethiopia]. 2008. The Health Sector Strategic Plan (HSDP). Addis Ababa, Ethiopia: Ministry of Health.

IUSS Working Group (2015): World Reference Base (WRB) for Soil Resources 2014, update 2015, International soil classification system for naming soils and creating legends for soil maps. World Soil Resources Reports No. 106. FAO, Rome.

Janoušek, V., Farrow, C.M., Erban, V. (2006): Interpretation of whole-rock geochemical data in igneous geochemistry: introducing Geochemical Data Toolkit (GCDkit). J Petrol 47, 1255–1259.

JICA (2012): The Study on Groundwater Resources Assessment in the Rift Valley Lakes Basin in the Federal Democratic Republic of Ethiopia. Japan International Cooperation Agency (JICA), Kokusai Kogyo Co., Ltd., Ministry of Water and Energy (MoWE), The Federal Democratic Republic of Ethiopia.

Jones, A., Breuning-Madsen, H., Brossard, M., Dampha, A., Deckers, J., Dewitte, O., Gallali, T., Hallett, S., Jones, R., Kilasara, M., Le Roux, P., Micheli, E., Montanarella, L., Spaargaren, O., Thiombiano, L., Van Ranst, E., Yemefack, M., Zougmore, R. (2013): Soil Atlas of Africa. European Commission, Publications Office of the European Union, Luxembourg. 176 pp.

Katoh, S., Nagaoka, S., WoldeGabriel, G., Renne, P., Snow, M.G., Beyene, Y., Suwa, G. (2000): Chronostratigraphy and correlation of the Plio-Pleistocene tephra layers of the Konso Formation, southern Main Ethiopian Rift, Ethiopia. Quaternary Science Reviews 19(13), 1305–1317.

Kazmin, V. (1972): Geological Map of Ethiopia. Geological Survey of Ethiopia: Addis Ababa, Ethiopia.

Kazmin, V. (1975): Explanation of the geological map of Ethiopia. Bulletin number one. Geological Survey of Ethiopia, Addis Ababa.

Kazmin, V. (1980): Transform faults in the East African Rift system. Atti Convegni Lincei 47, 65–73.

Kebede, S., Abdulkadir, M. (1987): Results of shallow wells drilling and geophysical review of Corbetti geothermal prospect. Report: Ethiopian Institute of Geological Surveys. Geothermal exploration project Lakes District, 30 pp.

Kefale, T., Šíma, J. (2013): Hydrogeological and hydrochemical maps of Hosaina NB 37-2. Explanatory notes. Aquatest a.s., Praha, Czech Republic.

Koeppen NMSA (1989): Climatic and Agroclimatic Resources of Ethiopia. NMSA.

Lahmeyer International (2005): Genale-Dawa River Basin integrated resource development master plan study. Ministry of Water Resources.

Macdonald, R., Gibson, I.L. (1969): Pantelleritic obsidians from the volcano Chabbi (Ethiopia). Contributions to Mineralogy and Petrology 24(3), 239–244.

Martin-Jones, C.M., Lane, C.S., Pearce, N.J.G., Smith, V.C., Lamb, H.F., Schaubitz, F., Viehberg, F., Brown, M.C., Frank, U., Asfawossen, A. (2017): Recurrent explosive eruptions from a high-risk Main Etiopian Rift volcano throughout the Holocene. Geology 45(12), 1127–1130.

McKenzie, M.J., Siegel, D., Patterson, W., McKenzie, D.J. (2001): A geochemical survey of spring water from the main Ethiopian rift valley, southern Ethiopia: implication for well head protection. Hydrogeol J. 9, 265–272.

Mengesha, T., Chernet, T., Haro, W. (1996): Geological map of Ethiopia at scale of 1 : 2,000,000, 2nd Edition. Geological survey of Ethiopia, Addis Ababa, Ethiopia.

Moges, A., Holden, M.N. (2008): Estimating the rate consequences of gully development, a case study of Umbulo catchment in southern Ethiopia. Land Degrad. Develop. 19.

Morgan, R.P.C. (1996): Soil erosion and conservation, 2nd edition. Longman, Harlow.

Morimoto, N., Fabries, J., Ferguson, A.K., Ginzburg, I.V., Ross, M., Seifert, F.A., Zussman, J., Aoki, K., Gottardi, G. (1988): Nomenclature of pyroxenes. Amer Miner 73, 1123–1133.

MoWR (2002): Negarit Gazeta No. 12/1990 and the Guidelines of Ministry of Water Resources.

MoWR (2005): Genale-Dawa and Wabe Shebelle River Basins integrated water Resources development. Master plan study, Ministry of Water Resource, Addis Ababa, Ethiopia.

NMA (2006): Annual Climatic Bulletin – Federal Democratic Republic of Ethiopia. Ministry of Water Resources, National Meteorological Agency (NMA), Climatological Service Team.

NMSA (1996): Assessment of Drought in Ethiopia. Meteorological Research Reports Series No. 2, Addis Ababa, Ethiopia.

Pearce, J.A. (1996): A user's guide to basalt discrimination diagrams. Trace element geochemistry of volcanic rocks: applications for massive sulphide exploration. Geological Association of Canada, Short Course Notes 12, 79–113.

Placek, A., Migoń P. (2007): Rock-landform relationships in the Sudetes in the light of rock strength assessment using the Schmidt hammer. Geomorphological Variations. Prague.

Pouchou, J.L., Pichoir, F. (1985): "PAP" (φρZ) procedure for improved quantitative microanalysis. In: Armstrong. JT (ed.): Microbeam Analysis. San Francisco Press, San Francisco, 104–106.

Rapprich, V., Kycl, P., Hroch, T., Verner, K., Nida, D., Biyuze, Y., Kopačková, V., Mišurec, J., Šíma, J., Málek, J., Malík, J., Tesema, T., Bekele, Y., Megerssa, L., Filfilu, E., Legesse, F., Tadesse, E., Bewketu, H., Demewoz, A., Negash, T., Pecskay, Z., Freymuth, H. (2014a): Explanation Booklet to the Geological Hazards and Engineering Geology Maps of Hosaina, NB 37-2. Czech Geological Survey, Prague; AQUATES a.s., Prague; Geological Survey of Ethiopia, Addis Ababa.

Rapprich, V., Habtamu, E., Kycl, P., Hroch T., Verner, K., Kopačková, V., Mišurec, J., Šíma, J., Málek, J., Malík, J., Tesema, T., Bekele, Y., Megerssa, L., Filfilu, E., Legesse, F., Tadesse, E., Bewketu, H., Demewoz, A., Negash, T., Pecskay, Z., Freymuth, H. (2014b):

Explanation Booklet to the Geological Hazards and Engineering Geology Maps of Dila, NB 37-6. Czech Geological Survey, Prague; AQUATEST a.s., Prague; Geological Survey of Ethiopia, Addis Ababa.

Rapprich, V., Žáček, V., Verner, K., Erban, V., Goslar, T., Bekele, Y., Legesa, F., Hroch, T., Hejtmánková, P. (2016): Wendo Koshe pumice: the latest Holocene silicic explosive eruption product of the Corbetti volcanic system (southern Ethiopia). J. Volcanol. Geotherm. Res. 310, 159–171.

Rogers, N.W., Macdonald, R., Fitton, J.G., George, R.M.M., Smith, M., Barreiro, B. (2000): Two mantle plumes beneath the East African rift system: Sr, Nd and Pb isotope evidence from Kenya Rift basalts. Earth Planet. Sci. Lett. 176, 387–400.

Rooney, T.O. (2010): Geochemical evidence of lithospheric thinning in the southern Main Ethiopian Rift. Lithos 117, 33–48.

Rooney, T.O., Hart, W.K., Hall, C.M., Ayalew, D., Ghioprso, M.S., Hidalgo, P.J., Yirgu, G. (2012): Peralkaline magma evolution and the tephra record in the Ethiopian Rift. Contrib. Mineral. Petrol., 164, 407–426.

RRC (1985): The Challenges of Drought, Ethiopia's decade of struggle in relief and rehabilitation. RRC, Addis Ababa, 280 p.

Saria, E., Calais, E., Stamps, D.S., Delvaux, D., Hartnady, C.J.H. (2014): Present-day kinematics of the East African Rift. J. Geophys. Res. Solid Earth 119, 3584–3600.

Schumann, H.H., Poland, J.F. (1970): Land subsidence, earth fissures and groundwater withdrawal insouth-central Arizona, USA. In: Tison, L.J. (ed.): Land Subsidence. International Association of Hydrological Sciences, Tokyo, Japan, 295–302.

Setegn, S.G. (2010): Modeling Hydrological and Hydrodynamic Processes in Lake Tana Basin, Ethiopia, KTH. TRITA-LWR, Ph.D. Thesis 1057.

Shinjo, R., Chekol, T., Meshesha, D., Tatsumi, Y., Itaya, T. (2011): Geochemistry and geochronology of the mafic lavas from the southeastern Ethiopian rift (the East African Rift System): assessment of models on magma sources, plume-lithosphere interaction and plume evolution. Contrib. Mineral. Petrol. 162, 209–230.

Šíma, J., Kebede, S., Belete, Y., Mamo, T. (2012): Mineral and Thermal Waters for Spa and Recreation-Lake Shalla. Geological Survey of Ethiopia. Report.

Singh, B., Gilkes, R.J. (1992): Properties and distribution of iron oxides and their association with minor elements in the soils of southwestern Australia. J. Soil Sci. 43, 77–98.

Stamps, D., Calais, E., Saria, E., Hartnady, C.J.H., Nocquet, J., Ebinger, C.J., Fernandez, R. (2008): A kinematic model for the East African Rift. Geophys. Res. Lett., L05304.

Steiger, R.H., Jäger, E. (1977): Subcommission on geochronology: Convention on the use of decay constants in geo- and cosmochronology. Earth and Planetary Science Letters 36, 359–362.

Stewart, K., Rogers, N. (1996): Mantle plume and lithosphere contributions to basalts from southern Ethiopia. Earth Planet. Sci. Lett. 139(1-2), 195–211.

Stocking, M., Murnaghan, N. (2000): Handbook for the Field Assessment of Land Degradation. Earthscan. 169 pp.

Tan, Z.X., Lal, R., Smeck, N.E., Calhoun, F.G. (2004): Relationships between surface soil organic carbon pool and site variables. Geoderma, 121, 185–187.

Trua, T., Deniel, C., Mazzuoli, R. (1999): Crustal control in the genesis of Plio-Quaternary bimodal magmatism of the Main Ethiopian Rift (MER): geochemical and isotopic (Sr, Nd, Pb) evidence. Chemical Geology 155(3), 201–231.

UNDP (1971): Ethiopia: Investigation of Geothermal Resources for Power Development (ETH 26): Geology, Geochemistry and Hydrology of Hot Springs of the Eastern African Rift System in Ethiopia.

Van Wambeke, A.R. (1962): Criteria for classifying tropical soils by age. Journal of soil science 13, 124–132.

WABCO (1990): Water Resources Development Master Plan for Ethiopia.

WHO (2006): World Health Statistics. *http://www.who.int/countries/eth/eth/en/*

Wolde, B., Widenfalk, L. (1994): Petrochemical and geochemical constraints on Cenozoic magmatism in Ethiopia. Afr Geosci Rev 1, 475–494.

WoldeGabriel, G. (1989): Geological map of Hagere Mariam in scale 1 : 250 000, MS GSE, Addis Ababa.

WoldeGabriel, G., Aronson, J.L., Walter, R.C. (1990): Geology, geochronology, and rift basin development in the central sector of the Main Ethiopian Rift, Geol. Soc. Am. Bull. 102, 439–458.

WoldeGabriel, G., Hart, W.K., Katoh, S., Beyene, Y., Suwa, G. (2005): Correlation of Plio–Pleistocene Tephra in Ethiopian and Kenyan rift basins: Temporal calibration of geological features and hominid fossil records. Journal of Volcanology and Geothermal Research 147(1), 81–108.

WoldeGabriel, G., Yemane, T., White, T., Asfaw, B., Suwa, G. (1991): Age of volcanism and fossils in the Burji-Soyoma area, Amaro Horst, southern Main Ethiopian Rift, J. Afr. Earth Sci. 13, 437–447.

Wolela, A. (2014): Volcanism, sedimentation, K/Ar and palynology studies, Yayu

and Delbi-Moye Basins, Southwestern Plateau of Ethiopia. Journal of African Earth Sciences 93, 1–13.

Wolfenden, E., Ebinger, C., Yirgu, G., Deino, A., Ayalew, D. (2004): Evolution of the northern Main Ethiopian rift: Birth of a triple junction, Earth Planet. Sci. Lett. 224, 213–228.

WWDSE (2001): Water Works Design and Supervision Enterprise: Integrated Master Plan study for Developing Lake Hawasa. Ministry of Water and Irrigation. Addis Ababa, Ethiopia.

WWDSE (2004): Study and Design of Gelana, Gidabo and Bilate Irrigation Project, Water Works Design and Supervision Enterprise, Addis Ababa.

WWDST (2003): Wabe Shebelle River Basin Integrated Development Master Plan Study, MoWR, Addis Ababa.

Yavitt, J.B., Wright, S.J. (2002): Charge characteristics of soil in a lowland tropical moist forest in Panama in response to dry-season irrigation. Aust. J. Soil Res. 40(2), 269–281.

Yemane, T., WoldeGabriel, G., Tesfaye, S., Berhe, S.M., Durary, S., Ebinger, C.J., Kelley, S.P. (1999): Temporal and geochemical characteristics of Tertiary volcanic rocks and tectonic history in the southern Main Ethiopian Rift and the adjacent volcanic fields. Acta Vulcanol. 11, 99–119.

Zanettin, B. (1978): The Evolution of the Chencha Escarpment and the Ganjuli Graben (Lake Abaya) in the Southern Ethiopian Rift. N. Jb. Geol. Paläont. Mh. 8, 473–490.

Zenaw, T., Tadesse, D. (2003). Hydrology and Engineering Geology of Awasa Lake Cahtchment, Geological survey of Ethiopia.

ANNEXES

Annex 1.

Table 1. Whole-rock compositions of volcanic rocks (oxide wt.% for major elements and ppm for trace elements, except Au)

Sample	DE001	DE025	DE035	KE001	TE028	DE201
rock	ignimbrite	ignimbrite	rhyolite	trachyte	rhyolite	basalt
wt. %						
SiO_2	75.13	71.94	73.16	73.97	73.66	45.39
Al_2O_3	10.9	10.39	12.76	12.27	12.52	15.05
Fe_2O_3	3.46	4.88	2.57	2.83	2.77	13.1
MgO	0.09	0.14	0.16	0.14	0.14	5.64
CaO	0.24	0.19	0.16	0.15	0.14	10.11
Na_2O	4.63	4.19	4.93	4.41	4.69	2.8
K_2O	4.57	4.88	5.18	5.03	5.04	0.87
TiO_2	0.22	0.34	0.35	0.31	0.33	2.95
P_2O_5	0.01	0.01	0.02	0.01	0.02	0.36
MnO	0.14	0.2	0.13	0.14	0.14	0.2
Cr_2O_3	< 0.002	< 0.002	< 0.002	< 0.002	< 0.002	0.008
LOI	0.4	2.5	0.4	0.6	0.4	3.2
Sum	99.78	99.71	99.81	99.82	99.82	99.73
ppm						
Mo	1.4	0.2	0.1	0.3	0.4	0.6
Cu	0.5	1.4	0.2	< 0.1	0.1	44.2
Pb	3.6	2.2	15.3	16.5	13.4	0.7
Zn	26	42	14	10	32	82
Ni	0.6	1.1	0.2	0.2	0.3	49.6
As	< 0.5	< 0.5	< 0.5	0.5	< 0.5	< 0.5
Cd	0.1	0.2	0.2	< 0.1	< 0.1	< 0.1
Sb	< 0.1	< 0.1	< 0.1	0.1	< 0.1	< 0.1
Bi	< 0.1	< 0.1	< 0.1	< 0.1	< 0.1	< 0.1
Ag	< 0.1	< 0.1	< 0.1	< 0.1	< 0.1	< 0.1
Au (ppb)	0.7	< 0.5	< 0.5	< 0.5	< 0.5	0.8
Hg	< 0.01	< 0.01	< 0.01	< 0.01	< 0.01	< 0.01
Tl	< 0.1	< 0.1	< 0.1	< 0.1	< 0.1	< 0.1
Se	< 0.5	< 0.5	0.7	< 0.5	< 0.5	< 0.5

Table 2. Trace element analyses of volcanic rocks (ppm)

Sample	DE001	DE025	DE035	KE001	TE028	DE201
Ba	17	150	10	16	24	272
Sc	5	4	6	6	6	25
Be	5	7	3	4	6	< 1
Co	6.7	3	4.3	2.1	2.6	44.9
Cs	0.6	1.5	0.4	0.4	0.2	< 0.1
Ga	25.5	26.9	25.4	26.2	27.8	17.9
Hf	22.1	27.6	18.8	22.6	20.8	4.1
Nb	109.7	145.7	95	106.1	99	22.7
Rb	99.9	122.9	119.2	143.6	134.5	20
Sn	6	8	6	6	7	1
Sr	8.6	14	3	3.2	3.6	527.4
Ta	6.9	8.7	5.8	6.8	6.8	1.5
Th	14.8	16.7	14.7	17.3	16.6	1.6
U	3.6	4.7	2.4	2.2	2	0.5
V	8	< 8	< 8	8	< 8	321
W	35.2	10.1	20.6	9.6	13.8	4.8
Zr	890.9	1140.3	770	891.4	746.3	144.5
Y	91.6	122.9	69.2	72.1	53	26.1
La	102.2	135.5	94.8	48.2	85.3	19.9
Ce	211	268.9	176	150.4	149.6	45.6
Pr	24.58	31.35	21.54	11.95	21.89	5.5
Nd	93.4	117	79.3	44.2	76.6	25
Sm	18.07	22.59	14.88	9.23	13.95	5.36
Eu	1.55	3.39	1.87	1.09	1.54	2.11
Gd	16.48	21.97	13.56	10.27	10.9	6.01
Tb	2.74	3.66	2.23	1.89	1.82	0.88
Dy	16.32	21.7	13.46	12.45	11.01	5.03
Ho	3.37	4.49	2.67	2.74	2.16	0.92
Er	9.49	13.36	8.03	8.29	6.84	2.49
Tm	1.46	2.01	1.22	1.27	1.06	0.33
Yb	9.72	12.72	8	8.53	7.58	2.07
Lu	1.49	1.99	1.25	1.32	1.21	0.28

Table 3. Representative chemical composition of pyroxenes

Rock	basalt	basalt	basalt	rhyolite	rhyolite	rhyolite	basalt	basalt
Sample	DE 013B	DE 013B	DE 013B	DE036	DE036	DE036	DE201	DE201
SiO_2	50.01	49.95	49.71	52.01	52.17	52.15	46.96	47.53
TiO_2	1.57	1.56	1.72	0.23	0.20	0.22	2.88	2.72
Al_2O_3	3.53	3.64	3.76	0.34	0.28	0.26	5.18	5.02
Cr_2O_3	0.41	0.42	0.25	0.00	0.01	0.04	0.07	0.08
Fe_2O_3	2.10	1.93	2.10	3.42	3.92	2.80	4.63	3.93
FeO	6.19	6.28	7.04	9.65	8.81	9.97	5.80	6.08
MnO	0.25	0.19	0.12	2.77	2.72	2.82	0.16	0.21
MgO	14.18	14.16	14.10	11.84	12.21	11.90	13.02	13.18
CaO	21.69	21.62	21.10	18.50	18.78	18.28	21.38	21.37
Na_2O	0.37	0.37	0.35	1.11	1.11	1.10	0.46	0.45
K_2O	0.00	0.00	0.02	0.01	0.02	0.00	0.02	0.01
Total	**100.30**	**100.12**	**100.25**	**99.87**	**100.23**	**99.53**	**100.56**	**100.56**
Si	1.857	1.857	1.849	1.978	1.973	1.988	1.756	1.774
Al	0.155	0.160	0.165	0.015	0.013	0.012	0.228	0.221
Fe^{2+}	0.192	0.195	0.219	0.307	0.279	0.318	0.181	0.190
Fe^{3+}	0.059	0.054	0.059	0.098	0.111	0.080	0.130	0.110
Cr	0.012	0.012	0.007	0.000	0.000	0.001	0.002	0.002
Ti	0.044	0.044	0.048	0.007	0.006	0.006	0.081	0.076
Mn	0.008	0.006	0.004	0.089	0.087	0.091	0.005	0.007
Mg	0.785	0.785	0.782	0.671	0.688	0.676	0.726	0.733
Ca	0.863	0.861	0.841	0.754	0.761	0.747	0.856	0.854
Na	0.026	0.027	0.025	0.081	0.081	0.081	0.033	0.033
K	0.000	0.000	0.001	0.000	0.001	0.000	0.001	0.000
TOTAL	**4.000**	**4.000**	**4.000**	**4.000**	**4.000**	**4.000**	**4.000**	**4.000**

Annex 2. Soil textural and chemical data

Sample	Depth	Sand	Silt	Clay	pH/H_2O	pH/KCl	P	K	Ca	Mg	TOC	CEC	BS	$CaCO_3$
	cm	%	%	%			mg/kg	mg/kg	mg/kg	mg/kg	%	$cmol_c/kg$	%	%
JJ038A	10–20	14.18	43.56	42.26	5.40	4.00	< 3.5	251	3288	557	1.83	32.94	76.15	< 0.20
JJ038B	40–50	10.48	60.12	29.40	6.20	4.70	< 3.5	195	4457	608	1.24	35.20	87.15	< 0.20
JJ039A	0–20	24.92	32.48	42.60	6.20	4.80	< 3.5	289	2178	332	2.30	21.04	58.14	< 0.20
JJ039B	40–50	17.33	46.64	36.03	6.30	4.50	< 3.5	202	1496	262	0.80	17.11	69.39	< 0.20
JJ040	20–40	8.99	18.11	72.90	7.40	5.90	< 3.5	380	2424	228	1.14	40.62	95.31	< 0.20
JJ041A	0–20	34.14	31.68	34.18	6.70	5.40	< 3.5	529	1276	133	1.47	16.38	63.67	< 0.20
JJ041B	40–60	16.27	37.21	46.52	8.10	5.60	< 3.5	248	8616	708	1.86	30.07	100.00	3.30
DE198	0–20	14.78	29.98	55.24	6.90	4.90	< 3.5	327	4574	359	1.80	37.27	76.37	< 0.20
JJ043A	0–20	41.46	40.69	17.85	6.30	4.90	< 3.5	578	1854	275	1.88	16.89	76.04	< 0.20
JJ043B	80–100	23.20	23.30	53.50	8.10	6.40	< 3.5	1731	2704	311	0.83	31.38	100.00	< 0.20
JJ045A	0–30	48.56	27.99	23.45	6.90	5.80	< 3.5	768	2103	256	1.47	15.58	74.02	< 0.20
JJ045B	60	24.17	38.56	37.27	6.00	4.50	< 3.5	353	2589	332	1.69	21.11	53.47	< 0.20
JJ046A	30	21.10	37.33	41.57	4.90	4.00	< 3.5	205	1388	233	3.48	22.55	38.36	< 0.20
JJ046B	130	18.89	18.55	62.56	5.20	3.80	< 3.5	176	645	148	0.83	21.33	25.22	< 0.20
JJ047A	0–20	19.38	34.43	46.19	4.50	3.90	< 3.5	86	665	113	2.25	23.66	22.53	< 0.20
JJ047B	100	17.43	25.63	56.94	4.80	3.90	< 3.5	174	571	85	0.86	16.23	17.88	< 0.20
JJ048	10–20	53.09	31.95	14.96	7.80	6.70	< 3.5	968	2729	216	0.44	15.65	100.00	< 0.20
JJ049A	10–20	27.79	53.21	19.00	6.40	4.70	< 3.5	456	1415	195	1.57	16.96	52.40	< 0.20
JJ049B	40–50	15.27	27.68	57.05	7.80	6.20	< 3.5	1735	3085	434	0.58	26.94	97.33	< 0.20
JJ049C	190–200	14.87	21.39	63.74	–	–	–	–	–	–	–	–	–	–
JJ050A	0–30	39.89	40.35	19.76	6.70	5.50	41.7	1370	2176	218	1.18	15.80	100.00	< 0.20
JJ050B	30–90	26.96	44.16	28.88	–	–	–	–	–	–	–	–	–	–

TOC – total organic carbon, BS – base saturation, CEC – cation exchange capacity
Laboratory data: National Reference Laboratory of the Central Institute for Supervising and Testing in Agriculture (Brno, Czech Republic) and laboratories of the Czech Geological Survey (TOC analyses).

Annex 3. Spring inventory

Site_ID	X	Y	Yield
JCS-115	433099	748126	0.07
JCS-125	437541	751298	0.08
JCS-137	438823	750450	0.10
JCS-144	431977	747615	0.10
JCS-154	438112	753209	0.11
JCS-161	437536	751170	0.13
JCS-163	436502	749142	0.13
JCS-194	438297	755273	0.25
JCS-213	431758	746456	0.33
JCS-222	438963	748127	0.50
JCS-244	437873	752286	1.00
JCS-246	437468	752319	1.10
JCS-247	430547	747376	1.10
JCS-248	444376	746350	1.20
JCS-253	437386	747676	1.50
JCS-262	443192	761468	5.00
JCS-444	437212	772292	9.50
JCS-67	441843	746379	0.01
JCS-78	440620	757212	0.03
JCS-79	437719	751764	0.03
JCS-80	431685	748591	0.03
WSP-23	437101	772060	15.00
WSP-24	442590	759154	3.00
WSP-25	437441	750968	3.00
WSP-26	436732	746512	30.00
ZCS-23	444693	770861	28.60
ZCS-24	436967	771909	72.00
ZCS-25	443000	760814	6.10
ZCS-32	438663	749981	2.16
ZCS-33	432051	750884	0.72
ZCS-34	430496	758225	0.18

Dug well inventory

SITE ID	EASTING	NORTHING
DW-11	422220	769622

Borehole inventory

ID	Woreda	Kebele	Village Name	Utm E	Utm N	Altitude	Depth	SWL	Yield l/s
OBH1	Dale	Tula	Aganca	443880	756527	1747			0
OBH2			Eyrba	430171	763437	1963	150	82	0
OBH3			Eyrba	429972	764729	1963	95		0
OBH4			Eyrba	430065	765374	1963			0
OBH5			Abela Lida	435563	769021	1810	128	54	0
OBH6			Sedine	439497	770573	1740	119	56	4.4
OBH7			Abela lida plantation	442801	766525	1910	143		0
OBH8				441456	770917	1750	119	56	0
OBH9				434384	759565	1840	197.4	61	2.17
OBH10			Erbya	430072	763837	0			0
OBH11				444519	771571	1700	8.2	7.8	0
OBH12			East of shemena Kedida	427574	773352	1730	39.4	38.9	0
OBH13				435474	761003	1844		8.2	0
OBH14			Gov. Building	437076	772052	1680			0
OBH15			Gemetto Gale	444757	771017	1690	0		0
OBH16				421535	755179	0	307		5.4
OBH17				430871	755458	0	78		2.5
OBH18				429000	760000	0	220		6
OBH19				429200	762000	0	0		0
OBH20				429600	753500	0	121		6,6
OBH21				432529	757914	0	0		0
OBH22				431250	752170	1800	0		0
OBH23				439454	758156	1845	180		20
OBH24				439758	758653	1838	180		8
OBH25			Boko (Alamura)	441515	771015	1748	0	52	0
OBH26	Awassa Zuriya	Alamura	Manjola Udo	441475	770947	1698	120		0

ID	Woreda	Kebele	Village Name	Utm E	Utm N	Altitude	Depth	SWL	Yield l/s
OBH27	Shebedino	Abela Lida	Abela Chefe	443872	764567	1980	160		0
OBH28	Shebedino	Dirama Anferara	Dirama Anferara Town	430879	755469	1884	125		0
OBH29	Shebedino	Dulacha Tebarko	Muracho	437104	767716	1897	120		0
OBH30	Shebedino	Horocho Shondolo	Gonoba	436630	763907	1885	0		0
OBH31	Shebedino	Konsore Arkie	Demgeto	430043	763616	1850	150		0
OBH32	Shebedino	Leku Kebele 03	Leku Kebele 03	438208	759559	1871	0		0
OBH33	Shebedino	Leku Kebele 03	Leku Kebele 03	438215	759029	1873	0		0
OBH34	Shebedino	Morocho Kontela	Morocho Kontela	439380	764027	1927	230		0
OBH35	Shebedino	Nure Dulacha	Kundarie	438682	770065	1754	0		0
OBH36	Shebedino	Yirba	Yirbe 01 Town	430206	765640	1850	170		0
OBH37	Dara	Adola	Adola	441697	758984	1511	0		1.3
OBH38	Dale	Sodo Simite	Sodo Simite	434382	755751	1732	0		3.5
OBH39	Dale	Semen Mesenkela	Semen Mesenkela	440447	755364	1739	0		6.6
OBH40	Shebedino	Remeda	Asharea	440855	762637	2378	55		0
JBH-17			Alawo Orke *	429316	762264				4.4
JBH-30			Tara Mesa *	438753	758658				2
JBH-31			Tara Mesa *	439686	758827				1
JBH-45			Tara Mesa *	439686	758827				1
WBH 9			Midre Genet, Shebadeno, Sidama	434539	759688				
WBH 10			Derara Yirbaboricha, Sidama	421542	755176				
WBH-17			Abela Lida, Sidama	442138	765346				
WSBH-10			Wacho, Dále, Sidama	438541	754367				4.3
JBH-153			Alawo Ano *	432358	760688				1

ID	Woreda	Kebele	Village Name	Utm E	Utm N	Altitude	Depth	SWL	Yield l/s
JBH-279			Telamo *	441999	754828				1.5
JBH-280			Tara Mesa *	440752	756085				2
JBH-281			Sedeqa *	439302	756099				2
JBH-282			Tara Mesa *	439758	758653				1.5
JBH-283			Sadamo Dikicha *	430942	764320				0.7
JBH-284			Sadamo Dikicha *	431087	764391				1.5
JBH-285			Sadamo Dikicha *	432044	762315				0.7
JBH-286			Sadamo Dikicha *	432077	762871				2
JBH-289			Sedeqa *	438790	755899				0.5
JBH-290			Sedeqa *	439333	756524				6.6
JBH-313			Semen Mesenkela *	431035	752301				4.3
ZBH-19			Tulu *	439503	772129				
ZBH-20			Alamura *	441368	770824				
ZBH-21			Nure Dulecha *	438502	769894				
ZBH-18			Gemeto Gale *	443564	772019				
ZBH-17			Gemeto Gale *	444037	772150				
ZBH-16			Gemeto Gale *	444538	773609				
ZBH-23			Abela Lida *	441992	765116				
ZBH-24			Murancho Kutala *	439218	763856				
ZBH-25			Morochi Shonidola *	436549	763701				
ZBH-22			Delecha Teberako *	436961	767555				
ZBH-27			Morochi Negasha *	436403	762149				
ZBH-26			Konlore Orke *	429990	763394				
ZBH-31			Dirimo Aferara *	430860	755251				

ID	Woreda	Kebele	Village Name	Utm E	Utm N	Altitude	Depth	SWL	Yield l/s
ZBH-28			Midire Genet *	434402	759495				
ZBH-29			Leku Town *	437964	759294				
ZBH-30			Fura *	437132	756611				
ZBH-32			Chume *	435537	752720				
ZBH-33			Semen Mesenkela *	431250	752160				
ZBH-34			Tula *	431271	747833				
TBH-72			Finicahwa *	439279	770876				

Water chemistry (data in mg/l)

ID	Na	K	Ca	Mg	HCO_3	CO_3	Cl	F	SO_4	NO_3	HBO	SiO_2	Ph	EC	TDS_calc
ZBH-19	430	27.3	22.45	14.24	964	–	47	2.51	0	0	0	–	0	0	1507.5
ZBH-17	68	10	32	13	255	–	40	0.93	33	0	0	–	0	0	451.93
ZDW-100	123	10.6	23	8	410	–	12	3.57	11	0	–	–	0	0	601.17
ZDW-103	420	34	87.5	30	1262	–	161	7.94	82	0	–	–	0	0	2084.44
ZDW-89	475	24.8	15	7.5	931	–	163	10.46	74	0	–	–	0	0	1700.76
TDW-5	288	20	18	5	756	0	36	8.7	3	0	–	62	8	0	1198.1
ZBH-26	37	6	19	4	198	–	4	2.25	1	0	0	–	0	0	271.25
BH-10	29.9	7.34	13.1	3.7	0	122	2.2	1.08	0.05	0.05	0.1	99.51	6.62	226	279.03
ZBH-16	77	7.2	19	9	286	–	15	0.58	7	0	0	–	0	0	420.78
ZCS-34	29	6.1	6	2	63	–	19	0.3	5	0	–	–	0	0	130.4
ZDW-106	30	28	24	6	218	–	15	0.64	3	0	–	–	0	0	324.64
DW-1	30.8	12.45	10.6	1.6	0	70	4.68	0.88	34.8	1.77	–	39.53	6.21	738	207.21
BH-GID3	19	7.8	9.12	5.02	102.48	–	1.82	0.57	1	9.21	0	–	6.16	181	156.02
BH-GID8	27	6.2	12.9	3.2	110.2	–	6.6	0.11	1.71	6.33	0	–	6.4	181	174.25
ZBH-24	49	3.3	2.2	0.7	156	–	3	1.08	3	0	0	–	0	0	218.28
ZBH-28	29	9	9	2.2	132	–	3	0.75	1	0	0	–	0	0	185.95
ZBH-29	23	7	8	2	83	–	10	0.37	2	0	0	–	0	0	135.37
ZBH-30	13	4	11	1.4	95	–	5	0.24	1	0	0	–	0	0	130.64
ZBH-31	22	4	9.3	3	112	–	3	0.5	1	0	0	–	0	0	154.8
ZBH-32	16	5	14.3	2.3	109	–	10	0.41	1	0	0	–	0	0	158.01
ZBH-33	15	5	11	2	104	–	3	0.36	1	0	0	–	0	0	141.36
ZBH-34	16	7	12.4	2.4	105	–	7	0.33	1	0	0	–	0	0	151.13

DBH-42	9.9	6.16	8.7	2.1	0	62	2.06	0.13	0.05	4.87	0.17	86.67	6.59	117.1	182.81
SBH-10	13.7	6.2	10.7	2.1	0	73.2	5.81	0.23	2.8	0.05	0.11	92	5.91	189.2	206.9
BH-9	31.1	10.14	6.2	1.6	0	109.8	1.06	0.79	0.05	0.05	0.1	96.3	6.35	181	257.19
ZBH-20	44	7	10	5	236	–	4	1.21	1	0	0	–	0	0	308.21
ZBH-21	32	5.6	10.5	4	134	–	5	1.25	1	0	0	–	0	0	193.35
ZBH-25	28.5	7.2	12	4	137	–	5	1.04	1	0	0	–	0	0	195.74
BH-17	45.3	7.24	2.4	0.8	0	122	2.13	1.28	0.05	0.05	0.1	101.65	6.41	209	283
JSP-155	18	6.4	4.56	2.28	61.49	–	2.73	0.59	2.95	28.43	0	–	5.71	135	127.43
ZCS-25	7.4	6.4	6	1.4	49	–	6	0.15	3	0	0	–	0	0	79.35
ZCS-32	13	6	7	2	83	–	7	0.23	2	0	0	–	0	0	120.23
ZCS-33	27.5	10.1	4.7	1.5	104	–	9	1.04	3	0	0	–	0	0	160.84
sp-24	8.1	7.28	6.9	1.5	0	39.04	5.53	0.23	3.3	9.3	0.05	89.88	5.32	118	171.11
sp-25	13.8	5.14	3.3	0.8	0	41.48	5.81	0.23	4.5	8.86	0.05	86.7	5.39	111	170.67
sp-26	14.7	10.97	13.2	3.2	0	41.48	12.27	0.2	12.9	21.26	0.05	107	5.6	154	237.23
ZCS-23	2.3	5	14	4	124	–	5	0.35	1.3	0	0	–	0	0	155.95
ZCS-24	35.5	4.7	8.5	3	131	–	5	1.01	5	0	0	–	0	0	193.71
sp-23	36.7	4.53	9.1	2.8	0	162.26	4.68	1.45	2.9	0.05	0.1	84.5	7.34	224	309.07
ZDW-107	12	8	12	0.8	107	–	3	0.22	3	0	–	–	0	0	146.02
TDW-1	50	18	47	12	249	0	39	0.8	53	0	1	90	0	0	559.8
DW1	30.8	12.45	10.6	1.6	70	–	4.68	0.88	34.8	1.77	0.1	39.53	–	–	207.21
Bedesa River	24.2	9.5	2	0.9	85	–	6	0.52	–	3.54	0.03	391	–	–	522.69
Bilate River	40	8.9	7.9	1.6	122	–	13	1.4	0.4	3.54	0.14	31	–	–	229.88
Lake Awassa	151	25.4	10	5	412	12	29	6.08	1.03	–	–		–	–	651.51